Functional and animal studies of short-chain 3-hydroxyacyl-CoA dehydrogenase (SCHAD), a fatty acid beta-oxidation enzyme involved in congenital hyperinsulinism of infancy

Johanna St-Louis

Thesis for the degree of Philosophiae Doctor (PhD)
University of Bergen, Norway
2021

UNIVERSITY OF BERGEN

Functional and animal studies of short-chain 3-hydroxyacyl-CoA dehydrogenase (SCHAD), a fatty acid beta-oxidation enzyme involved in congenital hyperinsulinism of infancy

Johanna St-Louis

Thesis for the degree of Philosophiae Doctor (PhD)
at the University of Bergen

Date of defense: 16.02.2021

Year: 2021

Title: Functional and animal studies of short-chain 3-hydroxyacyl-CoA dehydrogenase (SCHAD), a fatty acid beta-oxidation enzyme involved in congenital hyperinsulinism of infancy

Name: Johanna St-Louis

Print: Skipnes Kommunikasjon / University of Bergen

Scientific environment

The studies of this dissertation were performed at:

Gade Laboratory for Pathology
Department of Clinical Medicine
Faculty of Medicine
University of Bergen
Bergen, Norway

and

Department of Pathology
Haukeland University Hospital
Bergen, Norway

In collaboration with:

Center for Diabetes Research
Department of Clinical Science
Faculty of Medicine
University of Bergen
Bergen, Norway

and

Islet Cell and Regenerative Biology
Joslin Diabetes Center
Harvard Medical School
Boston, USA

The research performed at the University of Bergen was supported by a PhD fellowship and an Overseas Research Grant from the Research Council of Norway (FRIMEDBIO program project #240788). Grants were also received from the Western Norway Regional Health Authority (Helse Vest #912258) and Novo Nordisk Foundation (NNF16OC0021050).

Acknowledgements

I would like to express my sincere gratitude to my main supervisor Prof. Anders Molven. You have been the most inspiring, motivating and patient mentor for me. I am incredibly grateful that you have given me the opportunity to grow as a scientist, not only in your own laboratory but also abroad at the Joslin Diabetes Center. I would also like to thank my co-supervisor Prof. Rohit Kulkarni for hosting and mentoring me in your laboratory at the Joslin Diabetes Center, Boston. Our discussions, your knowledge and insights have taught me many lessons along the way. To my co-supervisor Kelly Velasco, thank you for your scientific input and constant support on the SCHAD project. It was a wild ride! Your infectious enthusiasm for acquiring new knowledge and learning new methods taught me to push myself and grow not only as a scientist, but also as a person. To co-supervisor Prof. Pål R. Njølstad, I am grateful for your support and for leading the diabetes research environment in Bergen during my time there.

I would like to extend my sincere gratitude the Research Council of Norway for the funding that made this thesis possible. I am also indebted to Novo Nordisk Foundation and Western Norway Health Authority (Helse Vest) for supporting the SCHAD project over the years.

During my PhD period I received magnificent support and input from the MODY group in Bergen as well as the Kulkarni lab, and joint meeting groups, in Boston. Special thanks are directed to Karianne Fjeld, Ingvild Aukrust, and our students Nels Thompson, Benedict Man Hung Choi and Henrikke Nilsen Hovland. I would also like to extend a sincere thank you to Jiang Hu (Jane), Dario De Jesus, Brittany Slipp and Jennifer Hollister-Lock. Your help with Paper II of my thesis was invaluable!

Finally, I would like to thank my family and friends for your love, encouragement, and overall support throughout the years. Especially, I would like to thank my mother and late father for giving me the opportunity to follow my dreams. I would also like to thank my husband, Ronald. Not only have our scientific discussions helped me along the way, but you also provide for our family and gave me the greatest gift in our daughter Sara Isabelle. It is wonderful to have you all in my life, and I cannot wait to see what our future will hold!

Boston and Bergen, November 15th, 2020

Johanna L. St-Louis

Abstract

Short-chain 3-hydroxyacyl-CoA dehydrogenase (SCHAD) is a mitochondrial enzyme involved in fatty acid β-oxidation and the regulation of β-cell insulin secretion. Its role in insulin secretion became apparent in 2001 when the first report linking SCHAD deficiency with congenital hyperinsulinism of infancy (CHI) was published. Since then research into the mechanism of SCHAD-CHI has led to the view that SCHAD serves a β-cell specific function and that the mechanism involves inhibition of glutamate dehydrogenase. In this thesis, we studied functional differences of pathogenic and non-pathogenic SCHAD missense variants, investigated the β-cell specificity of SCHAD deficiency in an animal model, and sought to identify novel interaction partners of the protein.

In Paper 1, we found that missense SCHAD variants occurring in datasets from human populations mostly behaved like the wild type protein, whereas CHI-associated SCHAD variants had altered properties with regard to protein stability, enzymatic function and interaction with GDH. Four of the seven studied CHI variants showed reduced protein expression when expressed in HEK293 cells. The remaining three pathogenic variants had stable expression but reduced enzymatic activity and binding to GDH.

In Paper II, we generated conditional SCHAD knockout mice and studied the cell-type specific effects of SCHAD deficiency in β-cells and hepatocytes. We noted that the SCHAD protein was highly expressed in pancreatic β- and δ-cells, but virtually absent from the α-cells. The mice harboring a β-cell-specific deficiency in SCHAD expression were hypoglycemic under various conditions, and their islets were sensitive to amino acid-stimulated insulin secretion. Analysis of the transcriptome of isolated SCHAD knockout islets identified global changes in expression of genes involved in metabolism and β-cell identity. Overall, this study strengthened the hypothesis that SCHAD serves a specific function in the β-cells and that β-cell SCHAD deficiency is sufficient to cause hypoglycemia.

In Paper III, we sought to identify novel protein interactions partners of SCHAD by performing a yeast two-hybrid screen in a library from human islets of Langerhans. We identified keratin 8 (K8) as a putative binding partner and found additional evidence of an interaction by co-immunoprecipitation experiments. We also analyzed SCHAD expression in a K8 knockout mouse and K8 expression in the SCHAD knockout mouse. However, the lack of one potential interaction partner did not affect expression of the other, except when K8 knockout mice were

fed a ketogenic diet. The dietary challenge resulted in an upregulation of SCHAD in the pancreas of WT animals and this was blunted in the absence of K8. More experiments need to be carried out in order to explore the possible biological relevance of the proposed SCHAD-K8 interaction.

In summary, this thesis increased our knowledge on the impact of missense variants on SCHAD function and may therefore aid in the clinical evaluation of rare variants found in patients with phenotypes related to β-cell function. We developed a new mouse model for SCHAD-CHI, which highlighted the importance for SCHAD expression in the β-cell as well as the heterogeneous expression of the enzyme in islet cell populations. Lastly, we found evidence for a novel and surprising protein interaction of SCHAD with K8 that remains to be further validated.

List of Publications

Paper I

Kelly Velasco, Johanna L. St-Louis, Henrikke N. Hovland, Nels Thompson, Åsta Ottesen, Man Hung Choi, Line Pedersen, Pål R. Njølstad, Thomas Arnesen, Karianne Fjeld, Ingvild Aukrust, Line M. Myklebust, Anders Molven (2020). Functional evaluation of sixteen SCHAD missense variants: Only amino acid substitutions causing congenital hyperinsulinism of infancy lead to loss-of-function phenotypes in vitro. *Journal of Inherited* Metab*olic Disease* 2020 (doi: 10.1002/jimd.12309, online ahead of print)

Paper II

Johanna L. St-Louis, Dario F. De Jesus, Brittany A. Slipp, Jiang Hu, Solrun J. Steine, Geir Helgeland, Kelly Velasco, Rohit N. Kulkarni*, Anders Molven* (2020). Amino acid-sensitive hypoglycemia caused by a specific deficiency of the metabolic enzyme SCHAD within pancreatic β-cells. *Manuscript.*

* Joint senior authors

Paper III

Johanna L. St-Louis[#], Kelly Velasco[#], Jonas S.G. Silvander, Sarah Baghestani, Pål R. Njølstad, Rohit N. Kulkarni, Diana M. Toivola, Anders Molven (2020). Searching for novel interaction partners of short-chain 3-hydroxyacyl-CoA dehydrogenase (SCHAD): A role for keratin 8?

Manuscript.

Joint first authors

Selected abbreviations

CHI	Congenital hyperinsulinism of infancy
FAO	Fatty acid oxidation
FOXA2	Forkhead box A2
GDH	Glutamate dehydrogenase
GK	Glucokinase
GLP-1	Glucagon-like peptide
HADH	Short-chain 3-hydroxyacyl-CoA dehydrogenase gene
HK1	Hexokinase 1
HNF1α	Hepatocyte nuclear factor 1-alpha
HNF4α	Hepatocyte nuclear factor 4-alpha
K_{ATP} channel	ATP-sensitive potassium channel
Kir6.2	Inwardly rectifying potassium channel
KO	Knockout
K8	Keratin 8
KRT8	Keratin 8 gene
MCT-1	Monocarboxylate transporter 1
MIS	Mitochondrial import signal
MODY	Maturity onset diabetes of the young
SCHAD	Short-chain 3-hydroxyacyl-CoA dehydrogenase
SCHADKO	SCHAD knockout mouse
SST	Somatostatin
SUR1	Sulfonylurea receptor 1
VGCC	Voltage gated calcium channels
Y2H	Yeast-2-hybrid

Table of contents

1. Introduction

1.1. The human and mouse pancreas

The pancreas serves dual roles in the endocrine and digestive systems of vertebrates. The endocrine pancreas secretes hormones into the blood stream that regulate glucose homeostasis, and the exocrine pancreas produces and secretes digestive enzymes into the duodenum to aid digestion.

The human pancreas is an organ of approximately 14 – 18 cm length, weighing between 50 to 100 g. It is commonly divided into a head, body and tail region. The head of the pancreas aligns with the C-bend of the duodenum. The body stretches horizontally below the stomach and the tail is in contact with the spleen (Figure 1A).

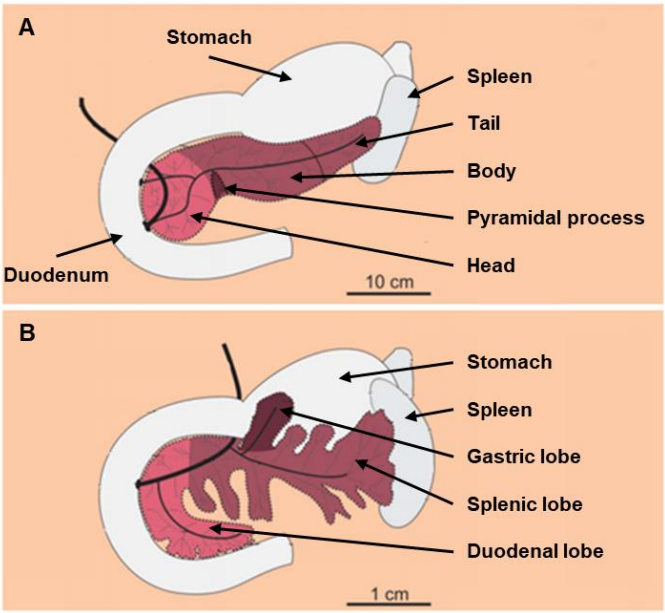

Figure 1 Anatomic comparison of the human and mouse pancreas. (A) The human pancreas stretches from the C-bend of the duodenum to the spleen and is usually divided into three regions: head, body, and tail. **(B)** The mouse pancreas is structurally less defined but can also be divided into three regions: the duodenal, splenic, and gastric lobes. Homology in pancreas structure between man and mouse is indicated by color. Ducts are represented as full black lines going through the pancreas. Adapted from (1).

The mouse pancreas has a more diffuse morphology but can still be divided into three major lobes. The duodenal lobe is analogous to the head of the human pancreas and lies embedded in the mesentery around the duodenum. The splenic lobe is the largest part of the mouse pancreas and equivalent to the body and tail of the human pancreas. The smallest part of the mouse pancreas, the gastric lobe, extends upwards from the splenic lobe attaches to the stomach. This part may be analogous to the pyramidal process, a structure seen in only 50% of human pancreata (Figure 1B) (1).

1.1.1. The endocrine pancreas - islets of Langerhans

The endocrine pancreas consists of micro-organs called islets of Langerhans that are embedded in the exocrine parenchyma. These islets constitute up to 15% of the pancreas volume in neonates but this fraction decreases to 2 – 3% in adults (2).

The islets of Langerhans contain five distinct endocrine cell types that originate from a common progenitor cell expressing neurogenin 3 (Ngn3) (3): the glucagon-secreting α-cell, the insulin-secreting β-cell, the somatostatin (SST)-secreting δ-cell, the pancreatic polypeptide-secreting PP-cells and the ghrelin-secreting ε-cells. β-cells form the largest group of islet cells and contribute to 50-70% of islet cell mass in humans and 60-80% in mice. Alpha cells are the second most abundant cell type, comprising 20 – 40% of islet cells in humans and 10 – 20% in mice, followed by δ-cells which contribute 5 – 10%. PP-cells form only around 5% of islet cells, but the posterior head of the human pancreas contains a specific subset of islets that are enriched in PP-cells and low in α- and β-cells. ε-cells are the least frequent cell type comprising 1% of total islet cells.

In the mouse, islets are mostly organized in rounded or oval structures, in which a cluster of β-cells is surrounded by a mantle of other islet cells (Figure 2A,B). Human islets are overall more complex in architecture and non-β-cells are frequently observed in the islet core (Figure 2C,D). The islets are distributed heterogeneously throughout the pancreas. In humans the tail of the pancreas has the highest density of islets per unit volume. In the mouse, the gastric lobe contains the highest and the splenic lobe the lowest number of islets per unit of tissue volume (1). Pancreatic islets are strongly perfused (Figure 2B,D). Even though they comprise only 2-3% of the pancreas tissue mass, they receive up to 20% of pancreatic blood supply originating from the splenic artery. Blood exits the islet through the splanchnic veins and ultimately drains

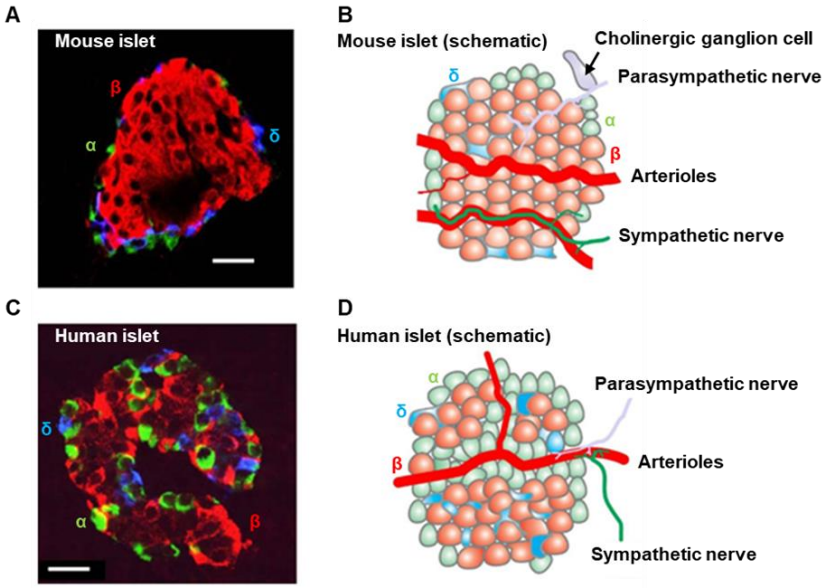

Figure 2. Structure and composition of the mouse and human islet of Langerhans. (A) Immunohistochemistry of a mouse islet stained for insulin (red), glucagon (green) and somatostatin (blue). **(B)** Schematic of mouse islet composition showing β-cells (red), α-cells (green) and δ-cells (blue), innervation and blood supply. **(C)** Immunohistochemistry of a human islet. Colors are the same as in (A). **(D)** Schematic of human islet. Colors are the same as in (B). Scale bars in (A) and (C): 20 µm. Adapted from (4)

into the hepatic portal vein. Blood supply from the splenic artery ensures that islet cells receive systemic stimuli such as glucose and amino acids for hormone secretion (4).

Besides from inputs via the blood supply, the islet receives stimuli from sympathetic, parasympathetic, and additionally in the mouse, cholinergic nerves (Figure 2B,D). Mouse islets are highly innervated, and the nerves make direct contact with the endocrine cells. In humans, innervation is less pronounced and the nerves make contact with smooth muscle cells instead of endocrine cells (4).

1.1.2. The insulin-secreting pancreatic β-cell

The β-cells are the best studied of the five islet cell types and, together with the less numerous α-cell, they play a central role in the regulation of glucose homeostasis. β-cells have a polygonal shape and contain about 10,000 granules that store insulin as Zn_2-insulin$_6$ crystals. These granules have an electron-dense core with clear edges and a surrounding electron-lucent ring on electron microscopy images of islets.

The main function of β-cells is the secretion of the hormone insulin in response to an increase in blood glucose levels. Insulin is encoded by the *INS* gene. The mRNA first yields preproinsulin which undergoes cleavage to proinsulin upon entry into the endoplasmic reticulum (ER). Proinsulin contains a carboxy-terminal A chain and an amino-terminal B chain separated by stretch of amino acids called the C-peptide. Once it arrives in the Golgi apparatus, proinsulin is packaged into secretory vesicles. Here, the C-peptide is excised from the precursor to yield mature insulin and free C-peptide (5).

Insulin is secreted in response to neurotransmitters, incretins (e.g. glucagon-like-peptide (GLP-1), gastric inhibitory polypeptide (GIP)), and nutrients such as glucose and amino acids. The regulation of insulin secretion will be discussed in detail in Chapter 1.2. However, the main stimulus is hyperglycemia, and insulin's major function is to reduce increased blood glucose levels to normoglycemic levels. This is achieved by stimulation of glucose uptake in muscle and adipose tissue, stimulation of glycogen synthesis, glycolysis, and conversion of pyruvate to Acetyl Co-A (for ATP production in the Krebs cycle or fatty acid synthesis). Insulin also inhibits glycogen breakdown and gluconeogenesis.

Besides glucose metabolism, insulin also influences lipid metabolism and protein synthesis. In liver and adipose tissue, insulin stimulates fatty acid synthesis, inhibits fatty acid β-oxidation, and increases formation and storage of triglycerides. It also stimulates cholesterol synthesis. Insulin affects gene expression throughout the body. Some examples include augmentation of liver glucokinase, fatty acid synthase and albumin, and adipose tissue pyruvate carboxylase expression (6). Lastly, β-cells interact with local islet cell populations through autocrine and paracrine mechanisms. Insulin regulates β-cell mass, insulin synthesis and β-cell calcium flux. Insulin, zinc ions and gamma-aminobutyric acid (GABA), which are co-secreted with insulin, reduce glucagon secretion from α-cells (7).

1.1.3. Other islet cell types

α-cell

α-cells are located in the islet periphery surrounding the β-cell core. In humans, α-cells may also be found within the core, lining arterioles and capillaries (4). α-cells secrete glucagon, which together with insulin regulates blood glucose levels. Glucagon is produced by cleavage of preproglucagon by prohormone convertase 2. Other cell types such as the L-cells in the

gastrointestinal tract, also produce the preproglucagon but process the precursor protein to yield GLP-1 and other hormones (8).

In many ways, glucagon functions opposite of insulin. The hormone stimulates hepatic glycogenolysis and gluconeogenesis during hypoglycaemic conditions to increase hepatic glucose release and achieve normoglycemia. Glucagon also stimulates lipolysis and increases energy expenditure. Within the islet, glucagon has paracrine functions to stimulate insulin and SST secretion (8,9).

The regulation of glucagon secretion is not as well defined as insulin secretion from β-cells. Studies suggest that glucagon secretion is regulated by glucose and amino acid levels, as well as paracrine factors. During low glucose conditions, ATP-sensitive potassium channels (K_{ATP}-channels) are activated to generate a membrane potential of 60 mV. This opens low voltage-gated calcium channels, and subsequently sodium and high voltage calcium channels. The influx of calcium then induces the exocytosis of glucagon granules. During high glucose conditions, ATP production increases which results in closure of K_{ATP} channels and inhibits glucagon secretion. However, high glucose has been reported to potently stimulate glucagon secretion from isolated alpha cells, an effect that is absent in intact islets. In whole islets, glucagon secretion under high glucose conditions may be suppressed through paracrine action of insulin, SST, zinc ions and GABA (9,10).

δ-cell

δ-cells can also be found in the CNS and scattered throughout the gastrointestinal tract. In mouse islets, δ-cells mostly surround the core, with few cells being located in the islet center. In humans, δ-cells may be found scattered throughout the islet. δ-cells make tight contact with several α- and β-cells through neurite-like processes and negatively regulate insulin and glucagon secretion through secretion of SST and β- to δ-cell electrical coupling. β- and δ-cells share an immediate common progenitor and δ-cells have been reported to transdifferentiate into β-cells. Both cell types share common properties related to their secretory function such as the expression of glucokinase and K_{ATP} channel genes (ABCC8 and KCNJ11). Stimulants of SST secretion also include glucose, amino acids (leucine and arginine), neurotransmitters, hormones such as GABA, glucagon, GLP-1, ghrelin, urocortin 3, and possibly insulin. However, SST secretion is initiated at lower glucose levels than insulin secretion (3 vs. 6 mM

in the mouse) and contrary to α- and β-cells, δ-cell SST secretion is inhibited by palmitate. SST secretion is also inhibited by adrenaline and possibly by SST itself (11).

PP-cell

Most of the PP-cells are concentrated in the head of the pancreas. In mice, the majority of PP-cells, like α- and δ-cells, are found surrounding the islet core. In human islets, PP-cells are located in close proximity to blood vessels. Some PP-cells can also be found scattered throughout the exocrine parenchyma of the pancreas. They postprandially secrete pancreatic polypeptide (PPY) in response to vagus and enteric nerve stimulation and increased levels of amino acids (arginine). PPY negatively regulates gastric emptying as well as intestinal mobility and inhibits α-cell glucagon secretion under hypoglycemic conditions (8).

ε-cell

ε-cells are the least abundant islet cell type in adults but make up to 10% of the islet cells mass in neonates. Like other non-β-cells, most ε-cells are located in the islet periphery of mouse islets. Some ε-cells may also be found in pancreatic ducts or scattered throughout the exocrine parenchyma (12). They, in concert with P/D1 cells in the gastric fundus, produce the "hunger hormone" ghrelin as response to fasting and as hunger levels rise. Ghrelin acts in the central nervous system as a signal to initiate food intake and plays widespread systemic roles in the regulation of glucose homeostasis, energy expenditure and body weight development (13). It also plays a local role within the islet, as a paracrine inhibitor of insulin secretion during fasting. Even though ε-cells make a minor contribution to islet mass, evidence suggests that they are a significant source of circulating ghrelin in humans (12).

1.1.4. The exocrine pancreas

The exocrine parenchyma constitutes about 90% of the pancreas volume and contains acinar, stellate, and ductal cells. Acinar cells are specialized cells that synthesize and secrete digestive enzymes which are transported to the intestine through a network of pancreatic ducts. Acinar cells are characterized by a highly basophilic cytoplasm, basally located nucleus, and apically located secretory granules. They are organized in small clusters called acini which surround a lumen that connects to intercalating ducts. These ducts drain into intralobular ducts and further into interlobular ducts which open into the pancreato-hepatic duct. Ductal cells aid in the transport of the digestive enzymes by secreting bicarbonate and water which mix with the

enzymes and form the pancreatic juice. The stellate cell is the least numerous cell type within the exocrine pancreas. These cells uphold pancreas structure by regulating the formation and degradation of extracellular matrix and are central players in fibrotic processes in pancreatic exocrine disease (14).

Although the exocrine and endocrine pancreas generally have been treated as two separate organ compartments, there is now increasing evidence of endocrine-exocrine crosstalk and interdependence. Blood flow between the islets and exocrine tissue is interconnected allowing for paracrine regulation in either direction (15). Exocrine cells are exposed to high levels of islet hormones which serve as regulators of exocrine secretion (16). Moreover, the two compartments are not separated and are in intimate physical contact with each other. Peri-islet acinar cells in close contact with islet cells are morphologically and functionally different from the more distantly located tele-islet acinar cells. Evidence suggests crosstalk between islets and peri-islet acinar cells plays a role in islet expansion in diabetes (17).

Due to the interconnectedness of the endocrine and exocrine pancreas it is not surprising that dysfunction in either compartment has implications for the other. Indeed, exocrine dysfunction as seen in conditions such as chronic pancreatitis, cystic fibrosis and maturity-onset diabetes of the young type 8 (MODY8), is a risk factor for endocrine dysfunction and type 3c diabetes (18). On the other hand, diabetes has been found to be a risk factor for and to exacerbate acute pancreatitis (19) and there are links between diabetes and pancreatic cancer (20).

1.2. The regulation of insulin secretion

1.2.1. Glucose-stimulated insulin secretion

The postprandial rise in blood glucose levels is the most important physiological stimulus for insulin secretion (Figure 3). Glucose enters the β-cell via facilitated, insulin-independent transport. In humans, this is primarily mediated by the membrane protein solute carrier family 2 member 1 (GLUT1) and to a lesser extent solute carrier family 2 member 3 (GLUT3). Rodents mainly utilize solute carrier family 2 member 2 (Glut2) (21). The difference in glucose transporter expression may explain the distinct set points of normoglycemia in human and mouse. Humans maintain their blood glucose levels around 90 mg/dl and mice around 140

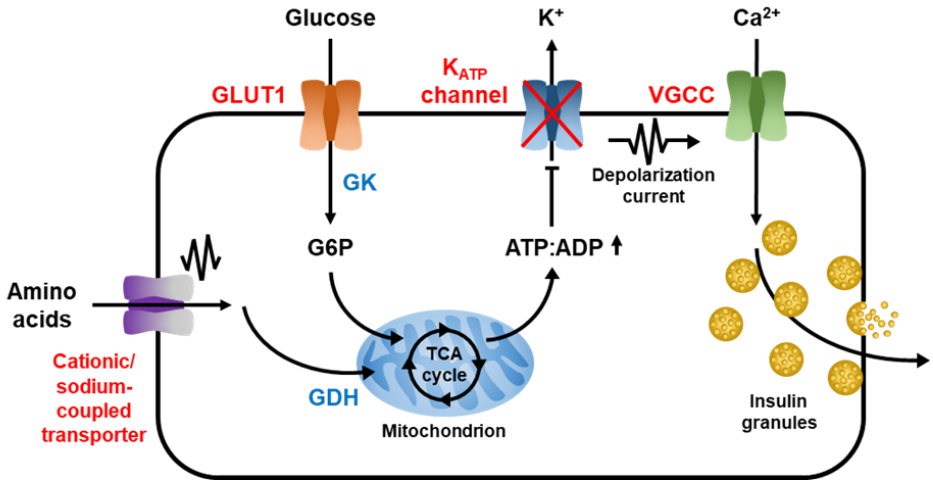

Figure 3. Insulin secretion in response to glucose and amino acids. Glucose enters the β-cell via facilitated transport through GLUT1 and GLUT3 (in the mouse Glut2). Glucokinase (GK) converts glucose to glucose-6-phosphate (G6P). G6P metabolism results in ATP production from the TCA cycle, a rise in the ATP:ADP ratio and closure of ATP-sensitive potassium channels (K_{ATP}-channel). This in turn blocks the export of positively charged potassium ions (K^+) and causes the loss of negative charge that triggers depolarization of the β-cell membrane. Voltage gated calcium channels (VGCC) then open to allow influx of calcium ions ($Ca2^+$). Finally, the import of Ca^{2+} stimulates exocytosis of insulin granules. Amino acids enter the cell through cationic or sodium coupled amino acid transporters and enhance insulin secretion via evocation of a depolarization current and metabolism in the TCA cycle which may be stimulated by glutamate dehydrogenase (GDH) activity.

mg/dL (22). GLUT1 and GLUT3 have lower K_m for glucose transport than Glut2 (6 mM and 1 mM vs. 11 mM), allowing for glucose transport at lower blood glucose levels (21).

After glucose enters the β-cell, it is converted to glucose-6-phoshate by glucokinase (GK), the glucose sensor of the β-cell. GK belongs to the hexokinase superfamily and is expressed in the β-cell, liver, and brain (23). Like other hexokinases, it catalyzes the conversion of glucose to glucose 6-phosphate (G6P). However, contrary to other hexokinases, GK is not inhibited by its product (24). Furthermore, glucokinase remains in an inactive configuration during low glucose conditions and as glucose levels rise, the substrate stimulates the switch to its active state (25). These attributes ensure low G6P production when blood glucose levels are low and high G6P production as glucose levels rise.

G6P subsequently serves as substrate for glycolysis and the TCA cycle, leading to a rise in ATP and a decrease in ADP levels. This change in β-cell energy status stimulates the closure of K_{ATP}-channels. When the β-cell is not stimulated, the K_{ATP} channel transports potassium ions out of the cell to maintain a resting potential. Closure of the K_{ATP} channel stops the export

of the positively charged potassium ions, which in turn causes a loss of negative charge and subsequent depolarization of the β-cell plasma membrane (26).

Membrane depolarization then stimulates the opening of voltage gated calcium channels (VGCC). Opening of VGCCs then allows for an influx of calcium ions which in turn trigger the fusion of the secretory granule with the plasma membrane in a process similar to neurotransmitter release (27).

The fusion of insulin granules with the β-cell plasma membrane is mediated by the SNARE complex. The SNARE complex is composed of soluble N-ethylmaleimide-sensitive factor attachment protein (SNAP) receptor proteins (SNAREs) and Sec1/Munc18-like (SM) proteins. Important SNARE proteins of the SNARE complex are the plasma membrane bound synaptosomal-associated protein of 25 kDa (SNAP-25) and syntaxin-1, as well as Vesicle Associated Membrane Protein 2 (VAMP) that is integrated into the insulin granule membrane. Insulin granule exocytosis is initiated by binding of calcium to synaptotagmin proteins within the vesicle membrane which then interact with SNAREs to facilitate membrane fusion (26).

Insulin release occurs in two phases. The β-cell contains ca. 10.000 mature insulin granules that are either pre-docked at the plasma membrane or stored deeper in the cell. First phase insulin secretion peaks between 3-5 minutes after stimulation and rapidly releases a small, pre-docked subset of insulin granules through the mechanism described above. Insulin secretion in the second phase is slower (5 – 40 granules/min) but can be sustained for long periods of time until normoglycemia has been achieved (28). Interestingly, while first phase insulin secretion can be stimulated by non-nutrient stimuli such as KCl, second phase insulin secretion is dependent on nutrients such as glucose (29).

1.2.2. Insulin secretion stimulated by other nutrients

Amino acids and lipids modulate insulin secretion in the presence of glucose. Amino acids enter the β-cell through cationic amino acid transporters and sodium-coupled neutral amino acid transporters (Figure 3). They are capable of evoking mild depolarization currents either by providing a positive charge themselves (e.g. arginine and lysine) or by requiring co-transport of positively charged sodium ions (e.g. alanine and glutamine). Uptake of these amino acids triggers depolarization in the presence of glucose, especially when glucose stimulation is mild and K_{ATP}-conductance is low (4). Additionally, alanine, glutamate, and glutamine serve as substrates for the TCA cycle. Their metabolism therefore increases the

ATP:ADP ratio to promote plasma membrane depolarization via closure of the K_{ATP}-channels (30). Glycine is co-secreted with insulin and serves as an autocrine potentiator of insulin secretion. It binds to ionotropic glycine receptors and triggers an influx of chloride ions which in turn leads to membrane depolarization (4).

Leucine plays a unique role in the stimulation of insulin secretion. It is the only amino acid that is capable of initiating insulin release independent of glucose action. It can serve as substrate for metabolism and ATP production, but it also stimulates the production of ATP via the TCA cycle by allosteric activation of glutamate dehydrogenase (GDH) (4).

Non-esterfied fatty acids acutely stimulate insulin secretion from isolated islets. Chronic incubation, on the other hand, negatively regulates insulin secretion. The mechanism underlying stimulation of insulin secretion by these fatty acids and its biological relevance are not fully elucidated. One suggested mechanism involves binding to free fatty acid receptor 1 on the β-cell surface. This leads to an influx of calcium ions and depolarization of the plasma membrane, thereby potentiating glucose-stimulated insulin secretion (4).

1.2.3. Paracrine regulation of insulin secretion by α- and δ-cells

α-, β-, and δ-cells form a tight network that regulates hormone secretion via paracrine mechanisms (Figure 4). β-cells suppress glucagon secretion from α-cells via paracrine action of insulin and other secreted factors (serotonin (5-HT), GABA, zinc ions). Conversely, β-cells stimulate SST secretion from δ-cells primarily via urocortin-3, which is co-secreted with insulin (30).

Glucagon derived from α-cells potentiates insulin secretion via binding to glucagon receptor (GCGR) and the related glucagon-like peptide receptor (GLP1R). Additionally, human α-cells secrete corticotropin-releasing hormone (CRH) and acetylcholine. Mouse α-cells neither secrete CRH (although mouse β-cells express the corresponding receptor), nor acetylcholine. Acetylcholine in mouse islets originates from parasympathetic neurons which make tight contact with endocrine cells (see Chapter 1.1.1). CRH and acetylcholine both potentiate insulin secretion directly by acting on β-cells via signaling through corticotropin-releasing hormone receptor 1 (CRHR1) and muscarinic acetylcholine receptor M3 (CHRM3), respectively. Additionally, acetylcholine inhibits SST secretion by binding to muscarinic acetylcholine receptor M3 (CHRM4) on δ-cells, thereby indirectly augmenting insulin secretion (30).

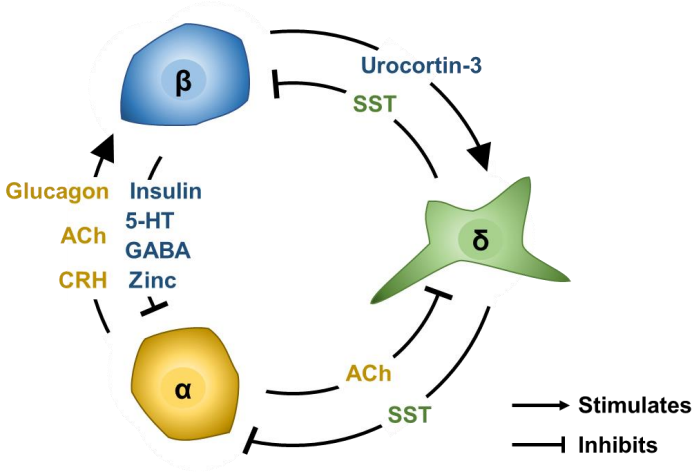

Figure 4. Paracrine interaction between α-, β-, and δ-cells. α-cell and α-cell-derived factors are indicated in yellow, β-cell and β-cell-derived factors in blue and δ-cell and δ-cell-derived factors in green. During hyperglycemia, β-cells secrete insulin, serotonin (5-HT), GABA and zinc ions, all of which suppress glucagon secretion from α-cells. α-cells on the other hand augment glucose-dependent insulin secretion by secretion of glucagon, acetylcholine (Ach) and corticotropin-releasing hormone (CRH). δ-cells negatively regulate both α- and β-cells via secretion of somatostatin (SST). β-cells stimulate SST secretion from δ-cells in a negative feedback loop by co-secretion of urocortin-3 with insulin. Finally, α-cell-derived ACh inhibits SST release from δ-cells. Drawn after (30).

Finally, δ-cells provide tonic inhibition of insulin and glucagon release from α- and β-cells. They secrete SST in response to glucose in a manner similar to glucose-stimulated insulin secretion (see Chapter 1.1.2). SST signals through somatostatin receptors (SSTR). SST prevents excess secretion of insulin and may be responsible for low glucagon secretion at high glucose levels, thereby providing important regulatory input for both α- and β-cells (30).

1.2.4. Other modulators of insulin secretion

Maintenance of glucose homeostasis involves a network of highly specialized cell types not only in the pancreas, but also within organs such as the brain, gastrointestinal tract, liver, adipose tissue, and muscle. Appropriate insulin secretion therefore requires input from these tissues.

Stimuli such as the smell or sight of food trigger the cephalic phase of insulin secretion that initiates insulin secretion before a meal. This mechanism is mediated by the autonomous nervous system via cholinergic and non-cholinergic stimulation and prepares the organism for food intake (31). Besides initiating insulin secretion, the autonomous nervous system modulates glucose-dependent insulin secretion. Pancreatic islets are highly innervated with

sympathetic and parasympathetic neurons (see Chapter 1.1.1), and neuron-derived factors, like norepinephrine and neuropeptide Y (NPY), are inhibitors while other neuropeptides such as pituitary adenylate cyclase-activating polypeptide and gastrin releasing peptide are stimulators of insulin secretion (26).

Up to 50% of insulin secretion after a meal is attributable to the incretin effect mediated by GLP-1 and GIP. These hormones are secreted in response to a mixed meal by gastrointestinal L- and K-cells, respectively. Both stimulate glucose-dependent insulin secretion by binding to their respective receptors on β-cells (GLP1R and GIPR). This initiates a signaling cascade that augments insulin secretion via increasing the insulin granule density at the plasma membrane, stimulating flux of calcium ions from internal stores into the cytoplasm, and modulating K_{ATP}-channel and calcium channel activity. Besides influencing insulin, GLP-1 inhibits, and GIP enhances glucagon release from α-cells. The gut also secretes decretins which inhibit insulin release during a fast. One of these, neuromedin U, suppresses insulin release directly in β-cells by signaling through its receptor (NmUR1) and possibly through stimulation of SST secretion (26).

Adipose tissue and muscle are highly regulated by insulin-dependent glucose uptake through GLUT4 and insulin signaling in general. In turn, adipocytes and myocytes secrete factors that modulate β-cell function underscoring the importance of inter-organ cross talk. Adipose tissue secretes the well-known hormones leptin and adiponectin that have opposite effects on insulin secretion. Leptin inhibits insulin secretion by reducing insulin gene expression and activation of K_{ATP}-channels. Adiponectin signaling, on the other hand, improves β-cell survival, insulin gene expression and secretion. Adipocytes and myocytes secrete interleukin 6 (IL-6), which influences insulin secretion indirectly via augmentation of glucagon secretion from α-cells and GLP-1 secretion from gastrointestinal L-cells (26).

1.3. Congenital hyperinsulinism of infancy

1.3.1. Definition and symptoms of CHI

CHI designates a group of genetically different disorders that are characterized by non-ketotic hypoglycemia and inappropriately elevated insulin secretion. It is a rare, inherited condition

with an incidence of 1:30,000 in northern Europe (32). However, in areas with high level of consanguinity, the incidence can rise up to 1:2,500 (33).

CHI is one of the most common causes of hypoglycemia in newborns and infants and poses a risk for the development of permanent brain damage. The condition is caused by mutations in genes that are involved in the regulation of insulin secretion and may manifest as a focal lesion or affect all β-cells within the pancreas. The symptoms range from mild to severe depending on the underlying mutation and form of CHI, making early diagnosis a necessity to prevent permanent neurological affection or even life-threatening hypoglycemia (34).

The hypoglycemia of CHI is most often transient but can also be persistent. Depending on which gene is mutated, low blood sugar levels can be elicited by fasting, protein-rich meals or exercise, or a combination of some of these. Symptoms are mostly related to the hypoglycemia and may range from increase or loss of appetite, pallor, sweating, and heart palpitations to seizures, unconsciousness, coma, and even death. Some forms of CHI present with increased birthweight (34). Moreover, some CHI forms are characterized by specific physiological defects that may aid in their diagnosis. One example is the occurrence of hyperammonemia in patients with activating mutations in *GLUD1* (35).

Besides being the hallmark of CHI, hyperinsulinemic hypoglycemia can be part of syndromes presenting with several functional and congenital anomalies. These syndromes include overgrowth disorders such as Beckwith-Wiedemann (36) and Sotos (37) syndrome, or multisystem disorders such as Kabuki (38) and Turner (39) syndrome.

1.3.2. Histological differentiation of CHI subtypes

CHI can be classified histologically into three forms: diffuse, focal and atypical CHI. The majority of CHI cases (60%) belong to the diffuse form, which affects the function and morphology of all β-cells in the pancreas (34). Focal CHI usually occurs sporadically and is caused by inheritance of a paternal loss-of-function mutation in *ABCC8* or *KCNJ11* together with somatic loss of the maternal allele (see below). This leads to proliferation of the affected β-cells and increased insulin secretion from the developing focal lesion (40). Atypical CHI does not fit the histological criteria of diffuse or focal CHI. This form is characterized by heterogeneous populations of islets. Some islets appear hyperactive with β-cells that contain large nuclei and cytoplasm, distinctive of increased hormone production, while other islets appear small and quiescent (34,41).

1.3.3. Genetic causes of CHI

Mutations in around 15 different genes have been reported to cause CHI (42), and the disease can be categorized in three groups based on the type of affected gene (Table 1; Figure 5). The first group is associated with mutations in channel and transporter proteins. This group, classically referred to as *channelopathies*, includes mutations in the genes that encode the subunits of the β-cell K_{ATP} channel, *ABCC8* and *KCNJ11*. Other channel and transporter genes implicated in CHI that can be classified as channelopathies are *CACNA1D*, *KCNQ1* and *SLC16A1* (42).

Table 1. Subgroups and molecular causes of CHI. D = autosomal dominant inheritance, R = autosomal recessive inheritance, IM = inactivating mutations, AM = activating mutations.

	Gene	Encoded protein	Inheritance	Mutation
Channelopathies	*ABCC8*	Sulfonylurea receptor-1 (SUR1)	D/R	IM
	KCNJ11	Inward rectifier K+ channel (Kir6.2)	D/R	IM
	CACNA1D	Voltage-dependent L-type calcium channel subunit alpha-1D (CACNA1D)	Sporadic	AM
	KCNQ1	potassium voltage-gated channel subfamily KQT member 1 (KvLQT1)	D	IM
	SLC16A1	Monocarboxylate transporter 1 (MCT1)	D	AM
Metabolopathies	*GCK*	Glucokinase (GCK)	D	AM
	GLUD1	Glutamate dehydrogenase (GDH)	D	AM
	HADH	Short chain L-3-hydroxyaxyl-CoA dehydrogenase (SCHAD)	R	IM
	HK1	Hexokinase (HK1)	D	AM
	PMM2	Phosphomannomutase 2 (PMM2)	R	IM
	UCP2	Mitochondrial uncoupling protein 2 (UCP2)	D	AM
Transcriptionopathies	*HNF1A*	Hepatocyte nuclear factor 1 alpha (HNF-1A)	D	IM
	HNF4A	Hepatocyte nuclear factor 4 alpha (HNF-4A)	D	IM
	FOXA2	Forkhead box A2 (FOXA2)	Sporadic	IM

The second group are the *metabolopathies*. The regulation of insulin secretion depends on nutrient sensing and tight control of nutrient flux. Therefore, mutations that perturb the normal regulatory framework of β-cell metabolism may stimulate insulin secretion under inappropriate conditions such as hypoglycemia. The most well-established genes in this group are *GCK*, *GLUD1* and *HADH*. Other members are *HK1*, *PMM2* and *UCP2*. The *HADH* gene and its CHI-causing mutations are the main focus of this thesis and will be discussed in detail in Chapter 1.4.

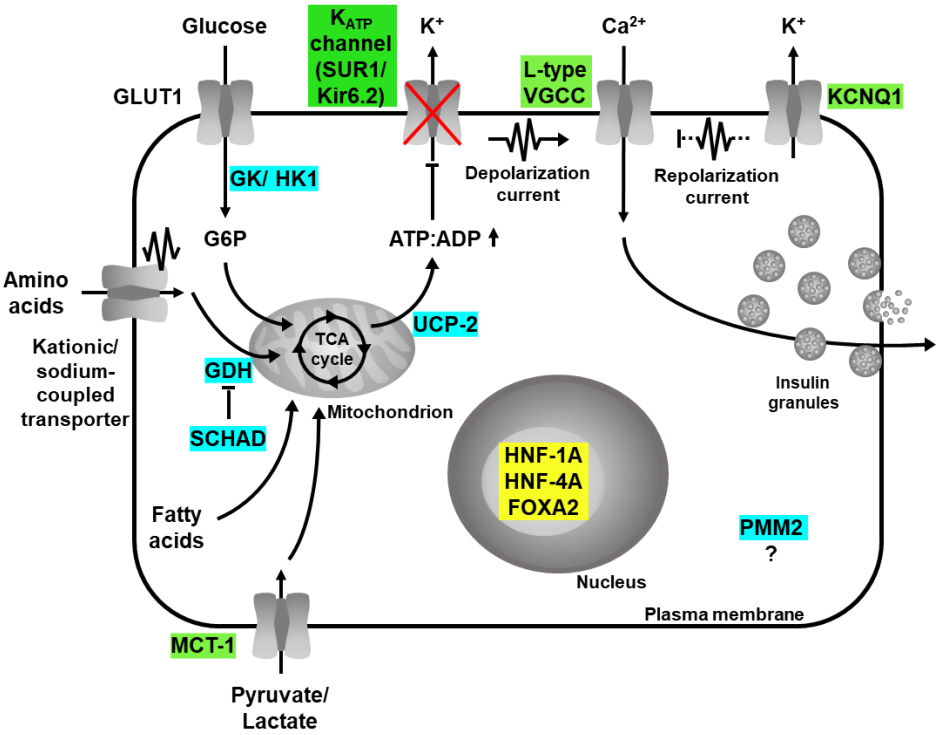

Figure 5. CHI-associated genes and their location in β-cell insulin secretion. Channelopathies are indicated in green, metabolopathies in blue and transcriptionopathies in yellow color. *Channelopathies* alter the transport of ions or metabolites across the β-cell plasma membrane. These are caused by mutations in the β-cell K_{ATP} channel subunits SUR1 and Kir6.2 L-type voltage-dependent Ca^{2+} channel (VGCC), the potassium voltage-gated channel subfamily KQT member 1 subunit of an inwardly rectifying K+ channel (Kir7.1.) and inappropriate expression of monocarboxylate transporter 1 (MCT-1). *Metabolopathies* increase insulin secretion by altering β-cell metabolism. These are caused by mutations in glutamate dehydrogenase (GDH), glucokinase (GK), inappropriate expression of hexokinase 1 (HK1) and inactivating mutations of short-chain hydroxyacyl-CoA dehydrogenase (SCHAD), uncoupling protein 2 (UCP-2) and phosphomannomutase 2 (PMM2). *Transcriptionopathies* includes transcription factors that regulate expression of genes important for β-cell metabolism. These genes are hepatocyte nuclear factor 1 and 4-alpha (HNF-1A, HNF-4A) and Forkhead box A2 (FOXA2).

The last and smallest group is characterized by mutations in transcription factors. Mutations in these genes affect β-cell metabolism due to altered transcriptional regulation. This group presently includes the *HNF-1A*, *HNF-4A* and *FOXA2* genes (42). As mentioned above, for the first two CHI groups, the umbrella terms "channelopathy" and "metabolopathy" are used to describe unifying characteristics of their associated gene mutations and their influence on β-cell biology. Since the common feature of the third CHI form is dysregulation caused by altered transcription factor activity, we propose to use the term "transcriptionopathy" to refer

to this subgroup. In the following subchapters, we will discuss the genetic etiology of CHI caused by channelopathies, metabolopathies, and transcriptionopathies.

1.3.4. Channelopathies

ABCC8/ KCNJ11

The most common and often most severe form of CHI is caused by mutations of the β-cell K_{ATP} channel. The channel is a hetero-octamer formed by assembly of four subunits of sulfonylurea receptor-1 (SUR1) and four subunits of the inwardly rectifying potassium channel (KIR6.2) which are encoded by the genes *ABCC8* and *KCNJ11*, respectively. The K_{ATP} channel plays a central role in the insulin secretion pathway (Figure 3) where it connects the energy state of the β-cell to insulin release by depolarization of the cell membrane, which subsequently activates voltage-gated calcium channels. Mutations in *ABCC8* and *KCNJ11* that perturb functional cell membrane expression of the K_{ATP} channel therefore lead to increased or continuous depolarization of the β-cell plasma membrane with subsequent stimulation of insulin release (42).

Several types of these mutations in *ABCC8* and *KCNJ11* have been described:

a) Recessive inactivating mutations that increase the turnover rate of SUR1 and KIR6.2, leading to complete absence of the K_{ATP} channel on the β-cell membrane in homozygous or compound heterozygous carriers (43). This is the most common subtype.
b) Recessive mutations that disrupt trafficking of SUR1 and Kir6.2 (44).
c) Recessive mutations that reduce K_{ATP} channel sensitivity to ADP, thereby allowing for ATP-mediated closure of the channel at lower ATP:ADP ratio (45).
d) Dominant inactivating mutations leading to reduced function of the K_{ATP} channel. These mutations usually cause the mildest form of K_{ATP} channel-CHI and sometimes transition to a diabetic phenotype later in life (46). This is a very rare subtype.
e) Focal CHI (described below)

ABCC8 and less often *KCNJ11* mutations also underlie the development of focal CHI. Focal CHI develops in response to multiple hits affecting the expression of K_{ATP} channel as well as multiple genes involved in cell proliferation. The first hit is paternal inheritance of a mutation in *ABCC8* or *KCNJ11* on chromosome 11. The second hit is somatic loss of the maternal region encompassing the K_{ATP} channel gene and multiple imprinted genes involved in cell

proliferation (*CDKN1C*, *IGF-II* and H19*)*. The maternally expressed genes *CDKN1C* and *H19* are inhibitors of cell proliferation, while the paternally expressed *IGF-II* promotes cell growth. Loss of the maternal segment thus causes imbalance in the regulation of cell proliferation leading to focal hyperplasia. Lastly, duplication of the paternal segment of chromosome 11 leads to isodisomy and homozygosity of the mutant K_{ATP} gene leading to dysregulated insulin secretion from the developing lesion (47).

CACNA1D

CACNA1D encodes the subunit alpha-1D of an L-type voltage-dependent Ca^{2+} channel (VGCC). Activating mutations in the gene are rare but have been described to force the channel into an open configuration at lower than normal membrane potential, leading to increased influx of Ca^{2+} ions and subsequent insulin secretion. Additionally, patients with activating mutations suffer from neuromuscular abnormalities, primary hyperaldosteronism, heart defects, and hypotonia (42,48).

KCNQ1

KCNQ1 encodes potassium voltage-gated channel subfamily KQT member 1 (Kir7.1), the pore-forming subunit of a potassium channel that mediates voltage-gated repolarization of the plasma membrane. *KCNQ1* is expressed in cardiomyocytes, pancreatic β-cells, cells of the inner ear and in the gastrointestinal track. Loss-of-function mutations in *KCNQ1* are associated with long QT syndrome, a group of conditions characterized by heart arrythmias caused by defective myocellular repolarization, syncope, deafness and sudden death (49). *KCNQ1* is also expressed on β-cells and mutations have been linked to postprandial hyperinsulinemic hypoglycemia most likely due to prolonged depolarization of the β-cell membrane (50).

SLC16A1

SLC16A1 encodes the monocarboxylate transporter 1 (MCT-1), which transports pyruvate and lactate into cells. MCT-1 expression, and therefore pyruvate and lactate levels, are low in β-cells. Normally, this prevents excessive ATP production and subsequent stimulation of insulin secretion during and after exercise, i.e. when blood levels of lactate are high. Dominant activating mutations in the promoter of *SLC16A1* disrupt this regulation by causing overexpression of the transporter protein in the β-cells. This causes an excessive influx of the metabolites, especially after strenuous exercise, leading to inappropriately high insulin

secretion stimulated by pyruvate metabolism (42,51). This form of CHI has also been classified as exercise-induced hyperinsulinism.

1.3.5. Metabolopathies

GLUD1

Dominant, activating mutations in *GLUD1* cause the hyperinsulinism/hyperammonemia syndrome, the second most common form CHI (35). *GLUD1* encodes the mitochondrial enzyme glutamate dehydrogenase (GDH) which is expressed at high levels in the pancreas, liver, kidney, and brain. The enzyme catalyzes the reversible conversion of glutamate to α-ketoglutarate and ammonia using NAD^+ or $NADP^+$ as co-enzymes. GDH activity is modulated by allosteric inhibitors such as GTP and ATP and activators such as leucine and ADP (52). CHI-causing mutations in *GLUD1* most commonly affect the sensitivity of GDH to its inhibitor GTP and lead to increased activity of the enzyme (53,54). In the β-cell, this is thought to lead to increased insulin secretion either through increased production of α-ketoglutarate which is then metabolized in the citric acid cycle to produce ATP or through increased production of glutamate which amplifies insulin secretion after uptake into insulin granules (55,56).

The phenotype of GDH-CHI is usually milder compared with the disease caused by K_{ATP} mutations. Characteristic features are fasting-induced hypoglycemia and protein sensitivity due to the stimulatory effect of leucine on GDH activity. Besides the hyperinsulinism phenotype, a hallmark of GDH-CHI is hyperammonemia (usually asymptomatic) due to increased GDH activity in the kidney (57). This phenotype is unique amongst CHI conditions and may aid in the diagnosis of GDH-CHI. Some forms of GDH-CHI are also associated with epilepsy and developmental delay (35).

GCK

Glucokinase (GK), also known as hexokinase 4, is expressed by the *GCK* gene. As stated in Chapter 2.1, it functions as the β-cell glucose sensor by linking plasma glucose levels to ATP production to insulin release (23). Due to GK playing such a central role in the insulin secretion pathway, β-cells are highly sensitive to changes in its activity. Mutations that reduce GK activity cause chronic mildly elevated glucose (GCK-MODY or MODY2) (58). On the other hand, mutations that increase the affinity of the enzyme to glucose, mostly by altering its

allosteric activator domain, cause CHI. Here, glucokinase is active at lower than normal glucose concentrations, causing inappropriate insulin secretion (59).

HK1

Similar to GK, hexokinase 1 (HK1) belongs to the hexokinase superfamily and catalyzes the phosphorylation of glucose to G6P. Unlike GK, the affinity for glucose remains high in low glucose conditions for HK1. Therefore, expression of HK1 when glucose is scarce is disadvantageous in β-cells since it would allow for the stimulation of insulin secretion under unfavorable conditions. The β-cell thus has evolved to suppress expression of HK1 when glucose levels are low (60). Dominant mutations in the non-coding region of the *HK1* gene may override the glucose-associated gene silencing at low glucose levels, allowing for inappropriate HK1 expression and stimulation of the insulin secretion pathway (61).

PMM2

Phosphomannomutase 2 is encoded by the *PMM2* gene. It is involved in glycoprotein synthesis, thereby enhancing stability of its target proteins. Homozygous, recessive loss-of-function mutations in *PMM2* cause congenital disorder of glycosylation (CDG), a complex disorder of varying severity and with a wide spectrum of symptoms related to glycosylation defects (62). Some forms of this condition (CDG type 1b and less often CDG type 1a and 1d), have been linked to diazoxide-responsive hyperinsulinemic hypoglycemia. The exact mechanism behind CHI in patients with CDG is still unclear, and hypoglycemia in CGD type 1a may also occur in the absence of hyperinsulinism (63).

UCP2

Inactivating mutations in *UCP2* are associated with CHI of varying severity. *UCP2* encodes mitochondrial uncoupling protein 2 (UCP-2), a member of the inner mitochondrial anion-carrier family. The protein plays a role in uncoupling of oxidative phosphorylation from ATP production. Loss of *UCP2* expression in β-cells leads to an increase in ATP production from glucose metabolism, followed by closure of K_{ATP} channels and subsequent insulin release (64).

1.3.6. "Transcriptionopathies"

HNF1A* and *HNF4A

Hepatocyte nuclear factor 1-alpha (HNF-1A) and hepatocyte nuclear factor 4-alpha (HNF-4A) are transcription factors of the nuclear receptor superfamily that control gene expression in several organs, including the liver and pancreatic islet (65). Amongst the regulated targets are genes involved in glucose-stimulated insulin secretion, such as *KCNJ11* (66,67). Heterozygous inactivating mutations in *HNF1A* or *HNF4A* in humans can sometimes result in macrosomia and transient, mild and diazoxide-responsive CHI in newborns, although this phenotype always transforms into MODY3 and MODY1, respectively, later in life (66,68).

FOXA2

Forkhead box A2 (FOXA2) is a transcription factor involved in the development of endoderm-derived tissues. In the pancreas, FOXA2 expression is necessary for normal organ development, due to its role in controlling PDX1 and other transcription factors that regulate differentiation of α- and β-cells (69,70). In the mouse, inactivating mutations in the *Foxa2* gene result in low numbers of α-cells and disproportionally large number of β-cells. Furthermore, FOXA2 also regulates expression of other CHI-associated genes, such as *ABCC8*, *KCNJ11* and *HADH* (71) which are down-regulated in patients with mutant *FOXA2* (72). The clinical phenotype of patients with *FOXA2* mutations has been described to include hyperinsulinemic hypoglycemia, congenital hypopituitarism, as well as craniofacial dysmorphism and developmental defects in the brain (pituitary, corpus callosum), liver, lung, gastrointestinal tract (72,73).

1.3.7. Diagnosis and treatment of CHI

Hypoglycemia with detectable plasma insulin and C-peptide is the hallmark of CHI. The exact definition of which level of plasma glucose is hypoglycemia has been widely debated, but the most common plasma glucose levels to define hypoglycemia are ≤ 50 mg/dL (2.8 mmol/L) or ≤ 45 mg/dL (2.5 mmol/L). It is not unusual for insulin and C-peptide to be low or undetectable in neonates and infants, and the severity of hypoglycemia does not correlate with measured blood insulin levels (74,75). Moreover, transient hypoglycemia in neonates is very common, and the severity and persistence of hypoglycemia will alert the caring physician to suspect CHI. Other markers may aid in the diagnosis of CHI. These include reduced plasma levels of

fatty acids and ketone bodies during hypoglycemia, and an increased glucose infusion requirement to maintain normoglycemia (76).

Hypoglycemia in neonates with CHI is often severe and puts the child at risk for irreversible brain damage. The first measure, therefore, is to stabilize blood glucose levels by administration of glucagon and glucose. Besides improving blood glucose levels, both measures aid in the diagnosis of CHI if they have the desired positive effect on the patient's condition. An elevated glucose infusion requirement above around 10 mg/kg/min to maintain normoglycemia is indicative of hyperinsulinism (77). Glucagon raises blood glucose levels by stimulating hepatic glucose output. Conditions such as glycogen storage disease (GSD) affect glycogen metabolism and impair hepatic glucose output, leading to hypoglycemia and rendering glucagon ineffective (78). A spike in blood glucose levels after glucagon administration thus rules out GSD. It supports the diagnosis CHI and is effective for treating the hypoglycemia (77).

Genetic screening can identify the mutant gene in the patient and family members who might be carriers. This facilitates the development of a treatment plan and helps reach a prognosis for the patient and possible future siblings. Some specific forms of CHI may also be identified due to phenotypical characteristics such as protein sensitivity and hyperammonemia in GDH-CHI, protein sensitivity and increased levels of 3-hydroxybutyryl-carnitine in blood and 3-hydroxyglutaric acid in urine in SCHAD-CHI, and exercise sensitivity in MCT1-CHI (42). Macrosomia is a common feature in CHI caused by mutations in genes such as *HNF1A* and *HNF4A* (79), as well as *ABCC8* (80). This phenotype most likely reflects the growth-promoting effects of increased insulin levels *in utero* and shortly after birth (81). However, macrosomia does not occur in all cases of CHI caused by mutations in these genes, and other forms of CHI, such as SCHAD-CHI (82), are not necessarily associated with increased birthweight. Thus, although macrosomia may aid in the diagnostic work-up of CHI, normal or low birthweight is not an exclusion criterion for this diagnosis.

Once the diagnosis of CHI is established, it needs to be determined whether the patient is presenting with focal or diffuse CHI. Focal CHI can be detected by ^{18}F-fluoro-L-dihydroxyphenylalanine (F-DOPA) PET scanning. This is a highly sensitive and accurate method for visualization of focal lesions due to enhanced uptake of F-DOPA by overactive compared to healthy β-cells (34). Patients with focal CHI are often unresponsive to drug-mediated suppression of insulin secretion. However, in these patients surgical resection of the

focal lesion is a viable option, leading to a cure for the condition in most patients (77). The most effective way to determine whether F-DOPA PET scanning should be investigated or not, is to make a genetic diagnosis. If homozygous or compound heterozygous mutations in *ABCC8* or *KCNJ11* are present, a diffuse CHI is present and a F-DOPA PET is not indicated. If a paternal heterozygous mutation in *ABCC8* or *KCNJ11* is present, a F-DOPA PET is indicated if the condition is severe (i.e. injection medical treatment is necessary to maintain stable glucose levels). If a maternal heterozygous mutation in *ABCC8* or *KCNJ11* is present, a focal lesion is less likely although many pediatricians will still order a F-DOPA PET to rule out a focal subtype.

The long-term treatment of CHI depends on the underlying mutation and severity of the disease. It usually involves medical intervention aimed to lower insulin secretion. The first approach is administration of the oral drug diazoxide. Diazoxide is a K_{ATP} channel activator ("channel opener") that binds to the SUR1 subunits of the β-cell K_{ATP} channel. Unfortunately, patients with mutations that affect the function or expression of SUR1 or Kir6.2 tend to be unresponsive to the drug. The next-in-line option for treatment of diazoxide unresponsive CHI are somatostatin analogues such as octreotide. These compounds inhibit insulin secretion by signaling through somatostatin receptors. Octreotide must be administered by injection, three times a day or via an insulin pump, due to the short half-life of the drug. Long-acting analogues are also available, which can be administered by an injection every 4-6 weeks. Other treatments that may be beneficial in the management of CHI are the immunosuppressant sirolimus and dietary changes. Continuous feeding with long-branched sugars is a crucial part of the treatment in addition to or without treatment with drugs. In addition, uncooked corn starch or ketogenic diet are sometimes used (34,83).

Surgery may be a last resort treatment for severe, drug-unresponsive diffuse CHI. Here, more than 95% of the pancreas will be removed, dramatically reducing the number of β-cells. While this procedure may improve glycemic control in some patients, many patients still experience hypoglycemia, while nearly all develop diabetes during or after puberty.

1.3.8. Mouse models of CHI

CHI-causing mutations alter the function or expression of genes involved in the regulation of insulin secretion. Consequently, studying the mechanisms behind the defects caused by these mutations offers unique insights into β-cell biology in health and disease. Mouse models are

an invaluable tool in this process. Thus, several transgenic and knockout (KO) mice have been developed for different CHI subgroups (Table 2). Some of these models such as overexpression of *Slc16a1* and whole-body KO of *Hadh* capture aspects of the human phenotype quite well. Like humans, mice with *Slc16a1* overexpression develop exercise-induced CHI and both humans and mice with disrupted *HADH* gene have elevated levels of plasma 3-hydroxybutyrylcarnitine and urinary 3-hydroxyglutarate (84,85).

Partial loss of one of the K_{ATP} channel genes, *Abcc8* or *Kcnj11*, accurately mimics the human phenotype of K_{ATP} channel mutations. In mice, this has been achieved by heterozygous KO of either gene, or β-cell-specific expression of dominant negative Kir6.2 (Kir6.2[AAA] or G132S point mutation). The full loss of either *Abcc8* or *Kcnj11* on the other hand does not cause a clear hyperinsulinism phenotype. Instead *Abcc8* KO and *Kcnj11* KO mice are characterized by impaired insulin secretion (86,87,96,97,88–95).

It may be possible that some K_{ATP}-channel function is necessary for a hyperinsulinism phenotype. In many humans with *ABCC8* or *KCNJ11* mutations, residual K_{ATP} channel expression is observed (45,98). Heterozygous KO of *Abcc8* or *Kcnj11,* and expression of Kir6.2[AAA] result in a reduction in K_{ATP} channel expression of ~60% and ~70%, respectively. Therefore, these mice might be a more accurate model for the human condition than the homozygous *Abcc8* or *Kcnj11* KO mice.

Moreover, some patients with K_{ATP}-channel mutations eventually develop diabetes, a phenotype seen in mice with the G132S point mutation in *Kcnj11* (71,72,80). These mice are hyperinsulinemic in youth but become diabetic in adulthood and may thus serve as a model for the study of the progression from K_{ATP}-channel-CHI to diabetes.

For some forms of CHI, mouse models exist, but no hyperinsulinemic phenotype has been described. This includes KO and transgenic models of *Kcnq1* and *Hnf1a* KO mice. *Kcnq1* KO animals mirror the human phenotype of long QT syndrome. No hyperinsulinism, but a decrease in plasma insulin and glucose levels has been reported. However, these mice had been published before the association of *Kcnq1* mutations with CHI was discovered (2001 and 2009 vs. 2014) (50,100,101). Therefore, a hyperinsulinism phenotype may have been missed since no other hyperinsulinism markers (e.g. plasma fatty acid and ketone body levels) were investigated.

Table 2. Published mouse models of CHI and their reported phenotypes. NA = no information available

	Channelopathies			
	Genetic alteration	**Targeted tissue**	**Mouse strain**	**Phenotype**
Abcc8	KO	Whole body	Mixed (C57Bl/6 and 129/SvJ) (90)	• Transient neonatal hypoglycemia • No first phase and reduced second phase insulin secretion • Fasting hypoglycemia in adults • Mild glucose intolerance
	KO	Whole body	Mixed (C57Bl/6 and 129/SvJ) Pure C57Bl/6 (91–93)	• Impaired GSIS • Impaired incretin response (GLP-1) • Normal insulin secretion after feeding • Impaired hypoglycemia- and arginine-induced glucagon secretion • β-cell dedifferentiation
	Knock-in of mouse equivalent of the human CHI-causing SUR1-E1506K mutation	Whole body	C57Bl/6 (102)	• Hyperinsulinemic hypoglycemia in young mice • Impaired insulin secretion and glucose intolerance by 6 months of age • Reduced β-cell insulin content at 6 months of age
Kcnj11	KO	Whole body	Outbred (94,95)	• Impaired GSIS • Improved insulin sensitivity • Mild glucose intolerance • Altered islet architecture • Hyperglycemia in aged animals • Increased bodyweight in aged animals
	Expression of dominant-negative, GFP-tagged Kir6.2 (Kir6.2[AAA]) under control of rat insulin 1 promoter	β-cell	C57Bl/6 or mixed C57Bl/6 and CD-1 (86,87)	• ~70% loss of Kir6.2 expression • Hyperinsulinism • Increased GSIS • Increased glucose tolerance
	Expression of dominant-negative Kir6.2 mutation (G132S) under control of the human insulin promoter	β-cell	C57Bl/6 (88,89)	• Hyperinsulinemic hypoglycemia in neonates • Hypoinsulinemic hyperglycemia in adults • Loss of β-cells in adults • Spontaneous recovery of β-cells and hyperglycemic phenotype in older animals (>25-week-old mice)

	Loss of Kir6.2 due to homozygous *Kcnj11*^{Y12STOP}	Whole body	Mixed (96)	• Impaired glucose tolerance • Increased insulin sensitivity • Reduced GSIS • Reduced incretin response (GLP-1 and GIP) • Increased basal insulin secretion from islets • Reduced islet insulin content
Abcc8/ Kcnj11	Heterozygous KO of *Abcc8* or *Kcnj11*	Whole body	C57Bl/6 (97)	• ~60% loss of Sur1 or Kir6.2 expression • Enhanced glucose tolerance and GSIS • Hyperinsulinism
Slc16a1	Doxycycline-inducible overexpression of MCT-1 using RIPrtTA	β-cell	C57Bl/6 (84)	• Hypoglycemia • Pyruvate sensitive insulin secretion • Exercise-induced hyperinsulinism
Kcnq1	KO	Whole body	Pure C57Bl/6 or mixed with 129/Sv (100,101)	• No hyperinsulinism described • Deafness • Shaker/waltzer phenotype (hyperactivity, head bobbing, circling) • Abnormal inner ear structure • Long QT syndrome • Increased insulin sensitivity • Improved glucose tolerance • Reduced fed and fasting plasma glucose and insulin
	Metabolopathies			
	Genetic alteration	**Targeted tissue**	**Mouse strain**	**Phenotype**
Glud1	Expression of human wild-type and H454Y mutant GDH under control of rat insulin promoter	β-cell	C57/Bl6 (103,104)	• Severe hypoglycemia • Reduced survival • Increased amino acid stimulated insulin secretion • Reduced GSIS • Hypoglucagonemia
Gck	Overexpression of Gck	Whole body	B6D2 hybrid (105,106)	• Hypoglycemia due to increased hepatic glucose uptake • Lower plasma glucose and insulin after HFD

	Overexpression of yeast hexokinase B	β-cell	ICR (107)	• Hyperinsulinemic hypoglycemia • Increased GSIS
Hadh	KO	Whole body	Mixed C57Bl/6 and Sv129/J (85)	• Hypoglycemic hyperinsulinism • Increased amino acid stimulated insulin secretion • Increased plasma 3-hydroxybutyrylcarnitine • Increased urinary 3-hydroxyglutarate
Ucp2	KO	Whole body	C57Bl/6 (108,109)	• Hyperinsulinemic hypoglycemia • Improved insulin secretion after high fat diet
	Transcriptionopathies			
	Genetic alteration	**Targeted tissue**	**Mouse strain**	**Phenotype**
Hnf1a	KO	Whole body	Possibly 129/Sv (110)	• No hyperinsulinism described • Failure to thrive and progressive wasting • Death around weaning • Liver enlargement • Phenylketonuria • Renal Fanconi syndrome
	EIIa-cre mediated KO	Whole body	Mixed C57Bl/6 and 129X1/SvJ (111–113)	• No hyperinsulinism described • Sterile • Laron-type dwarfism • Type 2 diabetes • No increase in mortality • Mild renal dysfunction • Hypercholesterolemia
Hnf4a	*Rip*-cre mediated KO	β-cells	CD1 (66)	• Hyperinsulinism • Impaired glucose tolerance • Impaired first-phase insulin secretion • Reduced β-cell expression of *Kcnj11*
	Rip-cre mediated KO	β-cells	Mixed C57Bl/6 and 129/SvJ (67)	• Impaired sulfonylurea and glucose stimulated insulin secretion • No hyperinsulinemic hypoglycemia • No diabetes by 6 months of age

				• Normal β-cell expression of *Abcc8* and *Kcnj11*
Foxa2	*Rip*-cre mediated KO	β-cells	NA (71,114)	• Severe glucose and amino acid sensitive hyperinsulinemic hypoglycemia • Growth retardation • Postnatal death • Altered islet architecture • Reduced β-cell expression of *Abcc8*, *Kcnj11* and *Hadh*
	Pdx1-cre mediated KO	*Pdx1* expressing cells	NA (115)	• α/β-cell ratio imbalance • Hypoglucagonemia • Hyperinsulinemic hypoglycemia

Mice harboring human long QT syndrome-causing point mutations in *Kcnq1* have also been described (116,117). Again, no hyperinsulinism was reported, but the mutations (T312I, A341V, A341E, and V207M) also differed from the mutations found in patients with long QT syndrome and hyperinsulinism (H363N, R366W, R401P, and Q530X) (50).

Two homozygous *Hnf1a* KO mice have been published. Both models have a complex phenotype including impaired growth, renal and liver abnormalities, and type 2 diabetes (110,111). One of the models, developed by Pontoglio et al. (110), was more severely impacted and showed increased mortality after weaning. The other model, developed by Lee et al. (111–113), did not show increased mortality. Hyperinsulinism was not reported for either model. Pontoglio et al. did not report insulin levels for their mouse, while Lee et al. stated that their mice were diabetic starting at 2 weeks of age and at 5 weeks plasma insulin levels were reduced compared to heterozygote KO mice. Overall, these mice are unlikely to reproduce the phenotype of *Hnf1a*-CHI. Instead these mice are diabetic and harbor some defects associated with *Hnf4*a-CHI, such as renal Fanconi syndrome. These findings may be explained by species differences. Alternatively, patients with *HNF1A* mutations may have some residual *HNF1A* expression and the full KO, like the full KO of K_{ATP} genes, results in a different phenotype characterized primarily by diabetes instead of CHI.

Lastly, many studies aimed to target expression of CHI-associated genes specifically in the pancreas or β-cells. For this endeavor *Pdx*-cre or *Rip*-cre transgenic mice have been used, respectively (118,119). However, we now know that these models introduced changes to the β-cell that could influence results significantly. These transgenic mice express Cre-recombinase under the control of the *Pdx* or rat insulin promoter (*Rip*). The constructs used to generate these animals included the human growth hormone (hGH) minigene to enhance the expression of Cre-recombinase. It was assumed that the hGH would not be expressed. However, in 2014 Brouwers et al. not only reported evidence for hGH expression in β-cells of these transgenic mice, but also that the expression of hGH altered β-cell function (120). This included pregnancy-like changes to β-cell mass and impaired GSIS. Interestingly, *Rip*-cre was used to generate β-cell specific *Hnf4a* KO mice by two separate groups (66,67). These mice were meant to serve as a model for MODY1, a condition that often presents with CHI in youth and transitions to a diabetic phenotype later in life (68). Even though both groups succeeded in generating the KO, the phenotypes of their mice were strikingly different. Gupta et al. reported a CHI phenotype for their mouse line (66), while the mouse generated by Miura et al. showed

impaired GSIS (67). This disparity may be explained by different genetic background of the two mouse lines (CD1 vs. mixed 129 Svj and C57BL/6), which could affect the phenotype directly or via different susceptibility for hGH expression. The latter may explain the reduced GSIS observed by Miura et al.

Fortunately, newer models for selective targeting of β-cells exist that do not include the hGH transgene. One such model is the *Ins1*-cre mouse model that uses the endogenous *Ins1* promoter for expression of Cre-recombinase (121). While this model reduces expression of the *Ins1* gene, insulin protein levels, insulin secretion and overall glucose homeostasis were not affected (121). This model therefore offers a more reliable approach for the study of β-cell function when beta-cell-specific KO of the gene in question is needed.

Overall, more than twenty models for eleven types of CHI have been developed and described. While some have been more successful in replicating the human condition, others have resulted in unexpected challenges. Ultimately, these models have substantially increased our understanding of the regulation of insulin secretion and the development and progression of CHI.

1.4. Short-Chain 3-Hydroxyacyl-CoA Dehydrogenase (SCHAD)

1.4.1. SCHAD gene and protein

Short-chain 3-hydroxyacyl-CoA dehydrogenase (SCHAD) is encoded by the hydroxyacyl-CoA dehydrogenase (*HADH*) gene located on chromosome 4q22-26. This gene contains nine exons and several predicted transcripts that are produced by alternative splicing, most of which have not been characterized. The best characterized transcript (NM_005327.7) does not include exon 7 and thus expresses 8 of the 9 exons (Figure 6A). The transcript has a length of 1803 base pairs. Translation produces a protein of 314 amino acids (aa) with a predicted molecular mass of ~34 kDa (Figure 6B).

The 314 aa monomer comprises three domains (Figure 6B,C). The N-terminus contains a mitochondrial import signal (MIS) of 12 amino acids length that is cleaved upon entry into the mitochondrion resulting in the mature protein product of ~34 kDa molecular mass. The protein contains an N-terminal NAD^+-binding domain spanning amino acids 12 – 201 connected via a

short and flexible linker region to a highly conserved C-terminal dimerization domain formed by residues 207 – 302 (122).

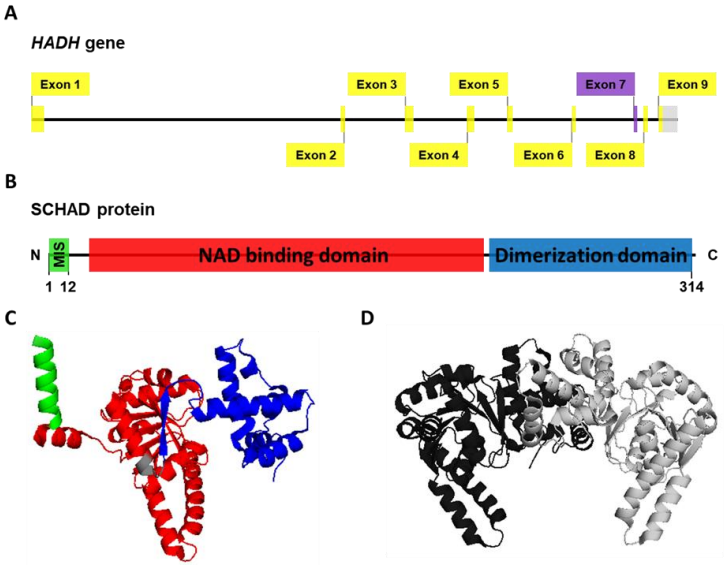

Figure 6. SCHAD gene and protein structure. A Schematic representation of the coding exons of the *HADH* gene**.** Exons expressed in the transcript NM_005327.7 are indicated in yellow. Exon 7, which is not included in this transcript is indicated in purple. **B** Schematic representation of the SCHAD protein. The SCHAD monomer has a total length of 314 aa. The N-terminal contains a mitochondrial import signal (MIS, green), followed by an NAD^+- binding domain (red) and a C-terminal dimerization domain (blue). **C** 3-dimensional model of SCHAD monomer. The MIS is indicated in green, NAD^+-binding domain in red and dimerization domain in blue color. The short linker region connecting NAD^+-binding with dimerization domain is indicated in grey. **D** 3D model of SCHAD homodimer. Individual monomers are indicated in black and grey color. 3-dimensional models were adapted from the SCHAD molecular model 3RQS obtained from the Protein Data Bank (PDB) using PyMol software. (http://www.rcsb.org/structure/3RQS).

SCHAD forms homodimers through hydrophobic interactions of α-helices within the C-terminal dimerization domains of the interacting monomers (Figure 6D). Formation of the homodimer is crucial for protein stability (123). The enzyme catalyzes the penultimate step of the fatty acid β-oxidation pathway which encompasses the conversion of 3-hydroxyacyl-CoA to 3-ketoacyl-CoA using NAD^+ as cofactor. The N-terminal NAD^+-binding domain is responsible for these catalytic functions. It is structurally composed of a β-α-β fold and contains an active site with a highly conserved His-Glu pair which functions as the catalytic domain and is responsible for cofactor (NAD^+) and substrate binding. Upon binding of NAD^+, affinity of SCHAD to its substrate increases. Binding of substrate to the active site then leads to deprotonation of the substrate by the histidine residue which acquires a positive charge that is subsequently neutralized by the adjacent glutamate residue (124).

1.4.2. The role of SCHAD in fatty acid β-oxidation

Fatty acid β-oxidation is the part of fatty acid oxidation (FAO) that takes place in the mitochondria. It is the major catabolic pathway of fatty acids and the main source of energy for some organs (kidney, heart, skeletal muscle) as well as an important source of energy in low glucose conditions throughout the body (125).

Long-chain fatty acids are imported into the mitochondria through the carnitine shuttle in the form of fatty acid acyl-CoA. Short- and medium-chain fatty acids enter the mitochondria through diffusion after which they are converted to fatty acid acyl-CoA (126). β-oxidation involves four enzymatic reactions that shorten fatty acid acyl-CoA by two carbon atoms to form acetyl-CoA which feeds into the TCA cycle for energy production or into ketogenesis for ketone body formation (Figure 7).

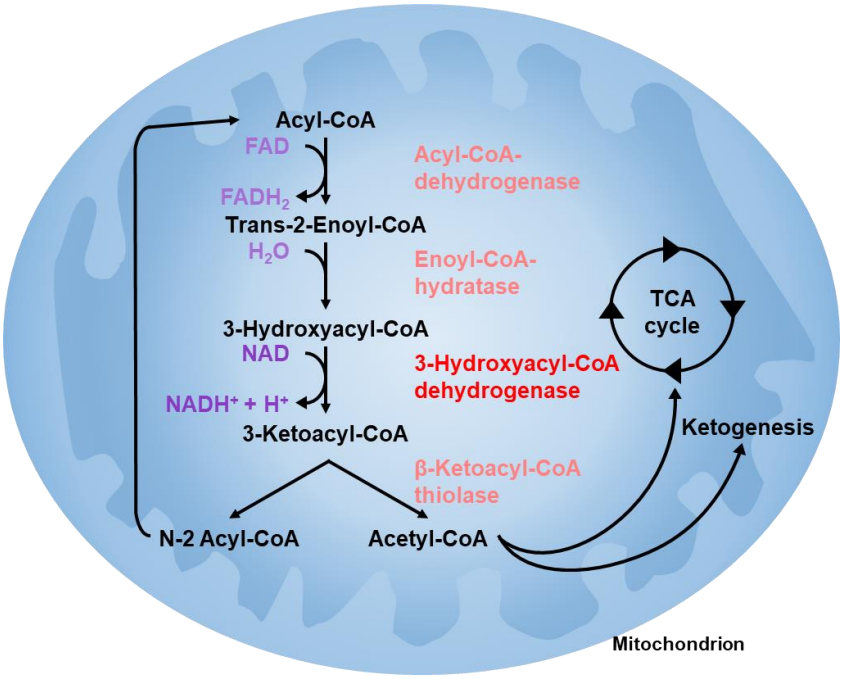

Figure 7. The fatty acid β-oxidation pathway. Enzymes are indicated in red and co-factors in purple. Fatty acid β-oxidation is a four-step process carried out by different enzymes specialized for different lengths of acyl-CoA degradation intermediates. SCHAD, a 3-hydroxyacyl-CoA dehydrogenase, carries out the penultimate step, i.e. the conversion of short- and medium-chain 3-hydroxyacyl-CoA to 3-ketoacyl-CoA. This reaction also requires the reduction of the co-factor NAD^+ to NADH. Drawn after (124).

In the first step, fatty acid acyl-CoA undergoes dehydrogenation to *trans*-2-enoyl-CoA by an acyl-CoA dehydrogenase. The acyl-CoA dehydrogenase in this reaction depends on the length of the fatty acid acyl-CoA molecule. Thus, the reaction is carried out by very-long chain (VLCAD), medium-chain (MCAD), or short-chain (SCAD) acyl-CoA dehydrogenase. Mice additionally rely on long-chain acyl CoA dehydrogenase (LCAD). The dehydrogenation of fatty acid acyl-CoA requires the reduction of FAD, which yields $FADH_2$ and is subsequently used as substrate in the respiratory chain (125).

The three last steps of β-oxidation are either carried out by mitochondrial trifunctional protein (MCP) located on the inner mitochondrial membrane or by separate enzymes within the mitochondrial matrix. MCP has affinity for long chain intermediates of fatty acid acyl-CoA while the other enzymes specialize on conversion of short- and medium- chain intermediates. Since SCHAD has affinity for short- and medium-chain intermediates, we will focus on degradation of these intermediates in the next paragraph.

Following dehydrogenation of fatty acid acyl-CoA, *trans*-2-enoyl-CoA is hydrated to 3-hydroxyacyl-CoA by the short-chain enoyl-COA hydratase, crotonase. 3-hydroxyacyl-CoA is subsequently dehydrogenated to 3-ketoacyl-CoA by SCHAD. This reaction requires the co-factor NAD^+ which is reduced to NADH and subsequently feeds into the respiratory chain. The last step in fatty acid β-oxidation is carried out by medium-chain β-ketoacyl-CoA thiolase, which cleaves 3-ketoacyl-CoA into acetyl-CoA and an acyl-CoA that has been shortened by two carbon atoms (N-2 acyl-COA). The shortened fatty acid acyl-CoA then re-enters in step 1 of the β-oxidation pathway until the final cycle, where there are two acetyl-CoA produced (125).

1.4.3. The discovery and phenotype of SCHAD-CHI

SCHAD was first associated with CHI by Clayton et al in 2001 (127). The authors described a female patient from a non-consanguineous family who presented with diazoxide-responsive hypoketotic hypoglycemia. Surprisingly, the patient also had elevated plasma hydroxybutyryl-carnitine levels that indicated a possible defect in fatty acid metabolism. Indeed, when the authors investigated the activity of FAO enzymes in fibroblasts of the patient and healthy controls, they found that activity of SCHAD was reduced to 35 – 40% of that of the control samples. This residual activity could be due to peroxisomal enzymes instead of reflecting residual SCHAD activity since further experiments showed a near lack of SCHAD protein

expression in fibroblasts of the patient. In line with this, enzyme activity was even further reduced when mitochondrial extracts were utilized for the assay. Finally, the authors identified a homozygous point mutation that changed a cytosine to thymine at position 773 in the *HADH* gene. This mutation results in the substitution of proline at position 258 with a leucine residue in the SCHAD protein transcript leading to SCHAD deficiency (127).

The association of SCHAD deficiency with CHI was still unclear at this point but was confirmed by Molven et al. in 2004 (128). The authors described a consanguineous family (Figure 8) where the parents were double first cousins and four children had severe neonatal hypoglycemia as well as elevated plasma 3-hydroxybutyryl-carnitine and urinary 3-hydroxyglutaric acid levels. The two eldest affected children died at four months of age due to hypoglycemia. The two younger affected children survived due to treatment involving frequent feeding, glucose administration, glucagon and eventually diazoxide therapy. The older of the surviving children developed mental retardation most likely due to hypoglycemic episodes in infancy.

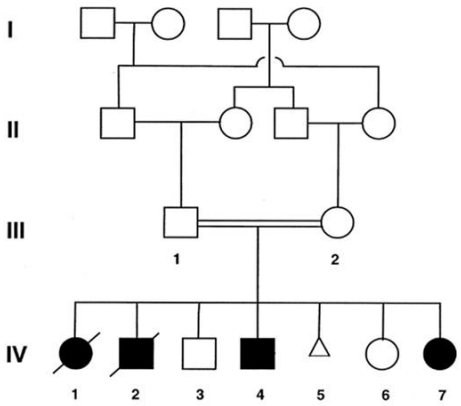

Figure 8. Pedigree of the consanguineous family with severe SCHAD-CHI described by Molven et al. Filled and open symbols denote subjects with CHI and healthy family members, respectively. Subjects IV 1 and 2 are deceased. Subject IV 5 was a miscarriage. Four generations of the family are shown to indicate the status of the parents as double first cousins. Figure from (126).

Since no mutations in known CHI-associated genes had been identified in this family, Molven et al. carried out a whole-genome scan with microsatellite markers searching for homozygous chromosomal segments. They identified a candidate region on 4q and revealed a deletion of six base pairs at the beginning of exon 5 of the *HADH* gene. The deletion disrupts a splice site and leads to omission of exon 5 causing the loss of approximately 30 aa in the final SCHAD

protein product. SCHAD activity was subsequently shown to be reduced in fibroblasts from the two affected children compared to controls (128).

These two reports linking SCHAD deficiency to CHI fully established *HADH* as a member of the metabolopathy subgroup of CHI genes. Today, at least 45 cases of SCHAD-CHI have been published (Table 3).

Table 3. Published patients with CHI-causing mutations in *HADH*. Mutations that affect splice sites and introns are reported at DNA level. Mutations that affect exons are reported at the level of protein sequence. NA = no information available. Table extended from (82). All mutations are homozygous except the compound heterozygous cases no. 5, 20, 26, and 48. Case no. 5 presented with a Reye-like syndrome instead of CHI.

Patient	Gender	Consanguinity	Ethnicity	Onset	Mutation	Reference
1	F	No	Indian	4 moths	P258L	(127)
2	M	Yes	Pakistani	3 days	IVS4-3DELCAGGTC	(128)
3	F	Yes	Pakistani	1.5 h	IVS4-3DELCAGGTC	(128)
4	M	Yes	Pakistani	4 months	IVS6-2A>G	(129)
5	F	No	Caucasian	10 months	D57G, Y226H	(130)
6	F	Yes	Bangladeshi	4 months	p.M188V	(131)
7	M	Yes	Caucasian	2 months	R236X	(132)
8	M	Yes	Caucasian	8 months	S196FfsX3	(133)
9	F	Yes	Caucasian	6 months	S196FfsX3	(133)
10	M	NA	Caucasian	14 months	S196FfsX3	(133)
11	M	No	Caucasian	7 months	IVS2+1G>A	(133)
12	M	Yes	Turkish	16 weeks	K136E	(134)
13	M	Yes	Turkish	16 weeks	Q163X	(134)
14	M	Yes	Turkish	2 weeks	R236X	(134)
15	M	Yes	Turkish	5 days	R236X	(134)
16	F	No	Turkish	1 week	R236X	(134)
17	M	Yes	Pakistani	2 days	R236X	(134)
18	F	No	Iranian	12 weeks	R236X	(134)
19	F	No	Iranian	1 day	R236X	(134)
20	M	No	Indian	26 weeks	K95SfsX3, IVS6 + 39C>G	(134)
21	M	No	Indian	2 days	Ex1deletion	(134)
22	M	No	Indian	24 weeks	Ex1deletion	(134)

23	NA	NA	NA	NA	G34R	(135)
24	NA	NA	NA	NA	K95fs	(135)
25	NA	NA	NA	NA	IVS8+39C>G	(135)
26	F	NA	Chinese	NA	R10P, V30E	(136)
27	F	No	Indian	12 weeks	I184F	(137)
28	F	No	Indian	16 weeks	I184F	(137)
29	M	Yes	Saudi	16 weeks	IVS2-1G>A	(138)
30	F	Yes	Saudi	12 weeks	IVS2-1G>A	(138)
31	M	Yes	Saudi	16 weeks	IVS2-1G>A	(138)
32	F	No	Turkish	4 weeks	IVS2-1G>A	(139)
33	M	Yes	Iranian	12 weeks	IVS2-1G>A	(140)
34	F	Yes	Iranian	1 year	IVS2-1G>A	(140)
35	M	Yes	Iranian	1 day	IVS2-1G>A	(140)
36	F	Yes	Iranian	4 days	IVS2-1G>A	(140)
37	M	Yes	Iranian	12 weeks	IVS2-1G>A	(140)
38	M	Yes	Iranian	6 weeks	IVS2-1G>A	(140)
39	M	Yes	Iranian	30 weeks	IVS2-1G>A	(140)
40	F	Yes	Iranian	1 day	IVS2-1G>A	(140)
41	M	Yes	Iranian	12 weeks	IVS2-1G>A	(140)
42	M	Yes	Iranian	12 weeks	IVS2-1G>A	(140)
43	M	Yes	Iranian	12 weeks	IVS2-1G>A	(140)
44	M	No	Caucasian	NA	G303S	(141)
45	M	No	Indian	34 weeks	T189fs	(142)
46	M	Yes	Turkish	Since birth	I143N	(143)
47	F	Yes	Turkish	Since birth	R236X	(143)
48	NA	NA	Chinese	3 days	c.419+1G>A + c.547-1G>C	(144)

SCHAD-CHI requires deficiency of both alleles and follows autosomal recessive inheritance. The hallmarks of the condition have been established to include mild to severe diazoxide-responsive hyperinsulinemic hypoglycemia, protein sensitivity (discussed in more detail in Chapter 1.4.4) and in most cases asymptomatic elevation of plasma 3-hydroxy-butyryl-carnitine and urinary 3-hydroxyglutaric acid. The birth weights are generally normal, and there

is an absence of FAO-related features (e.g. liver defects or enlargement, cardiomyopathy, skeletal muscle defects) (82).

1.4.4. Insights into the mechanism behind SCHAD-CHI

As mentioned, SCHAD-deficient patients lack the classical phenotype of a FAO disorder, and neither 3-hydroxybutyryl-carnitine nor 3-hydroxyglutaric acid is capable of stimulating insulin secretion (145). Therefore, it was hypothesized that SCHAD may play a role in the regulation of insulin secretion that is separate from its role in FAO and that this function could be specific to the β-cell. Indeed, SCHAD expression in the pancreas is highest in β-cells (Figure 9), and its level in β-cells is disproportionally high compared to that of other FAO enzymes (146). Knockdown of SCHAD in insulinoma cells and isolated islets results in increased insulin secretion (145,147). Moreover, SCHAD mRNA expression in β-cells is regulated by FOXA2 (71). As stated in Chapter 1.3.6, FOXA2 is another CHI-associated gene belonging to the transcriptionopathies. It is an important regulator of pancreas development and also regulates expression of the K_{ATP} channel genes (69,70,72).

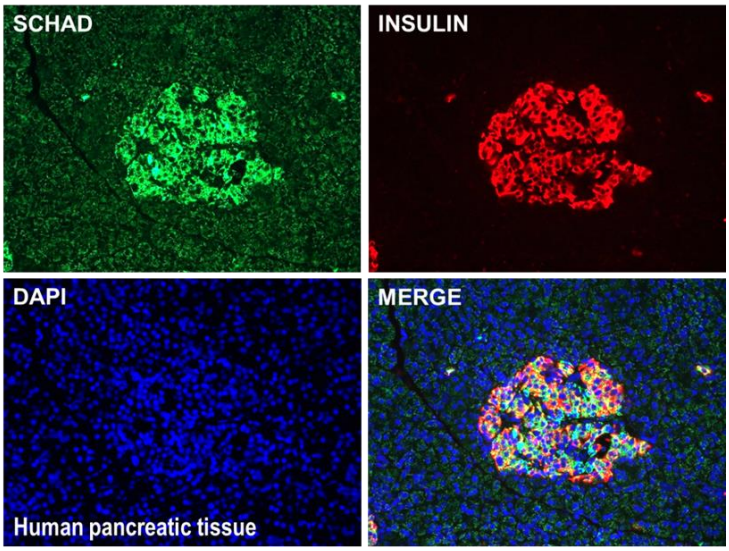

Figure 9. Immunohistochemistry of SCHAD and insulin expression in a human islet of Langerhans. Antibodies against SCHAD (green) and insulin (red) were used. Nuclei were stained with DAPI (blue). Source: Anders Molven and Jiang Hu, Joslin Diabetes Center.

Pull-down experiments using recombinant SCHAD protein as bait and human mitochondrial extracts derived from liver tissue as prey resulted in the discovery of a protein interaction between SCHAD and GDH (148). Activating mutations in the GDH-encoding gene, GLUD1, cause hyperinsulinism/hyperammonemia syndrome (see Chapter 1.3.5). Therefore, it was proposed that SCHAD may work as an inhibitor of GDH.

This was later confirmed by Li et al, who characterized the full body SCHAD knockout mouse (SCHADKO) (85). The animal model mirrors the human SCHAD-deficient phenotype of amino acid-sensitive, hyperinsulinemic hypoglycemia as well as the characteristic elevation in plasma and urinary fatty acid metabolites. Increased sensitivity to amino acids seems to be a hallmark of SCHAD-CHI (131) and is also characteristic for CHI caused by increased GDH activity. Indeed, Li et al. showed in experiments conducted on isolated islets that the amino acids leucine, glutamine and alanine are responsible for the spike in insulin secretion in SCHAD-CHI. This effect was dependent on the presence of leucine and greatly amplified by the other two amino acids. The three amino acids are related to GDH activity. Leucine is an allosteric activator of GDH, whereas oxidation of glutamine by glutaminase produces glutamate which serves as a substrate for GDH. Alanine can be utilized as substrate for the TCA cycle. The authors also confirmed the protein interaction between SCHAD and GDH, and they further showed that ablation of SCHAD protein increased islet GDH activity (85).

Overall, Li et al. demonstrated that the SCHADKO mouse is a good model for the study of SCHAD-CHI. However, how lack of GDH inhibition by SCHAD stimulates insulin secretion is still not fully understood. GDH catalyzes the reversible conversion of glutamate + NAD^+ (or $NADP^+$) to α-ketoglutarate + NH_3 + NADH. Both directions of this reaction have the potential to stimulate insulin secretion. α-ketoglutarate is used as substrate in the TCA cycle and its metabolism ultimately leads to a rise in the ATP:ADP ratio, which in turn stimulates insulin secretion through closure of K_{ATP} channels (55). Glutamate on the other hand can be taken up by insulin granules which then leads to amplification of insulin secretion (56). Glutamine oxidation to glutamate is increased in SCHADKO islets but administration of glutamine alone does not result in increased insulin secretion (85). This may suggest that glutamine is converted to glutamate for the conversion to α-ketoglutarate by GDH, instead of being taken up by insulin granules. However, other studies suggest that the specific β-cell environment favors the opposite reaction. Glucose stimulation increases the mitochondrial NADH:NAD^+ ratio which favors the production of glutamate over the production of α-ketoglutarate by GDH (149).

Ultimately, either way could lead to increased insulin secretion, and it is possible that both mechanisms exist simultaneously (Figure 10).

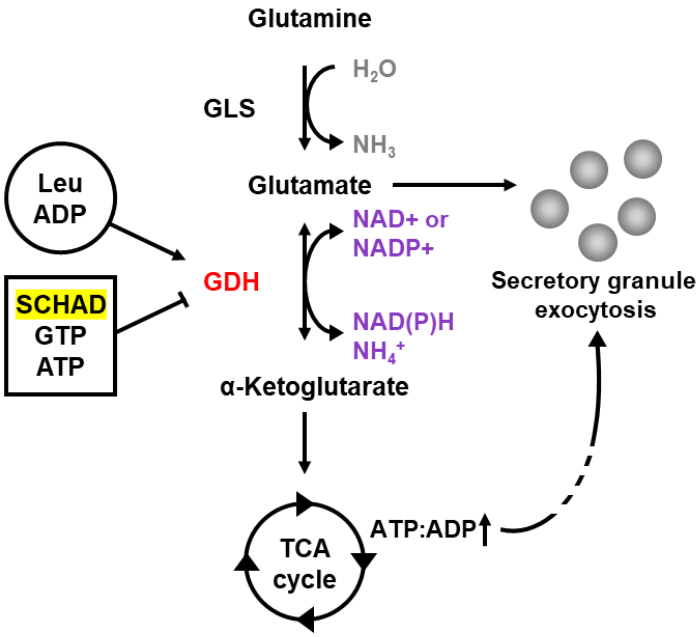

Figure 10. Proposed mechanism for regulation of GDH activity by SCHAD. GDH catalyzes the reversible conversion of glutamate to α-ketoglutarate and ammonia using NAD^+ or $NADP^+$ as cofactors. Its activity depends on stimulation by activators and inhibitors. In this proposed model, SCHAD is an inhibitor of GDH activity. SCHAD deficiency removes an inhibitory signal and increases GDH activity which leads to increased production of glutamate or α-ketoglutarate depending on the mitochondrial NADH:NAD^+ ratio. This would then stimulate insulin secretion by increasing the β-cell ATP:ADP ratio through metabolism of α-ketoglutarate or by amplifying insulin secretion through uptake of glutamate into secretory granules.

The above evidence confirms the hypothesis that SCHAD serves a second function outside of FAO, but the question remains whether this function is specific for the β-cell. Both SCHAD and GDH are ubiquitously expressed and some cases of SCHAD-CHI also report mild hyperammonemia, which poses the question whether liver or kidney defects may be involved in the pathophysiology (133). However, downregulation of SCHAD expression in rat insulinoma cells stimulates insulin secretion (145–147) and an islet transplantation study performed by Molven et al. suggests that the hypoglycemic phenotype of SCHAD deficiency is islet-autonomous (150). Molven et al. transplanted isolated islets from SCHADKO mice and controls under the kidney capsule of streptozotocin-diabetic mice. SCHADKO islets lowered the plasma glucose of recipient mice more potently than control islets. This suggests that SCHAD deficiency in the islet may be sufficient to cause hypoglycemia, but contribution of

different islet cell types and the influence of other tissues could not be studied by the transplantation approach.

Besides the interaction with GDH, one study indicated that SCHAD may interact with several other proteins, possibly within tissue-specific metabolic super-complexes (151). Pull-down and yeast-2 hybrid studies showed that the enzyme interacts with other mitochondrial and possibly cytosolic enzymes involved in metabolism of carbohydrates, glutamate, and lipids, urea cycle and others. Thus, even though the evidence strongly suggests a link between SCHAD and GDH in the pathophysiology of CHI, other interactions and pathways may be involved (151). Another limitation is that no structure of the postulated SCHAD-GDH complex has been presented.

In summary, the FAO enzyme SCHAD is fully implicated as member of the metabolopathy subgroup of CHI. So far, the data suggests that SCHAD serves two distinct functions, one in FAO and the other in β-cell insulin secretion, and that the latter is dependent on an interaction with GDH. Still, many questions concerning the mechanism behind SCHAD-CHI and the role of SCHAD within the β-cells remain unanswered.

2. Aims of the thesis

Almost two decades ago, the fatty acid-degrading enzyme SCHAD was identified as a regulator of insulin secretion because mutations in the *HADH* gene were shown to cause CHI. The overall aim of the present study was to obtain a deeper understanding of how the SCHAD protein is implicated in regulation of insulin secretion.

The specific aims of this thesis were as follows:

1. To establish the necessary methodology and to perform a functional evaluation of human *HADH* missense variants
2. To investigate the tissue specificity and phenotype of SCHAD deficiency in a conditional SCHAD KO mouse model
3. To identify and characterize novel protein interaction partners of the human SCHAD protein

3. Summary of results

Paper I

Functional evaluation of sixteen SCHAD missense variants: Only amino acid substitutions causing congenital hyperinsulinism of infancy lead to loss-of-function phenotypes in vitro.

Here we analyzed the stability, subcellular localization, enzymatic activity and GDH interaction of nine population variants of unknown significance, six previously published pathogenic variants and an unpublished pathogenic variant of the *HADH* gene. To this end, we developed tools for prokaryotic and eukaryotic expression and production of recombinant protein as well as a HEK293 SCHAD KO cell line for functional testing of variants in the absence of endogenous protein.

All variants localized to the mitochondria when expressed in HEK293 SCHAD KO cells. Seven of the nine population variants behaved in a similar manner to wildtype (WT) SCHAD regarding all tested properties. The exceptions were a higher molecular weight as assessed by western blot for the variant p.Phe92Cys and somewhat increased enzyme activity of p.Met188Val.

All CHI-causing variants differed from WT SCHAD in one or more respects. The variants p.Gly34Arg, p.Ile184Phe, p.Pro258Leu and p.Gly303Ser were expressed at significantly lower levels in HEK293 and SCHAD KO HEK293 cells. This is most likely due to abnormal folding followed by rapid degradation due to protein quality control since these variants could be expressed in a cell-free expression system devoid of functional quality control systems. Moreover, MG132-mediated blockage of the ubiquitin-proteasome system partially rescued protein expression of these variants in the HEK239 SCHAD KO cell line.

Regarding enzyme activity, SCHAD WT displayed a Vmax of 181 ± 3 µmol/min/mg. The three pathogenic variants p.His170Arg, p.Pro258Leu and p.Gly303Ser, had almost no enzyme activity (< 10 µmol/min/mg). The variants p.Lys136Glu and p.Met188Val had significantly reduced enzyme activity (127 ± 8 µmol/min/mg and 132 ± 29 µmol/min/mg, respectively).

Lastly, Co-IP experiments showed that three of the pathogenic variants with normal protein expression but reduced enzyme activity (p.Lys136Glu, p.His170Arg, and p.Met188Val) still interacted with GDH, albeit to a lower degree than WT SCHAD.

Overall, we showed that the tested population variants of unknown significance did not impair SCHAD protein function, while pathogenic variants affect protein stability, enzyme activity and GDH interaction to varying degrees.

Paper II

Amino acid-sensitive hypoglycemia caused by a specific deficiency of the metabolic enzyme SCHAD within pancreatic β-cells.

The focus of Paper II was to investigate whether SCHAD-CHI has a phenotype that can be attributed to specific loss-of-function in the pancreatic β-cells. Selective removal of SCHAD expression from specified mouse tissues was achieved by using ES cells and the Cre-Lox recombination system to generate *Hadh*$^{lox/lox}$ mice that harbored LoxP sites flanking exon 3 of the *Hadh* gene. These mice were then bred with Ins1-cre or Alb-cre mice to disrupt SCHAD expression in β-cells or hepatocytes, respectively. The KO was confirmed using PCR, western blot, and immunohistochemistry. Immunohistochemistry also demonstrated high expression of SCHAD in the δ-cells of the islets and an apparent absence of expression in the α-cells.

Male and female mice were analyzed for bodyweight development and glucose homeostasis. Hepatocyte SCHAD KO (L-SKO) mice had no evident phenotype and were not further analyzed. β-cell SCHAD KO (β-SKO) mice, on the other hand, had reduced blood glucose levels in the random fed, 16-h fasted and refed state, and the rise in blood glucose 4 h after refeeding was blunted. This happened despite normal food intake during refeeding in male and increased food intake in female β-SKO mice. Insulin and C-peptide levels in all three conditions did not indicate hyperinsulinism. Male, but not female 10-week-old β-SKO mice, had significantly impaired glucose tolerance, but this difference disappeared when re-tested at 30 weeks of age.

Feeding male β-SKO mice a diet enriched in the amino acids alanine, glutamine, and leucine exacerbated the hypoglycemic phenotype and slightly impaired glucose tolerance. Again, insulin levels did not indicate hyperinsulinism. However, isolated islets derived from male β-SKO mice displayed a marked increase in insulin secretion when stimulated with the above-mentioned amino acids in the presence of 3.3 mM, but not 16.7 mM glucose. These amino acids had no additional effect in stimulating insulin secretion from control islets at either

glucose concentration. Female β-SKO islets displayed a similar increase in insulin secretion when stimulated with amino acid mixture at 3.3 mM glucose. In contrast to male β-SKO islets, incubation with 16.7 mM glucose elicited a reduced insulin secretion response from female islets that was rescued by addition of amino acid mixture.

Analyzing the transcriptome of islets from 10-week-old male β-SKO mice revealed a global change in expression of genes involved in metabolism. Oxidative phosphorylation, amino acid, and protein metabolism were up-regulated, while lipid metabolism was down-regulated. Interestingly, the insulin secretion pathway was amongst the down-regulated pathways.

Furthermore, RNAseq showed evidence for β-dedifferentiation as dedifferentiation markers, *Aldh1a3*, *Aass,* and others were amongst the top up-regulated genes accompanied by a decrease in expression of genes involved in β-cell maturation, survival, and cell adhesion. Lastly, gene expression of proteins involved in calcium signaling and transport suggested an increase in calcium binding and uptake.

Overall, the data of Paper II demonstrated that ablation of SCHAD expression in the β-cells is sufficient to elicit an amino acid-sensitive, hypoglycemic phenotype akin to hypoglycemia seen in global SCHADKO mice and in SCHAD-deficient patients. KO of SCHAD in hepatocytes had no effect on glucose homeostasis and a role for the liver in SCHAD-CHI therefore seems unlikely.

Paper III

Searching for novel interaction partners of short-chain 3-hydroxyacyl-CoA dehydrogenase: A role for keratin 8?

SCHAD has been shown to interact with a variety of proteins, and it has been speculated that it is part of tissue-specific metabolic super-complexes of proteins. Specific interactions within the islets of Langerhans have not been addressed so far. Given the high β-cell expression levels and SCHAD's role in insulin regulation, we in Paper III aimed to identify novel SCHAD protein interactions that might be particularly relevant for its β-cell function. We therefore performed a yeast two-hybrid (Y2H) screen using a cDNA library from human islets.

By employing a bait consisting of SCHAD without its dimerization domain, we identified two proteins, keratin 8 (K8) and cytospin-A (SPECC1L), with very high confidence. K8 was the by far dominating hit. An interaction of SCHAD with K8 could be confirmed using co-immunoprecipitation approaches and was also supported by mass spectrometric analysis of co-IP samples.

SCHAD and K8 are confined to different subcellular compartments. SCHAD is transported to the mitochondria, while K8 is expressed in the cytosol. However, using a cytosolically expressed SCHAD variant (Δ1-12 SCHAD) as bait in SCHADKO HEK293 cells did not increase the amount of K8 in the co-IP fraction. In fact, we observed less interaction of K8 with Δ1-12 SCHAD, indicating that the interaction may be confined to the mitochondrial matrix.

K8 is a main keratin of the islet of Langerhans and with a potential role in the regulation of insulin secretion. We confirmed its presence in the endocrine pancreas by using immunohistochemistry on human and mouse tissue and by openly accessible single cell RNAseq data from the Tabula Muris database. Lastly, we performed a pilot study of SCHAD and K8 expression in their respective knockout mouse models. Absence of SCHAD expression did not affect K8 expression levels in whole pancreas but seemed to result in slight upregulation of K8 in islet preparations. Ablation of K8 expression alone had no overt effect on SCHAD expression in whole mouse pancreas and islets. However, when animals were fed a ketogenic diet, we observed significant upregulation of SCHAD in whole pancreas and this increase was blunted in animals lacking K8 expression.

In conclusion, Paper III identified a possible physical interaction between SCHAD and K8. Whether this interaction occurs within the pancreatic β-cell and, if so, its biological relevance needs to be determined in follow-up studies.

4. General discussion

4.1. Interpretation of *HADH* variants identified in a clinical setting

Whole-exome and whole-genome sequencing are powerful tools for the identification of underlying germline mutations in patients and families. This also holds true for rare, heritable genetic conditions of glucose homeostasis such as MODY and CHI. Analyzing the plethora of raw genetic information, however, poses a significant challenge. "Wildtype" humans do not exist, and every person harbors an array of rare genetic variants of unknown significance, in particular missense mutations, that will be picked up in the genetic screening. Missense mutations may or may not alter the function of the protein and, in the latter case, may or may not be pathogenic. Predicting functional effects of these mutations using bioinformatics tools is still notoriously unreliable. Thus, physicians and molecular biologists will in many cases be left with the conclusion that the variant is a VUS, i.e. a variant of unknown significance.

One example is a diabetes family recruited by the Norwegian MODY Registry and screened for pathogenic mutation at the Bergen Diabetes Research Center as part of the clinical workup some years ago (Figure 11). This multigenerational family includes several family members with diabetic phenotypes of varying severity. Whole-exome sequencing was performed on the seven available DNA samples from this family. Three family members were identified to be heterozygous for the known, pathogenic *GCK* mutation p.Ser453Leu. Thus, these patients were diagnosed with GCK-MODY (MODY2). The other four sequenced family members, who were previously diagnosed with either type I-like diabetes or impaired fasting glucose, did not harbor the *GCK* mutant but were found to be heterozygous for the rare *HADH* variant p.Pro215Thr. This *HADH* variant was absent in the family members with *GCK* mutations.

At the time of screening, the effect of p.Pro215Thr on SCHAD protein function was unknown. Thus, it was unclear whether the observation of the variant in the diabetes family depicted below was a spurious finding or if it represented a novel implication for SCHAD in β-cell function. Notably, *HADH* has not been associated with diabetes. In fact, there is an indication from the literature that rare variants of *HADH* might have a protective effect with regard to this disease (152). Still, it was not unreasonable to consider that some amino acid substitutions could alter SCHAD protein function in ways that could impair insulin secretion and cause a diabetic phenotype. This would be analogous to the situation for other central β-cell genes such

as *GCK*, *HNF1A*, *HNF4A* and *ABCC8* that can cause MODY or CHI depending on the type of mutation (68,153).

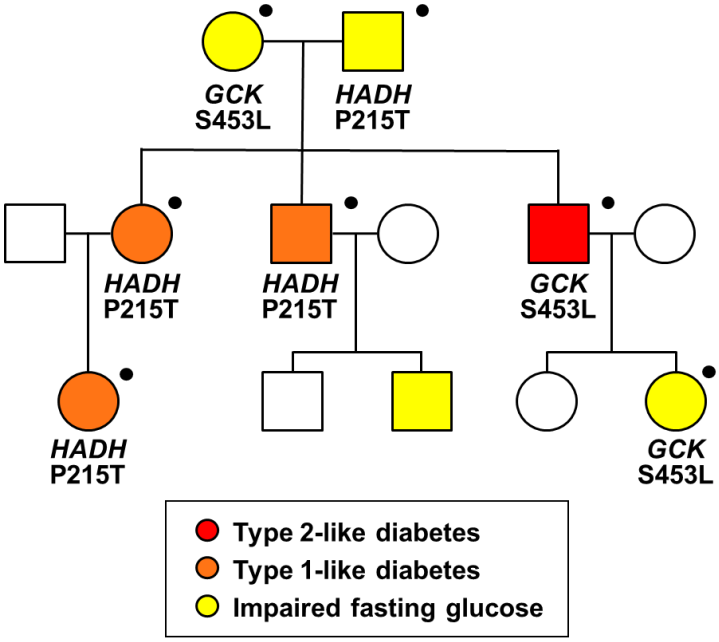

Figure 11. Multigenerational family with diabetes and impaired fasting blood glucose. Whole-exome sequencing was performed for the seven members for whom DNA was available (black dots). The color codes show their diagnoses before sequencing. Three members were found to carry the pathogenic *GCK* mutation p.Ser453Leu in the heterozygous state, leading to the conclusion that they have MODY2. In the four other sequenced members, *GCK* was normal. However, they were all heterozygous carriers of the rare *HADH* variant p.Pro215Thr. *HADH* was normal in the *GCK* mutation carriers.

In Paper I, we analyzed the protein products of 16 *HADH* missense variants for expression and function. This study also included p.Pro215Thr, which was examined for protein stability, intracellular localization and enzyme activity. Only the latter differed from that of the wildtype protein: the activity of p.Pro215Thr was slightly but significantly elevated. The effect on insulin secretion by increased β-cell SCHAD activity has so far not been investigated. However, since the p.Pro215Thr variant was present in the heterozygous state in the four affected family members, it was deemed unlikely that the very modest increase in enzyme activity could be linked to a diabetic phenotype. Based on the findings of Paper 1 and a carrier frequency of 0.00184 in the gnomAD database, we therefore concluded that the identification of the p.Pro215Thr variant was an unrelated, spurious finding and that the variant is likely benign. Thus, an underlying, genetic cause for the phenotype of the non-*GCK* mutation carriers of the family in Figure 11 has not yet been revealed.

Still, in future studies, overexpression of p.Pro215Thr in the presence or absence of endogenous wildtype SCHAD in β-cell models such as the lines INS-1E or EndoC-βH1 should be done. This might reveal if this variant has an insulin-reducing effect not seen for the CHI-causing variants of the *HADH* gene.

4.2. Heterogeneous expression of SCHAD in islet cell subtypes.

In Paper II, we created conditional SCHAD KO mice and deleted SCHAD expression specifically from β-cells using Ins1-cre mice. As part of the validation of the KO, we performed immunohistochemistry on pancreas sections of β-SKO mice and controls. The absence of SCHAD immunostaining in β-cells confirmed the successful KO, and also highlighted the high expression level of SCHAD in δ-cells and the very low or virtually absent expression of SCHAD in α-cells. This heterogeneous expression pattern in islets was previously reported by Lawlor *et al*. (154) and Martens *et al*. (155), and was further confirmed in Paper III by openly accessible single cell RNA sequencing data from Tabula Muris (156).

The different levels of SCHAD expression may reflect a closer developmental relationship between β- and δ- cells as opposed to β- and α- cells. As stated in Chapter 1.1.1, the endocrine cells of the pancreas share a common progenitor in neurogenin 3-positive (Ngn^+) cells. Ngn^+ cells start to emerge at embryonic day 8.5 (E8.5) in mice. Here, $Ngn3^+$ cells first give rise to α-cells at E9.5, followed by β-cells at E10.5, δ-cells at E14, and PP-cells at E18.5. In humans, endocrine cells develop between weeks 7 and 23 of gestation. Again, α-cells develop first during week 7, followed by the other endocrine cell types between week 8 and 10 of gestation (3).

The factors that determine cell fate during development are not fully understood and have so far mostly been studied in the mouse. Part of the process is the timed expression of a complex network of transcription factors (Figure 12). *Ngn3* regulates expression of many downstream transcription factors important for endocrine islet cell development, including neuronal differentiation 1 (*NeuroD1*), paired-box 6 (*Pax6*), ISL LIM homeobox 1 (*Isl1*), MAF BZIP transcription factor B (*Mafb*), NK2 homeobox 2 (*Nkx2.2*), and regulatory factor X6 (*Rfx6*). At E9.5, endocrine progenitors begin to express paired-box 4 (*Pax4*) and aristaless-related homeobox gene (*Arx*). These transcription factors are mutual inhibitors and are involved in the separation of the lineage into β/δ and α/PP cells. The former then gives rise to β-cells characterized by expression of insulin (*Ins*), MAF BZIP transcription factor A (*Mafa*), *Pax4/6*,

pancreatic and duodenal homeobox 1 (*Pdx1*), NK6 hHomeobox 1 (*Nkx6.1*), and *Nkx2.2*., as well as δ-cells characterized by expression of *Sst*. From the combined α/PP cells, α-cells arise, expressing glucagon (*Gcg*), *Arx*, *Mafb*, *Rfx6*, *Nkx2.2*, *NeuroD1*, and *Pax6*. PP-cells are characterized by expression of *Ppy* (157). Thus, α-cells develop earlier than β- and δ-cells, and β- and δ-cells share a common, immediate progenitor.

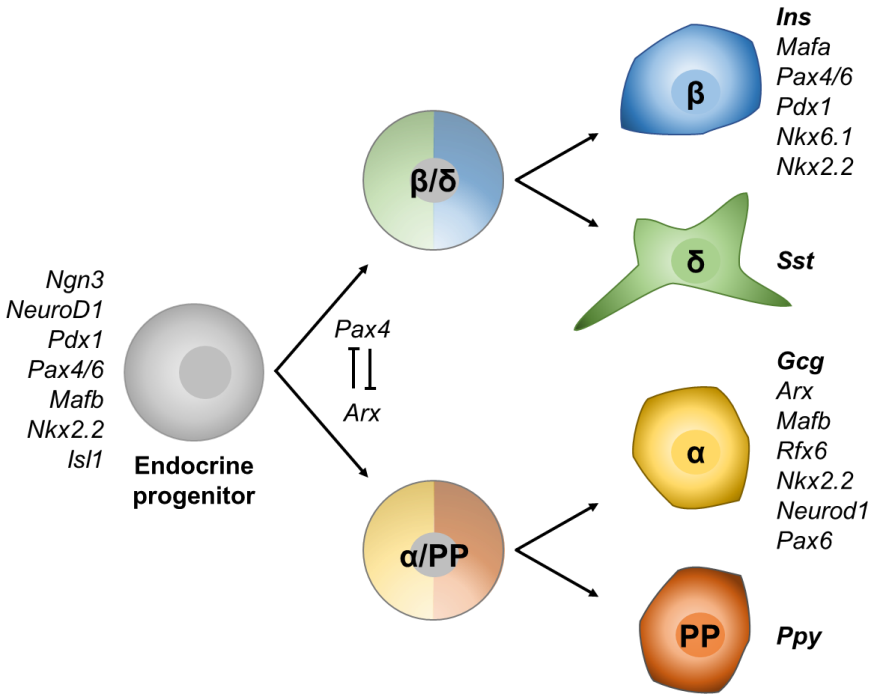

Figure 12. Transcription factors involved in differentiation of Ngn$^+$ cells into endocrine islet cell types. Hormones and transcription factors are indicated in bold and roman font, respectively. α-, β-, δ-, and PP-cells share a common neurogenin 3 (Ngn3)-expressing endocrine progenitor cell. Expression of the mutually inhibitory paired-box 4 (*Pax4*) or aristaless-related homeobox gene (*Arx*) drives the cells towards the β/δ or α/PP lineage. The former gives rise to mature insulin (*Ins*)-producing β-cells and somatostatin (*Sst*)-producing δ-cells while the latter diverges into glucagon (*Gcg*)-producing α-cells and pancreatic polypeptide (*Ppy*)-producing PP-cells. Drawn after (155).

Islet SCHAD expression rises during embryogenesis and peaks postnatally as islets mature (158). RNA sequencing data from Tabula Muris confirmed the high expression of SCHAD in β- and δ-cells and showed high expression of SCHAD in PP cells. SCHAD is also highly expressed in pancreatic ductal cells which diverge from common pancreatic progenitor cells before the emergence of the *Ngn3*$^+$ endocrine progenitor cell. It is thus possible that SCHAD expression is specifically silenced in α-cells after α/PP cell development. The developmental stage when SCHAD expression is suppressed in α-cells and identity of the transcription factors

that are involved in the process are not yet known. Obviously, high expression of SCHAD is a characteristic of mature β-cells. Identification of the developmental processes that regulate expression of *HADH* would be beneficial for understanding islet endocrine cell differentiation that could have implications for the development of β-cell-like cells from induced pluripotent stem cells (iPSC).

4.3. A role for SCHAD in amino acid sensing?

As discussed previously, β- and δ-cells express high levels of SCHAD while expression in α-cells is strikingly low. Besides reflecting similarities and differences in differentiation, the heterogeneous expression pattern suggests that it is of relevance for proper functioning of the different islet cell types. In particular, the striking differences between α- and β-cells is worth discussing.

In Chapter 1, we reviewed insulin secretion from β-cells and briefly discussed glucagon secretion from α-cells. Both cell types are intricately regulated by nutrients, paracrine, autocrine, and nervous system factors. Besides glucose, amino acids are potent stimuli or enhancers of insulin and glucagon secretion. Many amino acids enhance glucose-stimulated insulin secretion in mature islets, but only leucine is capable of eliciting an insulin secretion response by itself (4).

During embryogenesis, however, insulin secretion is differently regulated. Here, insulin secretion does not follow the rise and fall of blood glucose levels. Instead, insulin is continuously secreted and regulated by a steady supply of nutrients by the mother (159). A recent study showed that in utero, amino acids may play a larger role in stimulating insulin release than glucose (160). Glucose responsiveness, where insulin secretion in low-glucose conditions is suppressed and stimulated as glucose levels increase, develops shortly after birth when the newborn adapts from a constant supply of nutrients to an environment where nutrient levels change response to feeding and fasting. During this transition, β-cells mature to become primarily responsive to glucose whereas amino acids take on a secondary role (160).

We speculate that SCHAD is part of the machinery involved in regulating the switch from pre- and postnatal β-cell metabolism due to its role in β-cell amino acid metabolism. SCHAD expression rises during embryogenesis but only reaches full expression levels in mature islets (158). The enzyme most notably regulates amino acid metabolism through inhibition of GDH

(85). Neither CHI-causing GDH nor SCHAD mutations are associated with an increased risk for macrosomia (82,161). Thus, it is unlikely that these mutations cause fetal hyperinsulinism and that increased insulin secretion may develop in the postnatal period as β-cells mature. However, our RNA sequencing data in Paper II suggests a general increase in amino acid and protein metabolism and a loss of β-cell identity in islets that lack β-cell SCHAD expression. Perhaps, SCHAD controls amino acid metabolism beyond the scope of GDH inhibition. It is proposed to associate with tissue-specific metabolic super-complexes (151), yet little is known about β-cell-specific interactive networks of SCHAD. Thus, it is possible that SCHAD regulates function and/or activity of other metabolic enzymes involved with amino acid metabolism.

Lack of SCHAD expression could thus impair β-cell maturation and allow for the resurgence or continuance of some features of amino acid-stimulated insulin secretion seen *in utero*. In SCHAD-CHI patients, this may manifest as the increase in sensitivity to protein- and especially leucin-stimulated insulin secretion (162). It will be intriguing to reveal the full extent of SCHAD's role in amino acid sensing and β-cell maturation.

α-cells secrete glucagon, which in concert with insulin, tightly regulates glucose levels. However, α-cell function is also intimately intertwined with systemic amino acid metabolism. For example, α-cells secrete glucagon in response to amino acids such as arginine, alanine, and glutamine while being inhibited by isoleucine. Leucine stimulates glucagon secretion at physiologic levels; however, it becomes a negative regulator when leucine levels rise (163). Glucagon in turn regulates hepatic amino acid metabolism and disruption of hepatic glucagon signaling has widespread effects on α-cell function (164).

Studies in KO mice and mice with acute interruption of glucagon signaling showed that absence of glucagon signaling in the liver results in hyperaminoacidemia due to altered liver amino acid catabolism (165,166). The elevated serum amino acids, primarily glutamine, stimulated α-cell hyperplasia and hyperglucagonemia. In contrast, β- and δ-cell numbers did not change in response to increased amino acid levels (164). Interestingly, α-cell hyperplasia is partially driven by upregulation of the sodium-coupled neutral amino acid transporter Slc38a5. Expression of this transporter is usually restricted to embryogenesis. Slc38a5 may thus be part of the machinery that drives α-cell differentiation and proliferation during development and may reflect the difference in nutrient supply during embryogenesis (167,168). Overall, these experiments identified a role for α-cells in amino acid sensing and a

specialized liver-α-cell axis that controls systemic amino acid metabolism and α-cell proliferation regulated by glutamine. Disruption of α-cell amino acid sensing could therefore have detrimental effects on α-cell function.

Since α-cell hyperplasia is primarily driven by glutamine, GDH activity may be part of the mechanism connecting amino acid sensing to α-cell proliferation. As stated in Chapter 1.4.4 glutamine serves as substrate for GDH after conversion to glutamate. Furthermore, GDH has previously been proposed to function as an amino acid sensor in autophagy due to its activity being partially coupled to leucine availability (169). α-cells express exceptionally low levels of SCHAD and thus lack this level of GDH inhibition. Perhaps, α-cells rely on GDH-mediated amino acid sensing to a higher degree than β- and δ-cells due to glutamine-mediated regulation of α-cell proliferation. SCHAD expression and SCHAD-mediated inhibition of GDH could therefore be detrimental for α-cell function and the liver-α-cell axis. Overexpression studies of SCHAD in α-cells could potentially elucidate the role of SCHAD in amino acid sensing and should be pursued in future experiments.

4.4. Novel SCHAD interaction partners. A role for keratin 8?

SCHAD protein interactions have been investigated in a variety of tissues such as liver, heart, skeletal muscle, brain, and kidney (151). Associations were then found with tissue-specific proteins and even with cytosolic proteins. The idea of Paper III of this thesis was to search for novel SCHAD protein interactions that might be specific for the islets of Langerhans. We performed a Y2H screening and identified K8 as a possible interaction partner of SCHAD. That there was no hit for GDH in this screening, might at first glance appear surprising since a previous study identified GDH in a similar experiment (151). However, the authors used a human placental cDNA library and a shorter SCHAD peptide spanning residues 75 – 119 as prey and bait, respectively. Thus, the discrepancy in Y2H results may indicate different availability of prey proteins depending on the studied tissue. Our results do not exclude that SCHAD interacts with GDH in the β-cell. Instead they may indicate that the interaction with K8 is sufficiently strong to mask interactions with GDH in our experimental set-up. This would be analogous to what happened in the first Y2H screen performed in Paper 1, where SCHAD dimerization dominated all other interactions in the β-cell cDNA library.

In Paper III, we therefore decided to focus our studies regarding possible interactions of SCHAD on keratin K8 due to the overwhelming dominance of this interaction in the Y2H

screen. Moreover, a previous report on K8KO mice had demonstrated a role for K8 in β-cell function and glycemic control (170). Indeed, the K8KO mouse is, similar to the SCHADKO model, hypoglycemic. It has been hypothesized that the reason for this phenotype in the mice lacking K8 may be an increase in insulin action, glucose uptake, and hepatocyte glycogen storage (170,171) while hypoglycemia in SCHAD-deficient mice may be the consequence of increased β-cell sensitivity to amino acid-stimulated insulin secretion (85,150). However, K8KO mice show evidence for defects related to the insulin secretion pathway. β-cell ultrastructure, specifically insulin vesicle morphology and mitochondrial mobility, have been found abnormal, and GLUT2 is retained in the cytoplasm instead of in the β-cell membrane (170,172). Consequently, K8KO mice have impaired GSIS and are less sensitive to streptozotocin-induced β-cell damage. Amino acid-stimulated insulin secretion has not yet been studied in K8KO mice. Overall, both SCHAD and K8 are implicated in β-cell function and absence of either protein directly affects the insulin secretion pathway. Thus, the possibility exists that lack of an interaction between SCHAD and K8 is part of the defects seen in each mouse KO model.

5. Concluding remarks

CHI is a rare, inherited condition characterized by inappropriately elevated insulin secretion, hypoglycemia, and associated health complications. It is caused by mutations in genes involved in the regulation of insulin secretion from pancreatic β-cells. Thus far, around fifteen genes have been identified to cause CHI through changes at the level of small molecule transport, nutrient metabolism and gene expression. Studying CHI-associated genes therefore offers a unique opportunity to investigate β-cell biology and has the potential for identification of therapeutic targets not only for CHI, but also for diabetes mellitus.

In this thesis, I have examined the function and possible protein interactions of one such gene, *HADH,* which encodes the fatty acid oxidation enzyme SCHAD. In Paper I, we developed toolkits for the study of *HADH* missense variants and concluded that rare variants observed in the general population are not functionally affected. In Paper II, we investigated the tissue specificity of SCHAD-CHI using conditional SCHAD KO mice, demonstrating that it is primarily a β-cell disease. Finally, in Paper III, we aimed to identify novel islet-specific protein interaction partners of SCHAD.

Overall, the work presented in this thesis offers new insights into rare *HADH* variants and their effects on the SCHAD protein, the functional importance of SCHAD expression in β-cells, and – potentially – its islet-specific interactions. Our studies may hopefully aid in future research unravelling precisely how SCHAD is implicated in the insulin secretion pathway and which role it plays in islet responses to amino acids.

6. Future perspectives

The experimental systems for SCHAD functional studies developed in Paper I included eukaryotic and prokaryotic expression vectors, as well as a HEK293 SCHAD KO cell line for eukaryotic overexpression of the variants in the absence of endogenous SCHAD protein. In the paper, we studied a total of 16 missense variants, and the developed toolkit will facilitate studies of newly discovered missense variants.

Future experiments would also benefit from the development of a SCHAD-deficient β-cell line (e.g. INS-1E (173) or EndoC-βH1 (174)) and transgenic β-cell lines expressing pathogenic variants of SCHAD under the control of the *HADH* promoter. Using β-cell lines would offer the possibility to study the effect of overexpression of pathogenic variants and the effect of increased SCHAD enzyme activity of the non-pathogenic P215T variant on insulin secretion in the absence of endogenous wildtype SCHAD. These cells would also enable the identification of protein interaction partners in the β-cell using co-immunoprecipitation with either overexpressed wildtype SCHAD or missense mutants as bait. The latter could be generated by targeted mutagenesis using CRISPR technology and would allow for more comprehensive analysis of the effect of pathogenic missense mutations as SCHAD variants would be expressed at natural levels.

Since SCHAD-CHI is widely accepted to be caused by a lack of GDH inhibition by SCHAD (85), understanding the interaction of SCHAD with GDH is of utmost importance. The determination of the structure of the two proteins in complex would represent a major leap forward in understanding their mechanism of interaction. SCHAD is expressed at particularly high levels in β-cells compared to GDH or other FAO enzymes (146). Indeed, a SCHAD:GDH ratio of 3:1 is required for inhibitory action by SCHAD (85). Furthermore, SCHAD-CHI patients are sensitive to leucine, an allosteric activator of GDH (162). Whether SCHAD blocks GDH directly or prevents allosteric activation by leucine remains to be investigated. Using GDH enzyme activity assays in combination with recombinant SCHAD protein generated in Paper I, this inhibitory interaction could be modulated by addition of allosteric activators (e.g. leucine) or inhibitors (e.g. GTP). Lastly, using pull-down experiments we showed that the tested pathogenic missense variants with normal protein expression level (e.g. p.Lys136Glu, p.His170Arg, and p.Met188Val) interacted with GDH to a lower degree than wildtype SCHAD

protein. Using these mutant SCHAD proteins as inhibitors in a GDH activity assay could shed more light on their effect compared to wildtype SCHAD.

In Paper II, we demonstrated that SCHAD deficiency limited to the insulin producing β-cell is sufficient to cause a hypoglycemic phenotype in β-SKO mice and that this phenotype can be exacerbated by feeding of a diet enriched in leucine, alanine, and glutamine. There are a number of experiments that await completion. Firstly, we did not detect overt hyperinsulinism *in vivo*. However, we only measured plasma insulin and C-peptide levels at the time of hypoglycemia. Insulin is not a reliable biomarker of hyperinsulinism and frequently does not show up as elevated in blood samples from CHI patients (74). To establish a hyperinsulinemic phenotype in β-SKO mice we could measure additional markers such as IGFBP-1, b-hydroxybutyrate, and free fatty acids. Secondly, RNA sequencing performed on islet samples of β-SKO mice and controls showed global changes in gene expression related to metabolism and β-cell identity. To confirm our findings, we will perform immunohistochemistry of selected hits on pancreas sections of control and β-SKO mice. Thirdly, we have also performed mass spectrometry analysis on plasma samples from mice fed an amino acid-enriched diet. The goal is to investigate whether the feeding of the diet increased metabolites related to leucine, alanine, and glutamine metabolism in circulation. We are currently working on finalizing the data analysis and are designing experiments for result validation.

Due to the development of the *Hadh*$^{flox/flox}$ mouse, we now possess a tool to study the importance of SCHAD in any desired cell-type, provided that appropriate Cre-models exist to generate the conditional KO. Thus far, we have analyzed SCHAD KO in β-cells and hepatocytes. Future experiments should include the KO of SCHAD in δ-cells. δ-cells are of interest due to their regulatory role in hormone secretion in the islet of Langerhans. As stated in Chapter 1.1.3, SST secretion is similarly regulated as insulin secretion (11). Indeed, δ-cells express high levels of SCHAD (154) and thus SCHAD may play an important role in the SST secretory pathway. As of today, no models that allow for conditional KO of genes specifically in pancreatic δ-cells have been described. Until such a model is developed, the general SCHADKO mouse developed by Li et al. (85) could be used to investigate δ-cell function in the absence of SCHAD expression.

Finally, in Paper III, we identified an interaction of SCHAD with K8 using a human islet of Langerhans library in a Y2H screening experiment. Islets of Langerhans also include other endocrine pancreas cells and while we performed a validating Co-IP experiment in HEK293

cells, we have not yet studied the postulated interaction in β-cell lines. Since both proteins are implicated in β-cell function and glycemic control is perturbed in KO mouse models of either protein, future research should focus on the possible implications of this interaction in the insulin secretion pathway. Here, β-cell lines such as the human EndoC-βH1 cells (174) will be instrumental. These cells could also be used to identify the suggested mitochondrial pool of K8/K18 using advanced imaging techniques and to study the effect of β-cell stress (e.g. palmitate-induced and oxidative stress) on K8 and SCHAD expression.

7. References

1. Dolenšek J, Rupnik MS, Stožer A. Structural similarities and differences between the human and the mouse pancreas. Islets. 2015;7:e1024405.
2. Rahier J, Wallon J, Henquin JC. Cell populations in the endocrine pancreas of human neonates and infants. Diabetologia. 1981;20:540–6.
3. Romer AI, Sussel L. Pancreatic islet cell development and regeneration. Curr Opin Endocrinol Diabetes Obes. 2015;22:255–64.
4. Rorsman P, Ashcroft FM. Pancreatic β-Cell Electrical Activity and Insulin Secretion: Of Mice and Men. Physiol Rev. 2018;98:117–214.
5. Fu Z, R. Gilbert E, Liu D. Regulation of Insulin Synthesis and Secretion and Pancreatic Beta-Cell Dysfunction in Diabetes. Curr Diabetes Rev. 2012;9:25–53.
6. Wilcox G. Insulin and Insulin Resistance. Clin Biochem Rev. 2005;26:19–39.
7. Jain R, Lammert E. Cell-cell interactions in the endocrine pancreas. Diabetes, Obes Metab. 2009;11:159–67.
8. Brereton MF, Vergari E, Zhang Q, Clark A. Alpha-, Delta- and PP-cells. J Histochem Cytochem. 2015;63:575–91.
9. Ojha A, Ojha U, Mohammed R, Chandrashekar A, Ojha H. Current perspective on the role of insulin and glucagon in the pathogenesis and treatment of type 2 diabetes mellitus. Clin Pharmacol Adv Appl. 2019;11:57–65.
10. Yosten GLC. Alpha cell dysfunction in type 1 diabetes. Peptides. 2018;100:54–60.
11. Rorsman P, Huising MO. The somatostatin-secreting pancreatic δ-cell in health and disease. Nat Rev Endocrinol. 2018;14:404–14.
12. Wierup N, Sundler F, Heller RS. The islet ghrelin cell. J Mol Endocrinol. 2014;52:R35–49.
13. Müller TD, Nogueiras R, Andermann ML, Andrews ZB, Anker SD, Argente J, et al. Ghrelin. Mol Metab. 2015;4:437–60.
14. Pandiri AR. Overview of Exocrine Pancreatic Pathobiology. Toxicol Pathol. 2014;42:207–16.
15. Almaça J, Caicedo A. Blood Flow in the Pancreatic Islet: Not so Isolated Anymore. Diabetes. 2020;69:1336–8.
16. Barreto SG, Carati CJ, Toouli J, Saccone GTP. The islet-acinar axis of the pancreas: more than just insulin. Am J Physiol Liver Physiol. 2010;299:G10–22.
17. Egozi A, Bahar Halpern K, Farack L, Rotem H, Itzkovitz S. Zonation of Pancreatic Acinar Cells in Diabetic Mice. Cell Rep. 2020;32:108043.
18. Rickels MR, Norris AW, Hull RL. A tale of two pancreases: exocrine pathology and endocrine dysfunction. Diabetologia. 2020;63:2030–9.
19. Kikuta K. Impaired glucose tolerance in acute pancreatitis. World J Gastroenterol. 2015;21:7367.
20. Andersen DK, Korc M, Petersen GM, Eibl G, Li D, Rickels MR, et al. Diabetes, Pancreatogenic Diabetes, and Pancreatic Cancer. Diabetes. 2017;66:1103–10.
21. McCulloch LJ, van de Bunt M, Braun M, Frayn KN, Clark A, Gloyn AL. GLUT2 (SLC2A2) is not the principal glucose transporter in human pancreatic beta cells: Implications for understanding genetic association signals at this locus. Mol Genet Metab. 2011;104:648–53.
22. Rodriguez-Diaz R, Molano RD, Weitz JR, Abdulreda MH, Berman DM, Leibiger B, et al. Paracrine Interactions within the Pancreatic Islet Determine the Glycemic Set Point. Cell Metab. 2018;27:549-558.e4.
23. Iynedjian PB, Mobius G, Seitz HJ, Wollheim CB, Renold AE. Tissue-specific expression of glucokinase: identification of the gene product in liver and pancreatic islets. Proc Natl Acad Sci. 1986;83:1998–2001.
24. Cárdenas ML, Cornish-Bowden A, Ureta T. Evolution and regulatory role of the hexokinases. Biochim Biophys Acta - Mol Cell Res. 1998;1401:242–64.
25. Iynedjian PB. Molecular Physiology of Mammalian Glucokinase. Cell Mol Life Sci. 2009;66:27–42.
26. Röder P V., Wu B, Liu Y, Han W. Pancreatic regulation of glucose homeostasis. Exp Mol Med. 2016;48:e219–e219.
27. Rorsman P, Braun M. Regulation of Insulin Secretion in Human Pancreatic Islets. Annu Rev Physiol. 2013;75:155–79.
28. Barg S, Eliasson L, Renstrom E, Rorsman P. A Subset of 50 Secretory Granules in Close Contact With L-Type Ca2+ Channels Accounts for First-Phase Insulin Secretion in Mouse -Cells. Diabetes. 2002;51:S74–82.
29. Wang Z, Thurmond DC. Mechanisms of biphasic insulin-granule exocytosis - roles of the cytoskeleton, small GTPases and SNARE proteins. J Cell Sci. 2009;122:893–903.

30. Noguchi GM, Huising MO. Integrating the inputs that shape pancreatic islet hormone release. Nat Metab. 2019;1:1189–201.
31. Ahren B, Holst JJ. The Cephalic Insulin Response to Meal Ingestion in Humans Is Dependent on Both Cholinergic and Noncholinergic Mechanisms and Is Important for Postprandial Glycemia. Diabetes. 2001;50:1030–8.
32. Yau D, Laver TW, Dastamani A, Senniappan S, Houghton JAL, Shaikh G, et al. Using referral rates for genetic testing to determine the incidence of a rare disease: The minimal incidence of congenital hyperinsulinism in the UK is 1 in 28,389. PLoS One. 2020;15:e0228417.
33. Rahman SA, Nessa A, Hussain K. Molecular mechanisms of congenital hyperinsulinism. J Mol Endocrinol. 2015;54:R119–29.
34. Demirbilek H, Hussain K. Congenital Hyperinsulinism: Diagnosis and Treatment Update. J Clin Res Pediatr Endocrinol. 2018;9:69–87.
35. Palladino AA, Stanley CA. The hyperinsulinism/hyperammonemia syndrome. Rev Endocr Metab Disord. 2010;11:171–8.
36. DeBaun MR, King AA, White N. Hypoglycemia in Beckwith-Wiedemann syndrome. Semin Perinatol. 2000;24:164–71.
37. Nakamura Y, Takagi M, Yoshihashi H, Miura M, Narumi S, Hasegawa T, et al. A case with neonatal hyperinsulinemic hypoglycemia: It is a characteristic complication of sotos syndrome. Am J Med Genet Part A. 2015;167:1171–4.
38. Yap KL, Johnson AEK, Fischer D, Kandikatla P, Deml J, Nelakuditi V, et al. Congenital hyperinsulinism as the presenting feature of Kabuki syndrome: clinical and molecular characterization of 10 affected individuals. Genet Med. 2019;21:233–42.
39. Gibson CE, Boodhansingh KE, Li C, Conlin L, Chen P, Becker SA, et al. Congenital Hyperinsulinism in Infants with Turner Syndrome: Possible Association with Monosomy X and KDM6A Haploinsufficiency. Horm Res Paediatr. 2018;89:413–22.
40. Verkarre V, Fournet JC, de Lonlay P, Gross-Morand MS, Devillers M, Rahier J, et al. Paternal mutation of the sulfonylurea receptor (SUR1) gene and maternal loss of 11p15 imprinted genes lead to persistent hyperinsulinism in focal adenomatous hyperplasia. J Clin Invest. 1998;102:1286–91.
41. Sempoux C, Capito C, Bellanné-Chantelot C, Verkarre V, de Lonlay P, Aigrain Y, et al. Morphological Mosaicism of the Pancreatic Islets: A Novel Anatomopathological Form of Persistent Hyperinsulinemic Hypoglycemia of Infancy. J Clin Endocrinol Metab. 2011;96:3785–93.
42. Galcheva S, Demirbilek H, Al-Khawaga S, Hussain K. The Genetic and Molecular Mechanisms of Congenital Hyperinsulinism. Front Endocrinol (Lausanne). 2019;10:111.
43. Crane A, Aguilar-Bryan L. Assembly, Maturation, and Turnover of K ATP Channel Subunits. J Biol Chem. 2004;279:9080–90.
44. Yan F-F, Lin Y-W, MacMullen C, Ganguly A, Stanley CA, Shyng S-L. Congenital Hyperinsulinism Associated ABCC8 Mutations That Cause Defective Trafficking of ATP-Sensitive K+ Channels: Identification and Rescue. Diabetes. 2007;56:2339–48.
45. Shyng SL, Ferrigni T, Shepard JB, Nestorowicz A, Glaser B, Permutt MA, et al. Functional analyses of novel mutations in the sulfonylurea receptor 1 associated with persistent hyperinsulinemic hypoglycemia of infancy. Diabetes. 1998;47:1145–51.
46. Kapoor RR, Flanagan SE, James CT, McKiernan J, Thomas AM, Harmer SC, et al. Hyperinsulinaemic hypoglycaemia and diabetes mellitus due to dominant ABCC8/KCNJ11 mutations. Diabetologia. 2011;54:2575–83.
47. Damaj L, le Lorch M, Verkarre V, Werl C, Hubert L, Nihoul-Fékété C, et al. Chromosome 11p15 Paternal Isodisomy in Focal Forms of Neonatal Hyperinsulinism. J Clin Endocrinol Metab. 2008;93:4941–7.
48. Flanagan S, Vairo F, Johnson M, Caswell R, Laver T, Lango Allen H, et al. A CACNA1D mutation in a patient with persistent hyperinsulinaemic hypoglycaemia, heart defects, and severe hypotonia. Pediatr Diabetes. 2017;18:320–3.
49. Splawski I, Timothy KW, Vincent GM, Atkinson DL, Keating MT. Molecular basis of the long-QT syndrome associated with deafness. Proc Assoc Am Physicians. 1997;336:1562–7.
50. Torekov SS, Iepsen E, Christiansen M, Linneberg A, Pedersen O, Holst JJ, et al. KCNQ1 Long QT Syndrome Patients Have Hyperinsulinemia and Symptomatic Hypoglycemia. Diabetes. 2014;63:1315–25.
51. Otonkoski T, Kaminen N, Ustinov J, Lapatto R, Meissner T, Mayatepek E, et al. Physical Exercise-Induced Hyperinsulinemic Hypoglycemia Is an Autosomal-Dominant Trait Characterized by Abnormal Pyruvate-Induced Insulin Release. Diabetes. 2003;52:199–204.
52. Plaitakis A, Kalef-Ezra E, Kotzamani D, Zaganas I, Spanaki C. The Glutamate Dehydrogenase Pathway and Its Roles in Cell and Tissue Biology in Health and Disease. Biology (Basel). 2017;6:11.

53. Stanley CA, Fang J, Kutyna K, Hsu BYL, Ming JE, Glaser B, et al. Molecular basis and characterization of the hyperinsulinism/hyperammonemia syndrome: predominance of mutations in exons 11 and 12 of the glutamate dehydrogenase gene. HI/HA Contributing Investigators. Diabetes. 2000;49:667–73.
54. Santer R, Kinner M, Superti-Furga A, Schneppenheim R, Mayatepek E, Meissner T, et al. Novel missense mutations outside the allosteric domain of glutamate dehydrogenase are prevalent in European patients with the congenital hyperinsulinism-hyperammonemia syndrome. Hum Genet. 2001;108:66–71.
55. Li C, Najafi H, Daikhin Y, Nissim IB, Collins HW, Yudkoff M, et al. Regulation of Leucine-stimulated Insulin Secretion and Glutamine Metabolism in Isolated Rat Islets. J Biol Chem. 2003;278:2853–8.
56. Maechler P, Wollheim CB. Mitochondrial glutamate acts as a messenger in glucose-induced insulin exocytosis. Nature. 1999;402:685–9.
57. Treberg JR, Clow KA, Greene KA, Brosnan ME, Brosnan JT. Systemic activation of glutamate dehydrogenase increases renal ammoniagenesis: implications for the hyperinsulinism/hyperammonemia syndrome. Am J Physiol Metab. 2010;298:E1219–25.
58. Gloyn AL, Odili S, Zelent D, Buettger C, Castleden HAJ, Steele AM, et al. Insights into the Structure and Regulation of Glucokinase from a Novel Mutation (V62M), Which Causes Maturity-onset Diabetes of the Young. J Biol Chem. 2005;280:14105–13.
59. Martínez R, Gutierrez-Nogués Á, Fernández-Ramos C, Velayos T, Vela A, Navas M-Á, et al. Heterogeneity in phenotype of hyperinsulinism caused by activating glucokinase mutations: a novel mutation and its functional characterization. Clin Endocrinol (Oxf). 2017;86:778–83.
60. Quintens R, Hendrickx N, Lemaire K, Schuit F. Why expression of some genes is disallowed in β-cells. Biochem Soc Trans. 2008;36:300–5.
61. Pinney SE, Ganapathy K, Bradfield J, Stokes D, Sasson A, Mackiewicz K, et al. Dominant Form of Congenital Hyperinsulinism Maps to HK1 Region on 10q. Horm Res Paediatr. 2013;80:18–27.
62. Matthijs G, Schollen E, Heykants L, Grünewald S. Phosphomannomutase Deficiency: The Molecular Basis of the Classical Jaeken Syndrome (CDGS Type Ia). Mol Genet Metab. 1999;68:220–6.
63. Shanti B, Silink M, Bhattacharya K, Howard NJ, Carpenter K, Fietz M, et al. Congenital disorder of glycosylation type Ia: Heterogeneity in the clinical presentation from multivisceral failure to hyperinsulinaemic hypoglycaemia as leading symptoms in three infants with phosphomannomutase deficiency. J Inherit Metab Dis. 2009;32:241–51.
64. González-Barroso MM, Giurgea I, Bouillaud F, Anedda A, Bellanné-Chantelot C, Hubert L, et al. Mutations in UCP2 in Congenital Hyperinsulinism Reveal a Role for Regulation of Insulin Secretion. PLoS One. 2008;3:e3850.
65. Odom DT. Control of Pancreas and Liver Gene Expression by HNF Transcription Factors. Science. 2004;303:1378–81.
66. Gupta RK, Vatamaniuk MZ, Lee CS, Flaschen RC, Fulmer JT, Matschinsky FM, et al. The MODY1 gene HNF-4α regulates selected genes involved in insulin secretion. J Clin Invest. 2005;115:1006–15.
67. Miura A, Yamagata K, Kakei M, Hatakeyama H, Takahashi N, Fukui K, et al. Hepatocyte Nuclear Factor-4α Is Essential for Glucose-stimulated Insulin Secretion by Pancreatic β-Cells. J Biol Chem. 2006;281:5246–57.
68. Stanescu DE, Hughes N, Kaplan B, Stanley CA, De León DD. Novel Presentations of Congenital Hyperinsulinism due to Mutations in the MODY genes: HNF1A and HNF4A. J Clin Endocrinol Metab. 2012;97:E2026–30.
69. Lee CS, Sund NJ, Behr R, Herrera PL, Kaestner KH. Foxa2 is required for the differentiation of pancreatic α-cells. Dev Biol. 2005;278:484–95.
70. Lee CS, Sund NJ, Vatamaniuk MZ, Matschinsky FM, Stoffers DA, Kaestner KH. Foxa2 Controls Pdx1 Gene Expression in Pancreatic Beta-Cells In Vivo. Diabetes. 2002;51:2546–51.
71. Lantz KA, Vatamaniuk MZ, Brestelli JE, Friedman JR, Matschinsky FM, Kaestner KH. Foxa2 regulates multiple pathways of insulin secretion. J Clin Invest. 2004;114:512–20.
72. Vajravelu ME, Chai J, Krock B, Baker S, Langdon D, Alter C, et al. Congenital Hyperinsulinism and Hypopituitarism Attributable to a Mutation in FOXA2. J Clin Endocrinol Metab. 2018;103:1042–7.
73. Giri D, Vignola M, Gualtieri A, Scagliotti V, McNamara P, Peak M, et al. Novel FOXA2 mutation causes Hyperinsulinism, Hypopituitarism with Craniofacial and Endoderm-derived organ abnormalities. Yearb Paediatr Endocrinol. 2018;26:4315–26.
74. Ferrara C, Patel P, Becker S, Stanley CA, Kelly A. Biomarkers of Insulin for the Diagnosis of Hyperinsulinemic Hypoglycemia in Infants and Children. J Pediatr. 2016;168:212–9.
75. Palladino AA, Bennett MJ, Stanley CA. Hyperinsulinism in Infancy and Childhood: When an Insulin Level Is Not Always Enough. Clin Chem. 2008;54:256–63.
76. Aynsley-Green A, Hussain K, Hall J, Saudubray J, Nihoul-Fékété C, De Lonlay-Debeney P, et al. Practical management of hyperinsulinism in infancy. Arch Dis Child - Fetal Neonatal Ed. 2000;82:F98–F107.

77. Arnoux J-B, Verkarre V, Saint-Martin C, Montravers F, Brassier A, Valayannopoulos V, et al. Congenital hyperinsulinism: current trends in diagnosis and therapy. Orphanet J Rare Dis. 2011;6:63.
78. Özen H. Glycogen storage diseases: New perspectives. World J Gastroenterol. 2007;13:2541.
79. Tung JY, Boodhansingh K, Stanley CA, De León DD. Clinical heterogeneity of hyperinsulinism due to HNF1A and HNF4A mutations. Pediatr Diabetes. 2018;19:910–6.
80. Sandal T, Laborie L, Brusgaard K, Eide S, Christesen H, Søvik O, et al. The spectrum of ABCC8 mutations in Norwegian patients with congenital hyperinsulinism of infancy. Clin Genet. 2009;75:440–8.
81. Pearson ER, Boj SF, Steele AM, Barrett T, Stals K, Shield JP, et al. Macrosomia and Hyperinsulinaemic Hypoglycaemia in Patients with Heterozygous Mutations in the HNF4A Gene. PLoS Med. 2007 Apr;4:e118.
82. Molven A, Helgeland G, Sandal T, Njølstad PR. The Molecular Genetics and Pathophysiology of Congenital Hyperinsulinism Caused by Short-Chain 3-Hydroxyacyl-CoA Dehydrogenase Deficiency. In: Monogenic Hyperinsulinemic Hypoglycemia Disorders. 2012. p. 137–45.
83. Maria G, Antonia D, Michael A, Kate M, Sian E, Sarah FE, et al. Sirolimus: Efficacy and Complications in Children With Hyperinsulinemic Hypoglycemia: A 5-Year Follow-Up Study. J Endocr Soc. 2019;3:699–713.
84. Pullen TJ, Sylow L, Sun G, Halestrap AP, Richter EA, Rutter GA. Overexpression of Monocarboxylate Transporter-1 (Slc16a1) in Mouse Pancreatic -Cells Leads to Relative Hyperinsulinism During Exercise. Diabetes. 2012;61:1719–25.
85. Li C, Chen P, Palladino A, Narayan S, Russell LK, Sayed S, et al. Mechanism of Hyperinsulinism in Short-chain 3-Hydroxyacyl-CoA Dehydrogenase Deficiency Involves Activation of Glutamate Dehydrogenase. J Biol Chem. 2010;285:31806–18.
86. Koster JC, Remedi MS, Flagg TP, Johnson JD, Markova KP, Marshall BA, et al. Hyperinsulinism induced by targeted suppression of beta cell KATP channels. Proc Natl Acad Sci. 2002;99:16992–7.
87. Koster J., Marshall B., Ensor N, Corbett J., Nichols C. Targeted Overactivity of β Cell KATP Channels Induces Profound Neonatal Diabetes. Cell. 2000;100:645–54.
88. Miki T, Tashiro F, Iwanaga T, Nagashima K, Yoshitomi H, Aihara H, et al. Abnormalities of pancreatic islets by targeted expression of a dominant-negative KATP channel. Proc Natl Acad Sci. 1997;94:11969–73.
89. Oyama K, Minami K, Ishizaki K, Fuse M, Miki T, Seino S. Spontaneous Recovery From Hyperglycemia by Regeneration of Pancreatic Beta-Cells in Kir6.2G132S Transgenic Mice. Diabetes. 2006;55:1930–8.
90. Seghers V, Nakazaki M, DeMayo F, Aguilar-Bryan L, Bryan J. Sur1 Knockout Mice. J Biol Chem. 2000;275:9270–7.
91. Shiota C, Larsson O, Shelton KD, Shiota M, Efanov AM, Høy M, et al. Sulfonylurea Receptor Type 1 Knock-out Mice Have Intact Feeding-stimulated Insulin Secretion despite Marked Impairment in Their Response to Glucose. J Biol Chem. 2002;277:37176–83.
92. Shiota C, Rocheleau J V., Shiota M, Piston DW, Magnuson MA. Impaired glucagon secretory responses in mice lacking the type 1 sulfonylurea receptor. Am J Physiol Metab. 2005;289:E570–7.
93. Stancill JS, Cartailler J-P, Clayton HW, O'Connor JT, Dickerson MT, Dadi PK, et al. Chronic β-Cell Depolarization Impairs β-Cell Identity by Disrupting a Network of Ca 2+ -Regulated Genes. Diabetes. 2017;66:2175–87.
94. Miki T, Nagashima K, Tashiro F, Kotake K, Yoshitomi H, Tamamoto A, et al. Defective insulin secretion and enhanced insulin action in KATP channel-deficient mice. Proc Natl Acad Sci. 1998;95:10402–6.
95. Winarto A, Miki T, Seino S, Iwanaga T. Morphological Changes in Pancreatic Islets of KATP Channel-Deficient Mice. The Involvement of KATP Channels in the Survival of Insulin Cells and the Maintenance of Islet Architecture. Arch Histol Cytol. 2001;64:59–67.
96. Hugill A, Shimomura K, Ashcroft FM, Cox RD. A mutation in KCNJ11 causing human hyperinsulinism (Y12X) results in a glucose-intolerant phenotype in the mouse. Diabetologia. 2010;53:2352–6.
97. Remedi MS, Rocheleau J V., Tong A, Patton BL, McDaniel ML, Piston DW, et al. Hyperinsulinism in mice with heterozygous loss of KATP channels. Diabetologia. 2006;49:2368–78.
98. Lin Y-W, MacMullen C, Ganguly A, Stanley CA, Shyng S-L. A Novel KCNJ11 Mutation Associated with Congenital Hyperinsulinism Reduces the Intrinsic Open Probability of β-Cell ATP-sensitive Potassium Channels. J Biol Chem. 2006;281:3006–12.
99. Grimberg A, Ferry RJ, Kelly A, Koo-McCoy S, Polonsky K, Glaser B, et al. Dysregulation of Insulin Secretion in Children With Congenital Hyperinsulinism due to Sulfonylurea Receptor Mutations. Diabetes. 2001;50:322–8.

100. Casimiro MC, Knollmann BC, Ebert SN, Vary JC, Greene AE, Franz MR, et al. Targeted disruption of the Kcnq1 gene produces a mouse model of Jervell and Lange- Nielsen Syndrome. Proc Natl Acad Sci. 2001;98:2526–31.
101. Boini KM, Graf D, Hennige AM, Koka S, Kempe DS, Wang K, et al. Enhanced insulin sensitivity of gene-targeted mice lacking functional KCNQ1. Am J Physiol Integr Comp Physiol. 2009;296:R1695–701.
102. Shimomura K, Tusa M, Iberl M, Brereton MF, Kaizik S, Proks P, et al. A Mouse Model of Human Hyperinsulinism Produced by the E1506K Mutation in the Sulphonylurea Receptor SUR1. Diabetes. 2013;62:3797–806.
103. Li C, Matter A, Kelly A, Petty TJ, Najafi H, MacMullen C, et al. Effects of a GTP-insensitive Mutation of Glutamate Dehydrogenase on Insulin Secretion in Transgenic Mice. J Biol Chem. 2006;281:15064–72.
104. Kibbey RG, Choi CS, Lee H-Y, Cabrera O, Pongratz RL, Zhao X, et al. Mitochondrial GTP Insensitivity Contributes to Hypoglycemia in Hyperinsulinemia Hyperammonemia by Inhibiting Glucagon Release. Diabetes. 2014;63:4218–29.
105. Niswender KD, Shiota M, Postic C, Cherrington AD, Magnuson MA. Effects of Increased Glucokinase Gene Copy Number on Glucose Homeostasis and Hepatic Glucose Metabolism. J Biol Chem. 1997;272:22570–5.
106. Shiota M, Postic C, Fujimoto Y, Jetton TL, Dixon K, Pan D, et al. Glucokinase Gene Locus Transgenic Mice Are Resistant to the Development of Obesity-Induced Type 2 Diabetes. Diabetes. 2001;50:622–9.
107. Epstein PN, Boschero AC, Atwater I, Cai X, Overbeek PA. Expression of yeast hexokinase in pancreatic beta cells of transgenic mice reduces blood glucose, enhances insulin secretion, and decreases diabetes. Proc Natl Acad Sci. 1992;89:12038–42.
108. Zhang C-Y, Baffy G, Perret P, Krauss S, Peroni O, Grujic D, et al. Uncoupling Protein-2 Negatively Regulates Insulin Secretion and Is a Major Link between Obesity, β Cell Dysfunction, and Type 2 Diabetes. Cell. 2001;105:745–55.
109. Joseph JW, Koshkin V, Zhang C-Y, Wang J, Lowell BB, Chan CB, et al. Uncoupling Protein 2 Knockout Mice Have Enhanced Insulin Secretory Capacity After a High-Fat Diet. Diabetes. 2002;51:3211–9.
110. Pontoglio M, Barra J, Hadchouel M, Doyen A, Kress C, Bach JP, et al. Hepatocyte Nuclear Factor 1 Inactivation Results in Hepatic Dysfunction, Phenylketonuria, and Renal Fanconi Syndrome. Cell. 1996;84:575–85.
111. Lee Y-H, Sauer B, Gonzalez FJ. Laron Dwarfism and Non-Insulin-Dependent Diabetes Mellitus in the Hnf-1α Knockout Mouse. Mol Cell Biol. 1998;18:3059–68.
112. Shih DQ, Bussen M, Sehayek E, Ananthanarayanan M, Shneider BL, Suchy FJ, et al. Hepatocyte nuclear factor-1α is an essential regulator of bile acid and plasma cholesterol metabolism. Nat Genet. 2001;27:375–82.
113. Shih DQ, Screenan S, Munoz KN, Philipson L, Pontoglio M, Yaniv M, et al. Loss of HNF-1 Function in Mice Leads to Abnormal Expression of Genes Involved in Pancreatic Islet Development and Metabolism. Diabetes. 2001;50:2472–80.
114. Sund NJ. Tissue-specific deletion of Foxa2 in pancreatic beta cells results in hyperinsulinemic hypoglycemia. Genes Dev. 2001;15:1706–15.
115. Zengbin Wu, MM, Aihua Fei, PhD, Yingbin Liu P, and Shuming Pan P. Conditional Tissue-Specific Foxa2 Ablation in Mouse Pancreas Causes Hyperinsulinemic Hypoglycemia. Am J Ther. 2017;24:e240.
116. Nishio H, Kuwahara M, Tsubone H, Koda Y, Sato T, Fukunishi S, et al. Identification of an ethnic-specific variant (V207M) of the KCNQ1 cardiac potassium channel gene in sudden unexplained death and implications from a knock-in mouse model. Int J Legal Med. 2009;123:253–7.
117. Casimiro MC, Knollmann BC, Yamoah EN, Nie L, Vary JC, Sirenko SG, et al. Targeted point mutagenesis of mouse Kcnq1: phenotypic analysis of mice with point mutations that cause Romano-Ward syndrome in humans. Genomics. 2004;84:555–64.
118. Herrera PL. Adult insulin- and glucagon-producing cells differentiate from two independent cell lineages. Development. 2000;127:2317–22.
119. Postic C, Shiota M, Niswender KD, Jetton TL, Chen Y, Moates JM, et al. Dual Roles for Glucokinase in Glucose Homeostasis as Determined by Liver and Pancreatic β Cell-specific Gene Knock-outs Using Cre Recombinase. J Biol Chem. 1999;274:305–15.
120. Brouwers B, de Faudeur G, Osipovich AB, Goyvaerts L, Lemaire K, Boesmans L, et al. Impaired Islet Function in Commonly Used Transgenic Mouse Lines due to Human Growth Hormone Minigene Expression. Cell Metab. 2014;20:979–90.
121. Thorens B, Tarussio D, Maestro MA, Rovira M, Heikkilä E, Ferrer J. Ins1 Cre knock-in mice for beta cell-specific gene recombination. Diabetologia. 2015;58:558–65.

122. Barycki JJ, O'Brien LK, Bratt JM, Zhang R, Sanishvili R, Strauss AW, et al. Biochemical Characterization and Crystal Structure Determination of Human Heart Short Chain-3-Hydroxyacyl-CoA Dehydrogenase Provide Insights into Catalytic Mechanism. Biochemistry. 1999;38:5786–98.
123. Xu Y, Li H, Jin Y-H, Fan J, Sun F. Dimerization Interface of 3-Hydroxyacyl-CoA Dehydrogenase Tunes the Formation of Its Catalytic Intermediate. PLoS One. 2014;9:e95965.
124. Barycki JJ. Sequestration of the active site by interdomain shifting: crystallographic and spectroscopic evidence for distinct conformations of L-3-Hydroxyacyl-CoA dehydrogenase. J Biol Chem. 2000;275:27186–96.
125. Houten SM, Violante S, Ventura F V., Wanders RJA. The Biochemistry and Physiology of Mitochondrial Fatty Acid β-Oxidation and Its Genetic Disorders. Annu Rev Physiol. 2016;78:23–44.
126. Schönfeld P, Wojtczak L. Short- and medium-chain fatty acids in energy metabolism: the cellular perspective. J Lipid Res. 2016;57:943–54.
127. Clayton PT, Eaton S, Aynsley-Green A, Edginton M, Hussain K, Krywawych S, et al. Hyperinsulinism in short-chain L-3-hydroxyacyl-CoA dehydrogenase deficiency reveals the importance of β-oxidation in insulin secretion. J Clin Invest. 2001;108:457–65.
128. Molven A, Matre GE, Duran M, Wanders RJ, Rishaug U, Njolstad PR, et al. Familial Hyperinsulinemic Hypoglycemia Caused by a Defect in the SCHAD Enzyme of Mitochondrial Fatty Acid Oxidation. Diabetes. 2004;53:221–7.
129. Hussain K, Clayton PT, Krywawych S, Chatziandreou I, Mills P, Ginbey DW, et al. Hyperinsulinism of infancy associated with a novel splice site mutation in the SCHAD gene. J Pediatr. 2005;146:706–8.
130. Bennett M, Russell L, Tokunaga C, Narayan S, Tan L, Seegmiller A, et al. Reye-like syndrome resulting from novel missense mutations in mitochondrial medium- and short-chain l-3-hydroxy-acyl-CoA dehydrogenase. Mol Genet Metab. 2006;89:74–9.
131. Kapoor RR, James C, Flanagan SE, Ellard S, Eaton S, Hussain K. 3-Hydroxyacyl-Coenzyme A Dehydrogenase Deficiency and Hyperinsulinemic Hypoglycemia: Characterization of a Novel Mutation and Severe Dietary Protein Sensitivity. J Clin Endocrinol Metab. 2009;94:2221–5.
132. Di Candia S, Gessi A, Pepe G, Sogno Valin P, Mangano E, Chiumello G, et al. Identification of a diffuse form of hyperinsulinemic hypoglycemia by 18-fluoro-l-3,4 dihydroxyphenylalanine positron emission tomography/CT in a patient carrying a novel mutation of the HADH gene. Eur J Endocrinol. 2009;160:1019–23.
133. Martins E, Cardoso ML, Rodrigues E, Barbot C, Ramos A, Bennett MJ, et al. Short-chain 3-hydroxyacyl-CoA dehydrogenase deficiency: the clinical relevance of an early diagnosis and report of four new cases. J Inherit Metab Dis. 2011;34:835–42.
134. Flanagan SE, Patch A-M, Locke JM, Akcay T, Simsek E, Alaei M, et al. Genome-Wide Homozygosity Analysis Reveals HADH Mutations as a Common Cause of Diazoxide-Responsive Hyperinsulinemic-Hypoglycemia in Consanguineous Pedigrees. J Clin Endocrinol Metab. 2011;96:E498–502.
135. Snider KE, Becker S, Boyajian L, Shyng S-L, MacMullen C, Hughes N, et al. Genotype and Phenotype Correlations in 417 Children With Congenital Hyperinsulinism. J Clin Endocrinol Metab. 2013;98:E355–63.
136. Fan Z, Ni J, Yang L, Hu L, Ma S, Mei M, et al. Uncovering the molecular pathogenesis of congenital hyperinsulinism by panel gene sequencing in 32 Chinese patients. Mol Genet Genomic Med. 2015;3:526–36.
137. Satapathy AK, Jain V, Ellard S, Flanagan SE. Hyperinsulinemic hypoglycemia of infancy due to novel HADH mutation in two siblings. Indian Pediatr. 2016;53:912–3.
138. Babiker O, Flanagan SE, Ellard S, Girim H Al, Hussain K, Senniappan S. Protein-induced hyperinsulinaemic hypoglycaemia due to a homozygous HADH mutation in three siblings of a Saudi family. J Pediatr Endocrinol Metab. 2015;28:1073–7.
139. Çamtosun E, Flanagan SE, Ellard S, Şıklar Z, Hussain K, Kocaay P, et al. A Deep Intronic HADH Splicing Mutation (c.636+471G>T) in a Congenital Hyperinsulinemic Hypoglycemia Case: Long Term Clinical Course. J Clin Res Pediatr Endocrinol. 2015;7:144–7.
140. Senniappan S, Sadeghizadeh A, Flanagan SE, Ellard S, Hashemipour M, Hosseinzadeh M, et al. Genotype and phenotype correlations in Iranian patients with hyperinsulinaemic hypoglycaemia. BMC Res Notes. 2015;8:350.
141. Vilarinho L, Sales Marques J, Rocha H, Ramos A, Lopes L, Narayan SB, et al. Diagnosis of a patient with a kinetic variant of medium and short-chain 3-hydroxyacyl-CoA dehydrogenase deficiency by newborn screening. Mol Genet Metab. 2012;106:277–80.
142. Popa FI, Perlini S, Teofoli F, Degani D, Funghini S, La Marca G, et al. 3-Hydroxyacyl-Coenzyme A Dehydrogenase Deficiency: Identification of a New Mutation Causing Hyperinsulinemic Hypoketotic Hypoglycemia, Altered Organic Acids and Acylcarnitines Concentrations. In: JIMD Reports. 2011. p. 71–7.

143. Susanne Weiss, Nadine Bachmann, Ertan Mayatepek, Carsten Bergmann, Thomas Meissner SK. Two patients with HADH (SCHAD) Hyperinsulinism in part without detectable 3-Hydroxybutyrylcarnitine/ 3-Hydroxyglutarate [Internet]. 2016. Available from: https://abstracts.eurospe.org/hrp/0086/hrp0086P1-P195
144. Xu Z-D, Zhang W, Liu M, Wang H-M, Hui P-P, Liang X-J, et al. Analysis on the pathogenic genes of 60 Chinese children with congenital hyperinsulinemia. Endocr Connect. 2018;7:1251–61.
145. Pepin É, Guay C, Delghingaro-Augusto V, Joly E, Madiraju SRM, Prentki M. Short-chain 3-hydroxyacyl-CoA dehydrogenase is a negative regulator of insulin secretion in response to fuel and non-fuel stimuli in INS832/13 β-cells. J Diabetes. 2010;2:157–67.
146. Martens GA, Vervoort A, Van de Casteele M, Stangé G, Hellemans K, Van Thi HV, et al. Specificity in Beta Cell Expression of l-3-Hydroxyacyl-CoA Dehydrogenase, Short Chain, and Potential Role in Down-regulating Insulin Release. J Biol Chem. 2007;282:21134–44.
147. Hardy OT, Hohmeier HE, Becker TC, Manduchi E, Doliba NM, Gupta RK, et al. Functional Genomics of the β-Cell: Short-Chain 3-Hydroxyacyl-Coenzyme A Dehydrogenase Regulates Insulin Secretion Independent of K+ Currents. Mol Endocrinol. 2007;21:765–73.
148. Filling C, Keller B, Hirschberg D, Marschall H-U, Jörnvall H, Bennett MJ, et al. Role of short-chain hydroxyacyl CoA dehydrogenases in SCHAD deficiency. Biochem Biophys Res Commun. 2008;368:6–11.
149. Frigerio F, Casimir M, Carobbio S, Maechler P. Tissue specificity of mitochondrial glutamate pathways and the control of metabolic homeostasis. Biochim Biophys Acta - Bioenerg. 2008;1777:965–72.
150. Molven A, Hollister-Lock J, Hu J, Martinez R, Njølstad PR, Liew CW, et al. The Hypoglycemic Phenotype Is Islet Cell–Autonomous in Short-Chain Hydroxyacyl-CoA Dehydrogenase–Deficient Mice. Diabetes. 2016;65:1672–8.
151. Narayan SB, Master SR, Sireci AN, Bierl C, Stanley PE, Li C, et al. Short-Chain 3-Hydroxyacyl-Coenzyme A Dehydrogenase Associates with a Protein Super-Complex Integrating Multiple Metabolic Pathways. PLoS One. 2012;7:e35048.
152. Fuchsberger C, Flannick J, Teslovich TM, Mahajan A, Agarwala V, Gaulton KJ, et al. The genetic architecture of type 2 diabetes. Nature. 2016;536:41–7.
153. Lu M, Li C. Nutrient sensing in pancreatic islets: lessons from congenital hyperinsulinism and monogenic diabetes. Ann N Y Acad Sci. 2018;1411:65–82.
154. Lawlor N, George J, Bolisetty M, Kursawe R, Sun L, Sivakamasundari V, et al. Single-cell transcriptomes identify human islet cell signatures and reveal cell-type–specific expression changes in type 2 diabetes. Genome Res. 2017;27:208–22.
155. Martens GA, Jiang L, Hellemans KH, Stangé G, Heimberg H, Nielsen FC, et al. Clusters of Conserved Beta Cell Marker Genes for Assessment of Beta Cell Phenotype. PLoS One. 2011;6:e24134.
156. Schaum N, Karkanias J, Neff NF, May AP, Quake SR, Wyss-Coray T, et al. Single-cell transcriptomics of 20 mouse organs creates a Tabula Muris. Nature. 2018;562:367–72.
157. Zhong F, Jiang Y. Endogenous Pancreatic β Cell Regeneration: A Potential Strategy for the Recovery of β Cell Deficiency in Diabetes. Front Endocrinol (Lausanne). 2019;10:101.
158. White P, Lee May C, Lamounier RN, Brestelli JE, Kaestner KH. Defining Pancreatic Endocrine Precursors and Their Descendants. Diabetes. 2008;57:654–68.
159. Herring CM, Bazer FW, Johnson GA, Wu G. Impacts of maternal dietary protein intake on fetal survival, growth, and development. Exp Biol Med. 2018;243:525–33.
160. Helman A, Cangelosi AL, Davis JC, Pham Q, Rothman A, Faust AL, et al. A Nutrient-Sensing Transition at Birth Triggers Glucose-Responsive Insulin Secretion. Cell Metab. 2020;31:1004-1016.e5.
161. Kapoor RR, Flanagan SE, Fulton P, Chakrapani A, Chadefaux B, Ben-Omran T, et al. Hyperinsulinism–hyperammonaemia syndrome: novel mutations in the GLUD1 gene and genotype–phenotype correlations. Eur J Endocrinol. 2009;161:731–5.
162. Heslegrave AJ, Kapoor RR, Eaton S, Chadefaux B, Akcay T, Simsek E, et al. Leucine-sensitive hyperinsulinaemic hypoglycaemia in patients with loss of function mutations in 3-Hydroxyacyl-CoA Dehydrogenase. Orphanet J Rare Dis. 2012;7:25.
163. Quesada I, Tudurí E, Ripoll C, Nadal Á. Physiology of the pancreatic α-cell and glucagon secretion: role in glucose homeostasis and diabetes. J Endocrinol. 2008;199:5–19.
164. Dean ED. A Primary Role for α-Cells as Amino Acid Sensors. Diabetes. 2020;69:542–9.
165. Yang J, MacDougall ML, McDowell MT, Xi L, Wei R, Zavadoski WJ, et al. Polyomic profiling reveals significant hepatic metabolic alterations in glucagon-receptor (GCGR) knockout mice: implications on anti-glucagon therapies for diabetes. BMC Genomics. 2011;12:281.
166. Solloway MJ, Madjidi A, Gu C, Eastham-Anderson J, Clarke HJ, Kljavin N, et al. Glucagon Couples Hepatic Amino Acid Catabolism to mTOR-Dependent Regulation of α-Cell Mass. Cell Rep. 2015;12:495–510.

167. Dean ED, Li M, Prasad N, Wisniewski SN, Von Deylen A, Spaeth J, et al. Interrupted Glucagon Signaling Reveals Hepatic α Cell Axis and Role for L-Glutamine in α Cell Proliferation. Cell Metab. 2017;25:1362-1373.e5.
168. Kim J, Okamoto H, Huang Z, Anguiano G, Chen S, Liu Q, et al. Amino Acid Transporter Slc38a5 Controls Glucagon Receptor Inhibition-Induced Pancreatic α Cell Hyperplasia in Mice. Cell Metab. 2017;25:1348-1361.e8.
169. Lorin S, Tol MJ, Bauvy C, Strijland A, Poüs C, Verhoeven AJ, et al. Glutamate dehydrogenase contributes to leucine sensing in the regulation of autophagy. Autophagy. 2013;9:850–60.
170. Alam CM, Silvander JSG, Daniel EN, Tao G-Z, Kvarnström SM, Alam P, et al. Keratin 8 modulates β-cell stress responses and normoglycaemia. J Cell Sci. 2013;126:5635–44.
171. Mathew J, Loranger A, Gilbert S, Faure R, Marceau N. Keratin 8/18 regulation of glucose metabolism in normal versus cancerous hepatic cells through differential modulation of hexokinase status and insulin signaling. Exp Cell Res. 2013;319:474–86.
172. Silvander JSG, Kvarnström SM, Kumari-Ilieva A, Shrestha A, Alam CM, Toivola DM. Keratins regulate β-cell mitochondrial morphology, motility, and homeostasis. FASEB J. 2017;31:4578–87.
173. Merglen A, Theander S, Rubi B, Chaffard G, Wollheim CB, Maechler P. Glucose Sensitivity and Metabolism-Secretion Coupling Studied during Two-Year Continuous Culture in INS-1E Insulinoma Cells. Endocrinology. 2004;145:667–78.
174. Ravassard P, Hazhouz Y, Pechberty S, Bricout-Neveu E, Armanet M, Czernichow P SR. A genetically engineered human pancreatic β cell line exhibiting glucose-inducible insulin secretion. J Clin Invest. 2011;121:3589–97.

I

Received: 11 September 2019 | Revised: 24 August 2020 | Accepted: 28 August 2020

DOI: 10.1002/jimd.12309

ORIGINAL ARTICLE

JIMD SSIEM WILEY

Functional evaluation of 16 SCHAD missense variants: Only amino acid substitutions causing congenital hyperinsulinism of infancy lead to loss-of-function phenotypes in vitro

Kelly Velasco[1] | **Johanna L. St-Louis**[1] | **Henrikke N. Hovland**[1] | **Nels Thompson**[1] | **Åsta Ottesen**[1] | **Man Hung Choi**[1,2] | **Line Pedersen**[1] | **Pål R. Njølstad**[3,4] | **Thomas Arnesen**[5,6,7] | **Karianne Fjeld**[1,8] | **Ingvild Aukrust**[3,8] | **Line M. Myklebust**[5,6] | **Anders Molven**[1,2,3]

[1]Gade Laboratory for Pathology, Department of Clinical Medicine, University of Bergen, Bergen, Norway

[2]Department of Pathology, Haukeland University Hospital, Bergen, Norway

[3]Center for Diabetes Research, Department of Clinical Science, University of Bergen, Bergen, Norway

[4]Department of Pediatrics and Adolescent Medicine, Haukeland University Hospital, Bergen, Norway

[5]Department of Biomedicine, University of Bergen, Bergen, Norway

[6]Department of Biological Sciences, University of Bergen, Bergen, Norway

[7]Department of Surgery, Haukeland University Hospital, Bergen, Norway

[8]Department of Medical Genetics, Haukeland University Hospital, Bergen, Norway

Correspondence
Anders Molven, Gade Laboratory for Pathology, Department of Clinical Medicine, Haukeland University Hospital, University of Bergen, N-5021 Bergen, Norway.
Email: anders.molven@uib.no

Funding information
Helse Vest Regionalt Helseføretak, Grant/Award Number: HV 912258; Norges Forskningsråd, Grant/Award Number: FRIMEDBIO 240788; Novo Nordisk Fonden, Grant/Award Number: NNF15OC0016330

Communicating Editor: Sander M Houten

Abstract

Short-chain 3-hydroxyacyl-CoA dehydrogenase (SCHAD), encoded by the *HADH* gene, is a ubiquitously expressed mitochondrial enzyme involved in fatty acid oxidation. This protein also plays a role in insulin secretion as recessive *HADH* mutations cause congenital hyperinsulinism of infancy (CHI) via loss of an inhibitory interaction with glutamate dehydrogenase (GDH). Here, we present a functional evaluation of 16 SCHAD missense variants identified either in CHI patients or by high-throughput sequencing projects in various populations. To avoid interactions with endogenously produced SCHAD protein, we assessed protein stability, subcellular localization, and GDH interaction in a SCHAD knockout HEK293 cell line constructed by CRISPR-Cas9 methodology. We also established methods for efficient SCHAD expression and purification in *E. coli*, and tested enzymatic activity of the variants. Our analyses showed that rare variants of unknown significance identified in populations generally had similar properties as normal SCHAD. However, the CHI-associated variants p.Gly34Arg, p.Ile184Phe, p.Pro258Leu, and p.Gly303Ser were unstable with low protein levels detectable when

expressed in HEK293 cells. Moreover, CHI variants p.Lys136Glu, p.His170Arg, and p.Met188Val presented normal protein levels but displayed clearly impaired enzymatic activity in vitro, and their interaction with GDH appeared reduced. Our results suggest that pathogenic missense variants of SCHAD either make the protein target of a post-translational quality control system or can impair the function of SCHAD without influencing its steady-state protein level. We did not find any evidence that rare SCHAD missense variants observed only in the general population and not in CHI patients are functionally affected.

KEYWORDS

congenital hyperinsulinism of infancy, *HADH*, loss-of-function mutations, SCHAD, short-chain 3-hydroxyacyl-CoA dehydrogenase, variants of unknown significance

1 | INTRODUCTION

An increasing challenge of clinical medicine is how to handle the wealth of information provided by high-throughput genetic analyses. For a given patient, techniques such as whole-exome and whole-genome sequencing may reveal multiple, rare genetic variants that are of unknown significance with regard to health implications.[1] Predicting the functional effect based on bioinformatics analyses alone is still unreliable, particularly for missense mutations; that is, when the genetic variant results in amino acid substitutions at the protein level. This problem has, for example, been illustrated by studies of *HNF1A* variants implicated in monogenic diabetes.[2]

A concerted effort to functionally evaluate missense variants of the *HADH* gene has so far not been performed. This gene encodes short-chain 3-hydroxyacyl-CoA dehydrogenase (SCHAD; EC 1.1.1.35), a mitochondrial protein expressed in all cells. It exerts a general metabolic function by catalyzing the third step of β-oxidation of short- and medium-chain fatty acids.[3] In addition, SCHAD has a specific role in glucose homeostasis by inhibiting insulin secretion in the pancreatic β-cells,[4-7] most likely through an inhibitory effect on the activity of another metabolic enzyme: glutamate dehydrogenase (GDH).[8,9] Thus, a number of recessive mutations in the *HADH* gene have been found to cause congenital hyperinsulinism of infancy (CHI; OMIM # 609975).[10-12] CHI is a disease characterized by inappropriately elevated plasma concentrations of insulin, resulting in episodes of hypoglycemia that may become life-threatening if not treated correctly.[13,14]

The gnomAD data set contains 155 *HADH* missense variants, of which 154 are rare with an allele frequency < 0.01.[15] Only few of the SCHAD-CHI case reports have examined protein expression and enzymatic activity of the mutation in question.[10,16,17] In addition, a study of the *C. elegans* SCHAD protein experimentally evaluated the structural and functional impact of two amino acid substitutions in the conserved dimerization interface of the protein.[18]

Here we have initiated a systematic assessment of SCHAD amino acid substitutions by establishing a toolkit of prokaryotic and eukaryotic expression vectors for producing the protein variants as well as a SCHAD knockout cell line for functional testing. We have tested 16 naturally occurring missense variants for stability, subcellular localization, enzymatic activity and GDH interaction. Overall, our data showed that SCHAD variants reported in CHI patients display various loss-of-function phenotypes, whereas functional defects were not seen in any rare variant of the general population.

2 | MATERIALS AND METHODS

2.1 | Plasmids

The complete coding sequence of the human *HADH* gene (transcript variant 2, NCBI reference sequence NM_005327.4) was synthesized (DNA 2.0) flanked by sites for the restriction enzymes *Eco*RI and *Xho*I. For eukaryotic SCHAD expression, the synthetic gene was transferred to expression vector pcDNA3.1/V5-His B (Invitrogen). The insert was cloned in-frame with the C-terminal V5/His tag using *Eco*RI/*Xho*I and the Quick Ligation Kit (NEB).

For prokaryotic expression, the synthetic gene served as template to amplify *HADH* without the mitochondrial import signal. Overhangs with *Bsm*I and *Nco*I sites were added in the 5′-end and an *Acc*65I site in the 3′-end. PCR

primers were 5′-CATCATCGTCTCCCATGGGATCC-TCCTCGTCCAC-3′ and 5′-CATCATGGTACCATCA-CTTGTATTTGTAAAATCCTTCTC-3′. Phusion High-Fidelity PCR polymerase (Thermo Fisher Scientific) was used with annealing at 53.2°C for 20 seconds. The PCR product was blunt-end-cloned into the vector pJet1.2 (CloneJET PCR Cloning Kit, Thermo Fisher Scientific). Subsequently, the *HADH* insert of the pJet1.2 vector was ligated to the pETM41-His/MBP expression vector in-frame with an N-terminal 6His/Maltose Binding Protein (MBP) tag (Quick Ligation Kit). Restriction enzymes *Acc*65I/*Bsm*BI were used for the insert and *Acc*65I/*Nco*I for the vector.

Sixteen missense variants chosen from the gnomAD data set[15] (transcript ENST00000309522) and from CHI case reports were introduced in the plasmids by using the QuickChange II XL Site Directed Mutagenesis Kit (Agilent). This kit was also used to delete the SCHAD mitochondrial import signal (Δ2-12 construct). Primers used to produce each variant are listed in Table S1.

The plasmid Plu-CMV-hGDH for over-expressing human GDH was kindly provided by Dr Charles Stanley, Philadelphia.

For propagation, all plasmids were heat shock-transformed into One Shot TOP10 competent *E. coli*. Plasmids were prepared by the QIAfilter Plasmid Midi Kit (QIAGEN) and controlled by linearization/agarose gel electrophoresis and Sanger sequencing.

Empty vector (EV) pcDNA3.1/V5-His B was used as negative control in the expression studies. Theoretical molecular masses were estimated using the ProtParam tool on the ExPASy server.[19] All sequence analyses for site-directed mutagenesis and for CRISPR-Cas9 genome editing (below) were performed by the SnapGene software (GSL Biotech).

2.2 | Antibodies

To detect SCHAD protein by western blotting, different polyclonal antibodies were used: rabbit anti-SCHAD (Atlas Antibodies, HPA039588; GeneTex, GTX105167) and goat anti-SCHAD (Novus Biologicals, NB100-77343). A custom-made monoclonal mouse anti-SCHAD antibody (epitope QTEDILAKSK) from Abmart was employed in some experiments. Mouse anti-V5 (R960-25), anti-mouse HRP conjugate (626520), anti-rabbit HRP conjugate (656120), anti-mouse Alexa Fluor 488 conjugate (A-11017), and goat anti-GLUD1/2 (PA5-19267) were from Thermo Fisher Scientific. Rabbit anti-β-tubulin (ab6046) and anti-β-catenin (ab32572) were from Abcam. Mouse IgG2a (X0943) was from DAKO.

2.3 | Establishment of a HEK293 SCHAD knockout (KO) cell line by CRISPR-Cas9

The gRNAs 5′-CACCGCACGGAACGCATGAACTGCC-3′ and 5′-AAACGGCAGTTCATGCGTTCCGTGC-3′, targeting the sequence 5′-CCAGGCAGTTCATGCG TTCCGTG- 3′ in the proximity of the *HADH* start codon were designed via the website http://crispr.mit.edu. After phosphorylation by T4 polynucleotide kinase, the gRNAs were kept at 95°C for 5 minutes, annealed by decreasing the temperature to 25°C (rate: 5°C/min), ligated into the pSpCas9(BB)-2A-Puro (PX459 v.2) plasmid (Addgene) using *Bbs*I sites, and transformed into One Shot TOP10 competent *E. coli*. Plasmid preparations were sequenced using the primer 5′-GAGGGCCTATTTCCCATGATT-3′. Human embryonic kidney (HEK293) cells (Clontech) were transfected for 48 hours using the calcium phosphate method. Cells carrying plasmid were then selected using 3 μg/mL puromycin in the growth medium for 96 hours. Surviving cells were detached with trypsin, and single cells were hand-picked and transferred to individual wells in a 96-well plate. *HADH* exon 1 was sequenced in surviving clones using the primers 5′-TCAACGCTGGGACGTTACA-3′ and 5′-GTGAAAACT CCCTGGTGTCG-3′. Finally, SCHAD expression in the generated cell lines was evaluated by western blotting.

2.4 | HEK293 cell culture, SCHAD-V5 plasmid expression, western blotting

HEK293 cells (WT and SCHAD KO) were cultured in DMEM medium supplemented with 10% FBS (Gibco) and PenStrep (Sigma-Aldrich), and maintained in 5% CO_2 at 37°C. Unless indicated otherwise, Lipofectamine 2000 (Thermo Fisher Scientific) was used for transfection.

Treatment with the proteasome inhibitor MG132 (Sigma-Aldrich) was done 24 hours after transfection. The culture medium was removed, and cells were incubated with 5 μM MG132 or an equivalent volume of DMSO in fresh medium for the specified amount of time.

To produce HEK293 whole-cell lysates, cells were incubated in RIPA buffer (Thermo Fisher Scientific) and centrifuged at 14 000*g* for 15 minutes at 4°C to obtain a clear supernatant. Protein concentration was measured using the Pierce BCA protein assay kit (Thermo Fisher Scientific).

For western blotting, the samples were mixed with loading buffer and reducing agent, heated at 70°C for 10 minutes and subjected to SDS-PAGE before transfer to a PVDF membrane. The proteins of interest were detected using specific antibodies and visualized by

enhanced chemiluminescence using Amersham ECL Prime Western Blotting detection reagent (GE Healthcare) and a GBOX I Chemi XR5 imager (Syngene).

2.5 | Cell-free expression of SCHAD-V5 plasmids

Cell-free expression of SCHAD variants was achieved by incubating the pcDNA3.1-SCHAD-V5-His plasmids in TNT T7 Quick Coupled Transcription/Translation master mix (Promega). Each reaction was incubated for 90 minutes at 30°C, and 3 μL were analyzed by western blotting.

2.6 | Immunostaining and microscopy

HEK293 SCHAD KO cells were grown on poly-L-lysine coated glass coverslips. To label the mitochondria, cells were incubated for 30 minutes in 200 nM MitoTracker Red CMXRos (Invitrogen) diluted in pre-warmed cell medium. Cells were fixed for 15 minutes with 4% paraformaldehyde, permeabilized with 0.2% Triton X-100 in PBS and blocked with 1% BSA, 22.5 mg/mL glycine, 0.1% Tween in PBS. To stain for SCHAD-V5, the cells were incubated consecutively with the anti-V5 and anti-mouse Alexa Fluor 488 conjugate antibodies. Each incubation was 1 hour at room temperature, with three PBS washes of 5 minutes in between. Coverslips were mounted in ProLong Gold Antifade Reagent with DAPI (Cell Signaling Technology). The confocal images were collected using a TCS SP5 confocal microscope with a 63×/1.4NA HCX Plan-Apochromat oil immersion objective, ~1.0 airy unit pinhole aperture, and appropriate filter combinations (Leica Microsystems). Images were acquired with 405 diode, argon and DPSS 561 lasers and processed using the LAS AF software.

2.7 | MBP-SCHAD protein expression and purification

MBP-SCHAD plasmids were transformed into BL-21 (DE3) *E. coli* cells (NEB) by the heat shock method. A single colony was inoculated and grown in LB medium with 1% glucose and 50 μg/mL kanamycin at 37°C. Protein expression was induced at OD_{600} = 0.6 by adding 0.1 mM IPTG. Bacteria were harvested after overnight incubation at 22°C and sonicated in a pH 7.8 buffer (50 mM NaH_2PO_4, 500 mM NaCl, 10 mM imidazole, 0.1 mM DTT, 10% glycerol) complemented with EDTA-free protease inhibitors (Roche). Recombinant SCHAD protein was purified by immobilized metal affinity chromatography (IMAC) on a HisTrap HP 5-mL column (GE Healthcare) followed by size exclusion chromatography (SEC) on a Superdex 200 16/60120-mL column (GE Healthcare). Buffers (pH 7.8) were as follows: IMAC wash buffer (50 mM NaH_2PO_4, 300 mM NaCl, 20 mM imidazole, 0.1 mM DTT, 10% glycerol), IMAC elution buffer (= wash buffer with 250 mM imidazole), SEC buffer (50 mM NaH_2PO_4, 150 mM NaCl, 0.1 mM DTT, 10% glycerol). Fractions were analyzed by SDS-PAGE and Coomassie staining (SimplyBlue SafeStain, Invitrogen) and protein concentration was determined by A_{280} measurements.

2.8 | Multiangle light scattering measurements

The molecular mass of MBP-SCHAD was calculated by SEC-MALS using a Superdex 200 HR 10/30 column coupled to a light-scattering device. Bovine serum albumin (BSA) was used as standard.

2.9 | SCHAD enzymatic assay

The enzymatic reaction was started by adding 0.07 μg of purified MBP-SCHAD protein to 1.0 mL 100 mM potassium phosphate buffer (pH 7.0) containing 0.1 mM DTT, 0.3 mg/mL BSA (fatty acid-free) and saturating concentrations of acetoacetyl-CoA (50 μM) and NADH (0.15 mM). Absorbance at 340 nm was measured every minute for 5 minutes at 37°C.

2.10 | Co-immunoprecipitation (co-IP)

HEK 293 SCHAD KO cells seeded in 10-cm Petri dishes were co-transfected with 2 μg Plu-CMV-hGDH and 6 μg of pcDNA3.1-SCHAD-V5-His variants using the calcium phosphate method. After 48 hours of transfection, cells were washed with PBS, incubated for 10 minutes with 1 mM disuccinimidyl glutarate and quenched for 15 minutes with 50 mM Tris, pH 7.5. Immediately after, co-IP was performed as follows (kit from Thermo Fisher Scientific): 6 μg of antibody were coupled to 10 μL AminoLink Plus Coupling resin, co-IP buffer was used for cell lysis (500 μL/plate) and washing (×7), 450 μL of cell lysate at 2.8 μg/μL were incubated for 1 hour with the antibody-coupled-resin, and elution (×1) was by

NuPAGE LDS Sample buffer (Thermo Fisher Scientific), followed by western blotting.

2.11 | Statistical analysis

The software R[20] with reshape2[21] and multcomp[22] was used. Plots were produced using the package ggplot2.[23] To evaluate differences in the enzymatic activity of the SCHAD variants, a one-way analysis of variance (ANOVA) and a post-hoc Dunnett's test were used. To evaluate differences in the amount of bound GDH, a one-sample *T*-test was used.

3 | RESULTS

3.1 | Selection of SCHAD variants for functional testing

To perform a systematic functional evaluation of SCHAD protein variants, we chose 16 missense variants present in human populations and CHI patients (Table 1). The population variants were selected to be distributed throughout the domains of SCHAD, and their positions are illustrated in Figures 1A and S1A. Specifically, nine variants were selected from the gnomAD data set,[15] most of them having an allele frequency in the range 0.0002 to 0.005 (Table 1). We also included p.Pro86Leu, which is the most frequent SCHAD coding variant and the only one with an allele frequency > 0.01.[27] Additionally, seven pathogenic variants found in CHI cases were included. Of these, six have been described in case reports[10,16,17,24-26] whereas one, p.His170Arg, has been identified in a CHI patient via our own clinical laboratory service (unpublished).

To characterize functional aspects of these variants in vitro, we introduced them by site-directed mutagenesis into plasmids pcDNA3.1 (for expression in mammalian cells as SCHAD-V5/His fusion protein) and pETM41-His/MBP (for expression in *E. coli* as MBP-SCHAD fusion protein).

3.2 | Expression of SCHAD missense variants in HEK293 cells

SCHAD is a ubiquitous protein that occurs as homodimer in its functional form.[18,28] To avoid the interference that dimerization with endogenous wildtype protein could cause in cellular studies with exogenously expressed variants, we produced a HEK293 SCHAD KO cell line using

TABLE 1 Overview of *HADH* variants and the studied amino acid substitutions

Nucleotide change[a]	Amino acid variant[b]	Exon	Reference SNP ID number[c]	Allele frequency[d]	Source
c.99C > G	p.Ile33Met	1	rs74428123	0.00040	gnomAD
c.100G > C	p.Gly34Arg	1	rs779135938	0.00001	24
c.171C > A	p.Asp57Glu	2	rs137853102	0.00001	gnomAD
c.257C > T	p.Pro86Leu	2	rs4956145	0.08480	gnomAD
c.275 T > G	p.Phe92Cys	3	rs61735992	0.00568	gnomAD
c.406A > G	p.Lys136Glu	3	rs1262186453	0.00003	25
c.456G > T	p.Gln152His	4	rs1051519	0.00175	gnomAD
c.509A > G	p.His170Arg	4	—	—	Unpublished[e]
c.550A > T	p.Ile184Phe	5	—	—	26
c.562A > G	p.Met188Val	5	—	—	16
c.614G > C	p.Gly205Ala	5	rs144699575	0.00023	gnomAD
c.643C > A	p.Pro215Thr	6	rs140413151	0.00184	gnomAD
c.662G > A	p.Arg221His	6	rs76476980	0.00117	gnomAD
c.773C > T	p.Pro258Leu	7	rs137853103	—	10
c.881A > G	p.Asn294Ser	8	rs36030668	0.00235	gnomAD
c.907G > A	p.Gly303Ser	8	rs201772964	0.00004	17

[a]According to NCBI reference sequence NM_005327.4.
[b]Predicted amino acid change. Notation according to NCBI reference sequence NP_005318.3.
[c]According to the Single Nucleotide Polymorphism Database (dbSNP) (https://www.ncbi.nlm.nih.gov).
[d]According to the gnomAD database (http://gnomad.broadinstitute.org).[15]
[e]Unpublished patient from own clinical laboratory service.

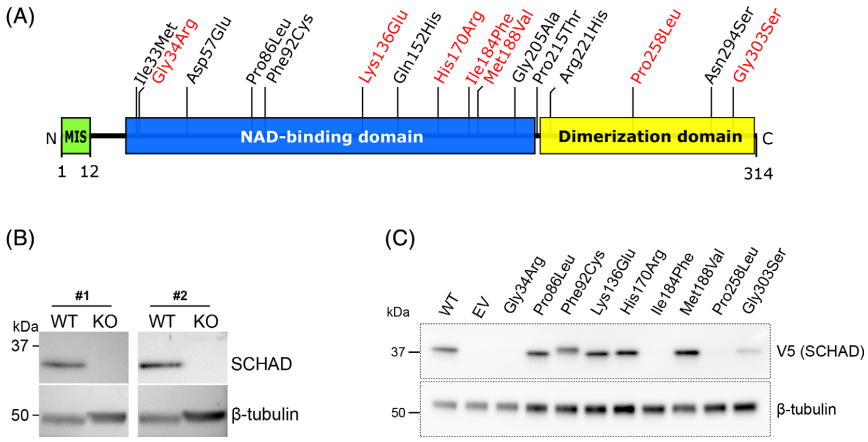

FIGURE 1 Location of the studied missense variants in the SCHAD protein, construction of SCHAD-deficient HEK293 cells, and expression of selected variants in these cells. A, SCHAD has three functional domains: the mitochondrial import signal (MIS; green), the NAD-binding domain (blue) and the dimerization domain (yellow). Protein variants of unknown significance found in populations are in black, while pathogenic variants found in CHI patients are displayed in red. Notation is according to the reference protein sequence NP_005318.3. For simplicity, the prefix "p." of the amino acid variants is not included in this and the other figures. B, Western blot of cell lysates from HEK293 cells expressing (wildtype, WT) and not expressing (knockout, KO) SCHAD protein. Membranes were probed with two different anti-SCHAD antibodies (#1, GeneTex; #2, Novus Biologicals). C, Western blot of whole-cell lysates of HEK293 SCHAD KO cells transfected with the indicated variants. One μg of protein was loaded in each lane, and the SCHAD variants were detected with anti-V5 antibody. A representative image of three experiments is shown. An anti-β-tubulin antibody was used for monitoring the loading in B and C. EV = empty vector

CRISPR-Cas9 targeted genome editing. Disruption of exon 1 of the *HADH* gene was verified through DNA sequencing of selected colonies (Figure S2). Knockout at the protein level was confirmed through western blotting using different anti-SCHAD antibodies (Figure 1B). A band of the expected molecular mass for SCHAD (~34 kDa) was observed only for the lysates of HEK293 WT cells, and not for SCHAD KO cells.

We then tested expression of the SCHAD variants by transiently transfecting the plasmids into HEK293 SCHAD KO cells. Figure 1C shows selected variants in HEK293 SCHAD KO cells to summarize the most relevant findings, whereas Figure S3 presents all 16 variants expressed in both HEK293 WT and SCHAD KO cells. Analysis of the cellular lysates by western blotting, using an anti-V5 antibody (Figure 1C) or an anti-SCHAD antibody (Figure S3), revealed a band of the expected molecular mass (~37 kDa) for the WT-V5/His fusion protein. Most missense variants exhibited the same size and expression levels as the WT protein. The five exceptions were p.Gly34Arg, p.Phe92Cys, p.Ile184Phe, p.Pro258Leu, and p.Gly303Ser. The p.Phe92Cys variant, found in the gnomAD dataset, displayed slower electrophoretic mobility than the WT protein, but had the same expression level. The four other variants, all CHI-associated, were consistently expressed at reduced levels. This reduction was more pronounced for p.Gly34Arg, p.Ile184Phe, and p.Pro258Leu than for the p.Gly303Ser variant. However, CHI variants p.Lys136Glu, p.His170Arg, and p.Met188Val appeared similar to the WT protein and the remaining population variants. All 16 variants yielded the same expression pattern in normal HEK293 (WT) as in the SCHAD KO cell line (Figure S3).

Next, we evaluated the expression and subcellular localization of the variants by immunofluorescence of transiently transfected KO cells. Figure 2 exemplifies how variants exhibiting reduced protein levels in Figure 1C, such as p.Pro258Leu and p.Gly303Ser, also resulted in lower amounts of SCHAD-V5 when directly visualized in the cells. Images of the other variants are presented in Figure S4. For variants with lower protein levels, we did not observe a uniform overall reduction in SCHAD levels within the expressing cells. A few cells displayed a fluorescence pattern comparable to that of WT-transfected cells, while most cells showed from very low to undetectable SCHAD levels.

By confocal microscopy, we found that all variants were correctly targeted to the mitochondria as shown by co-localization of SCHAD-V5 with a mitochondrial-specific stain (Figure S5).

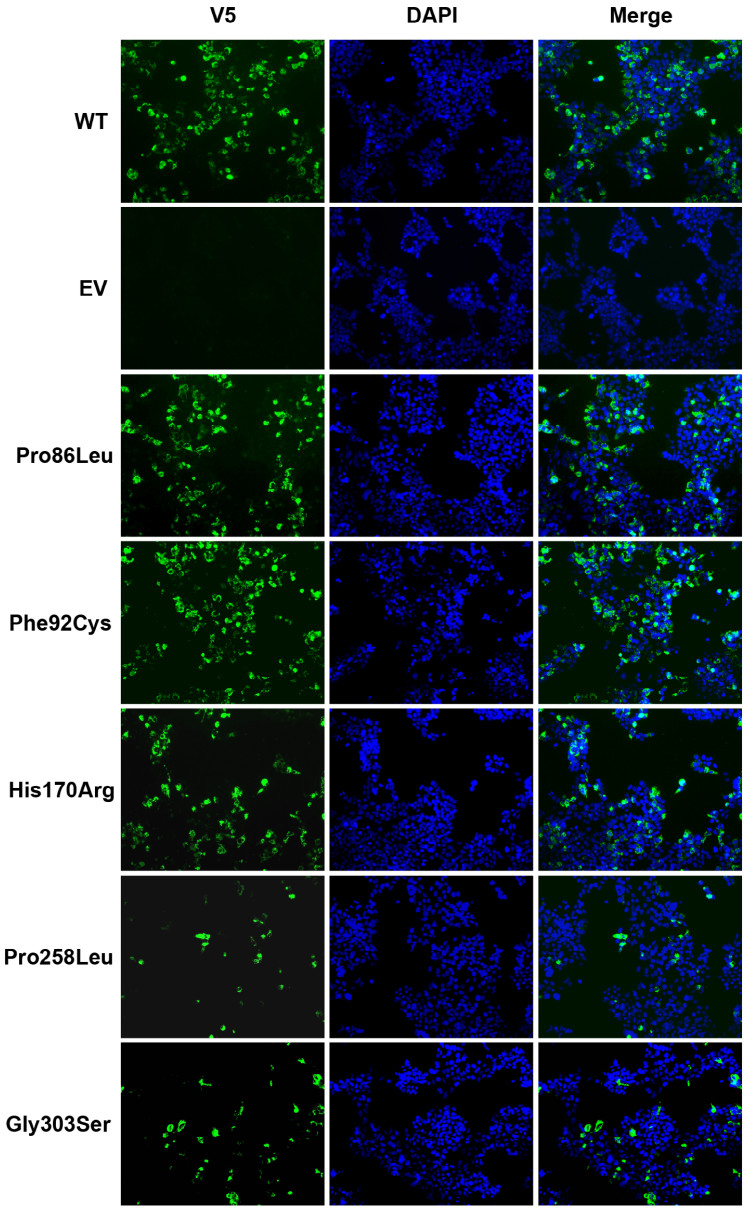

FIGURE 2 Expression of selected SCHAD variants in HEK293 SCHAD KO cells as determined by immunofluorescence. The cells were transiently transfected with the indicated V5-tagged SCHAD variants, fixed 48 hours-post transfection, stained using anti-V5 primary antibody and fluorescent anti-mouse IgG secondary antibody (green), and counterstained with DAPI (blue). Images are representative fields from two experiments, each with two technical replicates (×200). WT = wildtype, EV = empty vector

3.3 | Translation and protein degradation of SCHAD variants with reduced protein levels

To further test expression of variants p.Gly34Arg, p.Ile184Phe, p.Pro258Leu, and p.Gly303Ser, that is, those displaying low protein levels in HEK293 cells, we used a cell-free expression system. Equal amounts of the plasmids were incubated with the cell-free expression reaction mix followed by western blotting. In stark contrast to the results obtained with transfected cells, these four variants now displayed similar protein levels to WT SCHAD (Figure 3A). This confirmed that the plasmids were fully functional with protein synthesis being as efficient as from the WT plasmid. Moreover, this observation hinted at the activity of a cellular quality control

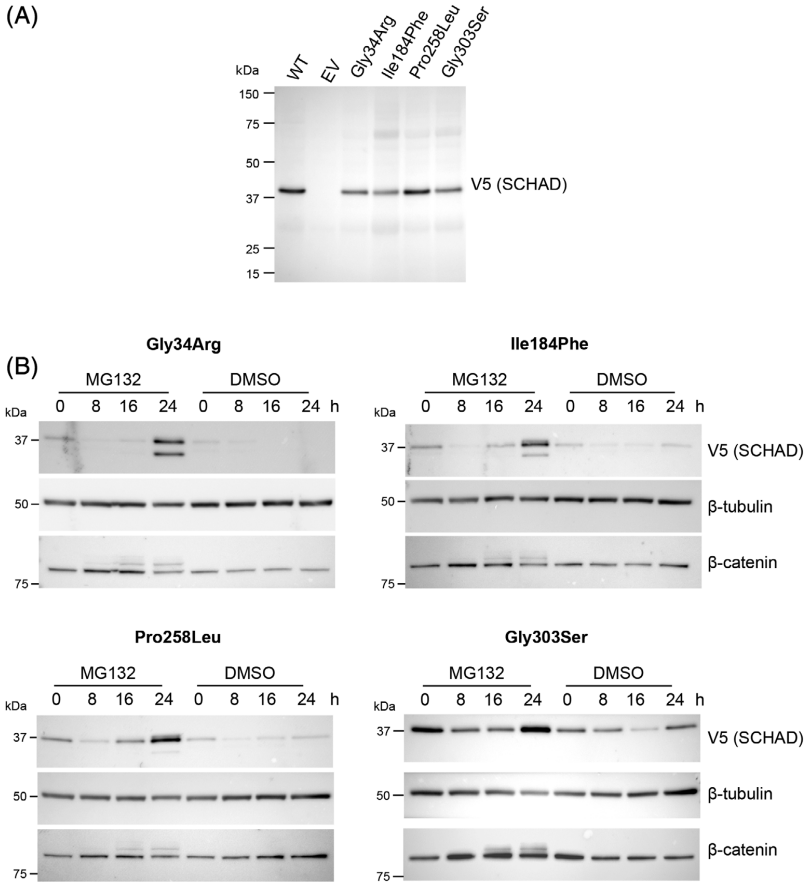

FIGURE 3 Expression of unstable SCHAD variants in a cell-free system and in HEK293 cells treated with a proteasome inhibitor. A, Equal amounts of the vectors expressing the indicated variants were incubated with the cell-free expression master mix for 90 minutes. Three microliters of each reaction were analyzed by western blot using an anti-V5 antibody. WT = wildtype, EV = empty vector. B, Twenty-four hours after transfection with the indicated variants, HEK293 SCHAD KO cells were treated with 5 μM MG132 or only DMSO for the specified times. To be able to visualize the unstable variants, we loaded five times the amount of whole-cell lysate (5 μg) per well than loaded in Figure 1C. The blots were analyzed by anti-V5 antibody, whereas anti-β-tubulin and anti-β-catenin antibodies were used for monitoring the loading and controlling the efficiency of MG132 treatment, respectively

mechanism, not present in the cell-free expression system, as explanation for the low variant levels in HEK293 cells.

To investigate whether the four variants were degraded by the ubiquitin-proteasome system, we blocked this pathway in transfected cells by using the proteasome inhibitor MG132. Figure 3B demonstrates that the variants p.Gly34Arg, p.Ile184Phe, and p.Pro258Leu exhibited clearly increased protein levels after 24 hours of MG132 treatment, suggesting that proteasomal degradation is of importance for their instability. There was also a certain effect on the level of p.Gly303Ser, an increase that was confirmed in two additional, independent experiments.

3.4 | Enzymatic activity of purified SCHAD variants

Although enzymatic activity of SCHAD can be measured in cell and tissue lysates,[3] we opted for using purified protein due to the greater flexibility of the assay and full control over the amount of SCHAD tested. Even though we were able to express all variants in *E. coli* cells, the purification efficiency differed considerably from variant to variant (Figure S6 and data not shown). In fact, the levels of p.Gly34Arg, p.Phe92Cys, and p.Ile184Phe were undetectable at the end of the SEC purification step and therefore no further work was performed on them. Notably, for all variants we employed a purification protocol optimized for WT SCHAD. Thus, none of the conditions were adjusted to the individual characteristics of any specific variant as an attempt to improve the yield.

We assessed the identity and purity of the samples by SDS-PAGE, western blotting and Coomassie staining. For all purified variants, a band around 75 kDa was detected by anti-SCHAD (Figure 4A) and anti-His (data not shown) antibodies. This agrees with the predicted molecular mass of ~77 kDa for MBP-SCHAD. Coomassie staining revealed a few additional, weak bands of higher molecular mass and unknown identity in all cases

(Figure S7A). Some variants, most notably p.Ile33Met, exhibited additional bands of lower molecular weight.

To test if recombinant MBP-SCHAD was purified in the functional dimeric form, we estimated the molecular mass of purified MBP-SCHAD WT by SEC-MALS (Figure S7B). While the predicted monomeric molecular mass was ~77 kDa, the calculated value by SEC-MALS analysis was ~168 kDa. This indicated that MBP-SCHAD WT was purified in the dimeric form. As the missense variants all eluted at the same rate as WT SCHAD (Figure S6), we expected them to be purified as dimers, too.

Next, we assessed the enzymatic activity of the variants in saturating conditions of substrate and co-factor (V_{max}). MBP-SCHAD WT exhibited V_{max} = 181 ± 3 μmol/min/mg (Figure 4B). Variants found in patients all showed reduced activity: p.His170Arg, p.Pro258Leu, and p.Gly303Ser had severely reduced V_{max} (<10 μmol/min/mg), while p.Lys136Glu (127 ± 8 μmol/min/mg) and p.Met188Val (132 ± 29 μmol/min/mg) displayed a smaller, but still significant, reduction. Interestingly, the population variant p.Pro215Thr had a slight increase in enzymatic activity (211 ± 5 μmol/min/mg).

3.5 | Interaction of pathogenic SCHAD variants with GDH

We were therefore left with principally two classes of SCHAD pathogenic variants, one with severely reduced cellular amounts of protein and another with impaired enzymatic activity in the presence of normal protein levels. The variants of the latter class might still have the capacity to inhibit GDH, thereby carrying out normal

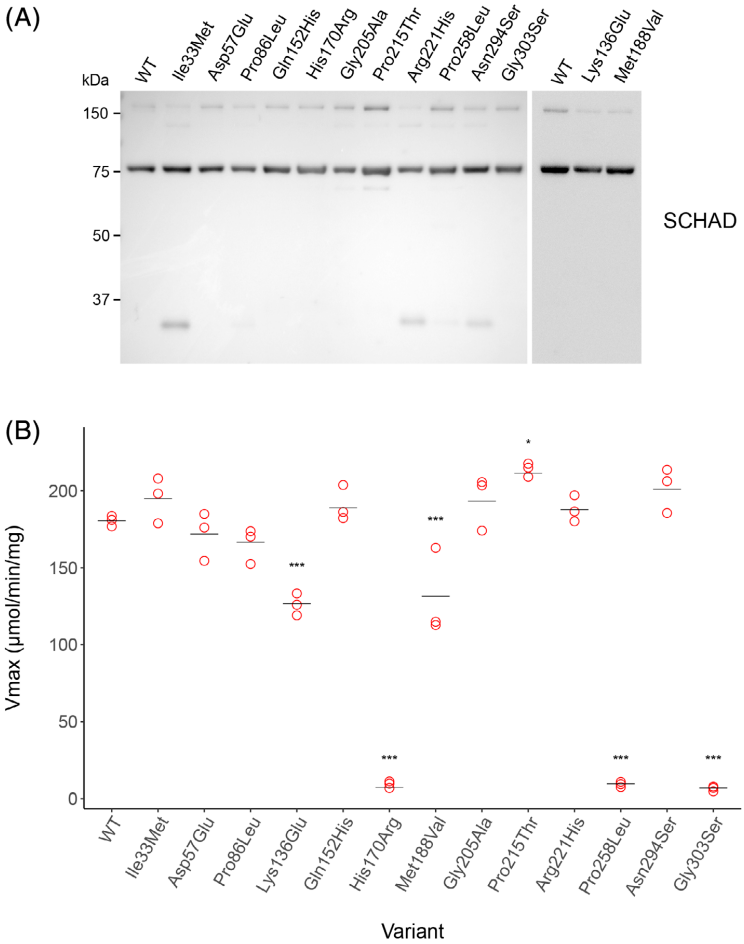

FIGURE 4 Purified recombinant MBP-SCHAD variants from *E. coli* and their enzymatic activity. A, Western blot of all successfully purified variants. Purified protein samples (0.3 μg) were analyzed using the Abmart anti-SCHAD antibody. B, The enzymatic activity of the purified variants was tested on three different days, each time with three measurements. Each dot represents the mean of a triplicate measurement and the horizontal lines show the overall mean. *$P < .05$, ***$P < .001$

SCHAD function in insulin secretion. We therefore evaluated the ability of the variants of the second class (p.Lys136Glu, p.His170Arg, and p.Met188Val) to bind GDH by using co-IP (Figures 5 and S8). We co-transfected HEK293 SCHAD KO cells with GDH and the SCHAD variant to be tested, and then treated the cells with a crosslinking reagent before cell lysis and co-IP. This ensured that we captured protein interactions within the mitochondria. The set-up was validated by including a SCHAD variant (Δ2-12) lacking the mitochondrial import signal and therefore unable to locate with GDH inside the mitochondria. The positive control (WT SCHAD) and all negative controls (EV, Δ2-12, IgG) behaved as intended. Somewhat unexpectedly, GDH was still able to co-IP with the three pathogenic SCHAD variants (Figure 5A, B). Nevertheless, the GDH levels were lower for the missense variants than for WT SCHAD in eight of nine independent Co-IPs tests performed (Figure 5C), although for each variant the reduction did not quite reach statistical significance when assessed separately.

4 | DISCUSSION

We here, for the first time, present a concerted functional assessment of naturally occurring SCHAD missense variants. We have evaluated protein expression, intracellular localization, enzymatic activity and GDH interaction. A strength of our study is that we used a cell line devoid of the SCHAD protein. Because this protein naturally forms dimers,[18,28] our approach allowed the functional testing of SCHAD variants without the interference of endogenous protein.

All tested SCHAD missense variants from verified CHI patients displayed loss-of-function phenotypes. This is in line with the other CHI mutations in the literature being nonsense mutations, exon deletions or mutations that affect the splicing machinery.[11] Thus, pathogenic *HADH* mutations are generally predicted to result in deficiency of SCHAD protein. They are recessively inherited in all reported pedigrees (eg, References 12 and 25). One functional *HADH* allele therefore provides a level of SCHAD protein function sufficient to avoid hypoglycemic episodes, and dominant-negative mutations are yet to be described.

We found altered properties for all seven CHI-associated SCHAD variants examined. A few case reports of missense mutations have investigated SCHAD protein levels and/or enzyme activity in patient fibroblasts. Consistent with our findings, Clayton et al[10] and Vilarinho et al[17] observed low protein levels for the variants p.Pro258Leu and p.Gly303Ser, respectively, whereas Kapoor et al[16] found decreased enzymatic activity for

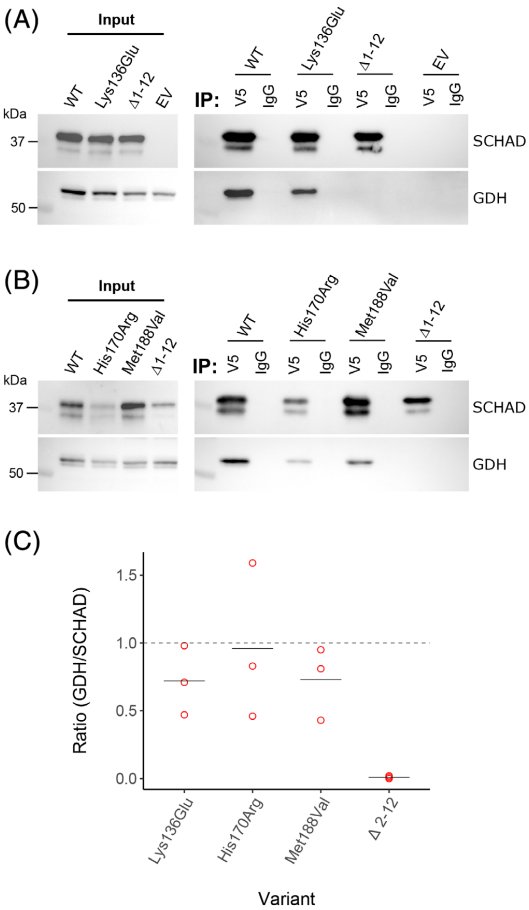

FIGURE 5 Co-immunoprecipitation of GDH with selected SCHAD variants. A,B, HEK 293 SCHAD KO cells were co-transfected with plasmids expressing GDH and selected SCHAD-V5 variants or with GDH and an empty plasmid vector (EV). The SCHAD variant Δ2-12 lacked the mitochondrial import signal. Forty-eight hours post transfection, cells were treated with a crosslinking reagent before lysis. Cell lysates (450 μL) with equal protein concentration (Input) were incubated with either V5 or IgG antibodies coupled to agarose beads. The proteins bound to the antibodies/beads (IP) were separated by SDS-PAGE, and SCHAD (GeneTex antibody) and GDH were visualized by western blotting. C, GDH and SCHAD western blot signals were quantified for the variants and normalized to the WT sample. The dots represent the calculated GDH/SCHAD ratio for each replicate with the horizontal lines showing the mean for each variant. The dashed line corresponds to the GDH/SCHAD ratio for the wildtype co-IP reaction

p.Met188Val. However, while we noted a drastically reduced V_{max} for recombinantly expressed and purified p.Gly303Ser, Vilarinho et al[17] in patient fibroblasts

observed a V_{max} comparable to the value of healthy controls. Still, they noted that the enzymatic function was affected by an increased K_m for binding to the cofactor NADH.

Our results suggest that SCHAD missense variants causing CHI exhibit at least two types of loss-of-function phenotypes. The first group, consisting of p.Gly34Arg, p.Ile184Phe, p.Pro258Leu, and p.Gly303Ser, displays the most common outcome for pathogenic missense mutations; that is, a decrease of the protein's half-life leading to lower amounts in the cell.[29] This can be explained by abnormal folding of the protein such that folding intermediates and/or improperly folded proteins are degraded through a protein-quality control system. Accordingly, we readily achieved protein expression in a cell-free eukaryotic system, and treatment with a proteasome inhibitor stabilized the protein levels in HEK293 cells. The small amounts of these variants still detectable by western blot and immunofluorescence may represent a fraction of the synthesized protein that managed to obtain a folded state and escape degradation before import to the mitochondria.[30]

A second loss-of-function phenotype was seen for CHI variants p.Lys136Glu, p.His170Arg, and p.Met188Val. Here, enzymatic activity of SCHAD was clearly impacted, but without visible affection of steady-state protein levels. It should be pointed out, though, that biophysical stress (such as high temperature) might have demonstrated protein instability also in this group of missense variants.

Among all CHI variants studied, p.His170Arg was the most atypical since it is the only one located directly in the active site of the enzyme. The His170 residue is part of the catalytic His-Glu pair and functions as a catalytic base, involved in proton abstraction from the substrate.[28] In the three-dimensional conformation of SCHAD, p.Lys136 and p.Met188 are both located on the surface of the NAD-binding domain, opposite to the catalytic site (Figure S1B). Due to the nature of these amino acids and their location, they could be involved in some interaction or binding, critical for proper functioning of the protein. Notably, Xu et al[18] have demonstrated that mutations distant from the catalytic site affect the enzymatic activity of *C. elegans* SCHAD by decreasing the stability of the catalytic intermediate formation. Considering that in the context of insulin regulation, SCHAD acts by inhibiting GDH,[8] we tested this particular protein-protein interaction, expecting that pathogenic variants with normal steady-state protein levels would exhibit abolished GDH binding. However, compared with WT SCHAD we found only a partial reduction of the GDH interaction. It is therefore not obvious how these three variants result in CHI.

Of the evaluated population variants, most had properties like that of normal SCHAD. Intriguingly, the p.Asp57Glu variant has been identified in a patient with fulminant hepatic failure consistent with a metabolic disorder involving defective fatty acid oxidation. The patient was heterozygous for p.Asp57Glu, which occurred together with the variant p.Ala40Thr.[31] In fact, a second variant in the Asp57 residue has been identified in a patient with Reye-like syndrome (p.Asp57Gly) who was compound heterozygous, carrying another unique variant, p.Tyr214His.[32] Possibly, these variants could affect the function of the SCHAD protein in fatty acid oxidation but not in insulin secretion.

Among the population variants, p.Phe92Cys stood out by consistently migrating with slower electrophoretic mobility. Still, its protein level was as for WT SCHAD, and we speculate that an extra post-translational modification involving the Cys92 residue might cause the apparent increase in molecular mass. As p.Phe92Cys was the only population variant that could not be purified after *E. coli* expression, we cannot rule out an effect on enzymatic function. Still, with an allele frequency of ~0.006, this variant is the second most frequent SCHAD amino acid substitution observed in populations, and we consider it unlikely to have a pathogenic phenotype.

There is only one common variant (allele frequency > 0.01) of the *HADH* gene that results in change of protein sequence, namely p.Pro86Leu. When expression levels and enzyme activity of p.Pro86Leu were evaluated in fibroblasts of heterozygous carriers, properties comparable for non-carriers were found.[27] Considering that around 0.7% of the population are predicted to be homozygous for this SNP (based on allele frequency of ~0.085 according to the gnomAD database), it was interesting to test the functional effects of this variant without any interference of the WT protein. We observed no obvious difference regarding expression or enzymatic activity when compared with normal SCHAD.

The phenotype of SCHAD deficiency is different from that of other genetic disorders in which genes encoding the enzymes of fatty acid oxidation are mutated. The protein has its highest expression level in the pancreatic β-cells,[5] and it is when the islet-specific function is disrupted that hypoglycemia ensues.[6] Notably, a recent analysis of the genetic architecture of diabetes indicated a small, protective effect of rare variants of the *HADH* gene (Figure 2c in Reference 33), an effect that might be explained by heterozygous carriers of rare *HADH* variants having increased capacity for insulin secretion. A limitation of the present study is therefore that the amino acid substitutions were not tested in cell lines that reflect the β-cell environment, such as INS-1 or EndoC-βH1. Hence, it is conceivable that a variant that in the present

study appears normal with regard to SCHAD expression and function, still could exhibit altered properties in β-cells.

Another limitation is that we included only one of the four SCHAD variants found in patients who had no signs of hyperinsulinism but presented with other metabolic diseases (fulminant hepatic failure and Reye-like syndrome). Only the enzyme kinetics of these non-CHI variants have so far been investigated.[31,32] It would have been interesting to investigate their properties both individually and in the combination that they appear in the patients, comparing with the CHI-causing variants. Finally, future studies should address whether the CHI variants with normal protein levels are unable to inhibit GDH despite being able to bind it, or whether these variants disturb other crucial interactions within the protein super complex in which SCHAD is postulated to be embedded.[34] Investigations of how GDH kinetics and protein complex formation are impacted by the normally expressed variants may be needed to fully clarify the mechanism of GDH activation in SCHAD-CHI.

Nevertheless, we have established a set of useful tools for functional testing of SCHAD protein variants. This toolkit includes a human cell line devoid of endogenous SCHAD expression as well as a series of eukaryotic/prokaryotic expression plasmids with missense variants distributed over the two major protein domains. We found no evidence that rare SCHAD amino acid substitutions not seen in CHI patients exhibited impaired function. This information will be of value when interpreting *HADH* genetic variants revealed by high-throughput sequencing projects and in clinical testing.

ACKNOWLEDGMENTS

We are indebted to Drs Charles Stanley and Changhong Li at the Children's Hospital of Philadelphia, Pennsylvania, USA for providing the plasmid Plu-CMV-hGDH and for valuable discussions. We thank Dr Sven Le Moine Bauer for assistance with statistical analyses and Dr Bjørn Dalhus, Structural Biology Core Facility, University of Oslo for assistance with the SEC-MALS analysis. The authors confirm independence from the sponsors; the content of the article has not been influenced by the sponsors.

CONFLICT OF INTEREST

The authors declare no potential conflict of interests.

ORCID

Kelly Velasco https://orcid.org/0000-0002-9376-6034
Anders Molven https://orcid.org/0000-0003-1847-3079

REFERENCES

1. Hitomi Y, Tokunaga K. Significance of functional disease-causal/susceptible variants identified by whole-genome analyses for the understanding of human diseases. *Proc Japan Acad Ser B*. 2017;93:657-676.
2. Najmi LA, Aukrust I, Flannick J, et al. Functional investigations of HNF1A identify rare variants as risk factors for type 2 diabetes in the general population. *Diabetes*. 2017;66:335-346.
3. Wanders RJA, Ruiter JPN, IJlst L, Waterham HR, Houten SM. The enzymology of mitochondrial fatty acid beta-oxidation and its application to follow-up analysis of positive neonatal screening results. *J Inherit Metab Dis*. 2010;33:479-494.
4. Hardy OT, Hohmeier HE, Becker TC, et al. Functional genomics of the β-cell: short-chain 3-Hydroxyacyl-coenzyme a dehydrogenase regulates insulin secretion independent of K+ currents. *Mol Endocrinol*. 2007;21:765-773.
5. Martens GA, Vervoort A, Van De Casteele M, et al. Specificity in beta cell expression of L-3-hydroxyacyl-CoA dehydrogenase, short chain, and potential role in down-regulating insulin release. *J Biol Chem*. 2007;282:21134-21144.
6. Molven A, Hollister-Lock J, Hu J, et al. The hypoglycemic phenotype is islet cell-autonomous in short-chain hydroxyacyl-CoA dehydrogenase-deficient mice. *Diabetes*. 2016;65:1672-1678.
7. Pepin É, Guay C, Delghingaro-Augusto V, et al. Short-chain 3-hydroxyacyl-CoA dehydrogenase is a negative regulator of insulin secretion in response to fuel and non-fuel stimuli in INS832/13 β-cells. *J Diabetes*. 2010;2:157-167.
8. Li C, Chen P, Palladino A, et al. Mechanism of hyperinsulinism in short-chain 3-hydroxyacyl-CoA dehydrogenase deficiency involves activation of glutamate dehydrogenase. *J Biol Chem*. 2010;285:31806-31818.
9. Smith HQ, Li C, Stanley CA, Smith TJ. Glutamate dehydrogenase, a complex enzyme at a crucial metabolic branch point. *Neurochem Res*. 2019;44:117-132.
10. Clayton PT, Eaton S, Aynsley-Green A, et al. Hyperinsulinism in short-chain L-3-hydroxyacyl-CoA dehydrogenase deficiency reveals the importance of β-oxidation in insulin secretion. *J Clin Invest*. 2001;108:457-465.
11. Molven A, Helgeland G, Sandal T, Njølstad PR (2012) The molecular genetics and pathophysiology of congenital hyperinsulinism caused by short-chain 3-hydroxyacyl-coA dehydrogenase deficiency. In: Stanley CA, De Leon DD (eds) *Monogenic Hyperinsulinemic Hypoglycemia Disorders. Frontiers in Diabetes*. Karger, Basel, pp. 137–145.
12. Molven A, Matre GE, Duran M, et al. Familial hyperinsulinemic hypoglycemia caused by a defect in the SCHAD enzyme of mitochondrial fatty acid oxidation. *Diabetes*. 2004; 53:221-227.
13. Arnoux JB, Verkarre V, Saint-Martin C, et al. Congenital hyperinsulinism: current trends in diagnosis and therapy. *Orphanet J Rare Dis*. 2011;6:1-14.
14. Stanley CA. Perspective on the genetics and diagnosis of congenital hyperinsulinism disorders. *J Clin Endocrinol Metab*. 2016;101:815-826.
15. Karczewski KJ, Francioli LC, Tiao G, et al. The mutational constraint spectrum quantified from variation in 141,456 humans. *Nature*. 2020;581:434-443.
16. Kapoor RR, James C, Flanagan SE, Ellard S, Eaton S, Hussain K. 3-Hydroxyacyl-coenzyme a dehydrogenase deficiency and hyperinsulinemic hypoglycemia: characterization of a novel mutation and severe dietary protein sensitivity. *J Clin Endocrinol Metab*. 2009;94:2221-2225.

17. Vilarinho L, Sales Marques J, Rocha H, et al. Diagnosis of a patient with a kinetic variant of medium and short-chain 3-hydroxyacyl-CoA dehydrogenase deficiency by newborn screening. *Mol Genet Metab*. 2012;106:277-280.
18. Xu Y, Li H, Jin Y-H, Fan J, Sun F. Dimerization interface of 3-hydroxyacyl-CoA dehydrogenase tunes the formation of its catalytic intermediate. *PLoS One*. 2014;9:e95965.
19. Artimo P, Jonnalagedda M, Arnold K, et al. ExPASy: SIB bioinformatics resource portal. *Nucleic Acids Res*. 2012;40:597-603.
20. R Core Team. *R: A Language and Environment for Statistical Computing*. Vienna: R Foundation for Statistical Computing; 2017.
21. Wickham H. Reshaping data with the {reshape} package. *J Stat Softw*. 2007;21:1-20.
22. Hothorn T, Bretz F, Westfall P. Simultaneous inference in general parametric models. *Biom J*. 2008;50:346-363.
23. Wickham H. *ggplot2: Elegant Graphics for Data Analysis*. New York: Springer-Verlag; 2016.
24. Snider KE, Becker S, Boyajian L, et al. Genotype and phenotype correlations in 417 children with congenital hyperinsulinism. *J Clin Endocrinol Metab*. 2013;98:E355-E363.
25. Flanagan SE, Patch AM, Locke JM, et al. Genome-wide homozygosity analysis reveals HADH mutations as a common cause of diazoxide-responsive hyperinsulinemic-hypoglycemia in consanguineous pedigrees. *J Clin Endocrinol Metab*. 2011;96:498-502.
26. Satapathy AK, Jain V, Ellard S, Flanagan SE. Hyperinsulinemic hypoglycemia of infancy due to novel HADH mutation in two siblings. *Indian Pediatr*. 2016;53:912-913.
27. van Hove EC, Hansen T, Dekker JM, et al. The HADHSC gene encoding short-chain L-3-hydroxyacyl-CoA dehydrogenase (SCHAD) and type 2 diabetes susceptibility: the DAMAGE study. *Diabetes*. 2006;55:3193-3196.
28. Barycki JJ, O'Brien LK, Bratt JM, et al. Biochemical characterization and crystal structure determination of human heart short chain L-3-hydroxyacyl-CoA dehydrogenase provide insights into catalytic mechanism. *Biochemistry*. 1999;38:5786-5798.
29. Gregersen N, Bross P, Jørgensen MM, Corydon TJ, Andresen BS. Defective folding and rapid degradation of mutant proteins is a common disease mechanism in genetic disorders. *J Inherit Metab Dis*. 2000;23:441-447.
30. Wu Y, Whitman I, Molmenti E, Moore K, Hippenmeyer P, Perlmutter DH. A lag in intracellular degradation of mutant α1-antitrypsin correlates with the liver disease phenotype in homozygous PiZZ α1-antitrypsin deficiency. *Proc Natl Acad Sci*. 1994;91:9014-9018.
31. O'Brien LK, Rinaldo P, Sims HF, et al. Fulminant hepatic failure associated with mutations in the medium and short chain L-3-hydroxyacyl-CoA dehydrogenase gene. *J Inherit Metab Dis*. 2000;23:127.
32. Bennett MJ, Russell LK, Tokunaga C, et al. Reye-like syndrome resulting from novel missense mutations in mitochondrial medium- and short-chain L-3-hydroxy-acyl-CoA dehydrogenase. *Mol Genet Metab*. 2006;89:74-79.
33. Fuchsberger C, Flannick J, Teslovich TM, et al. The genetic architecture of type 2 diabetes. *Nature*. 2016;536:41-47.
34. Narayan SB, Master SR, Sireci AN, et al. Short-chain 3-hydroxyacyl-coenzyme a dehydrogenase associates with a protein super-complex integrating multiple metabolic pathways. *PLoS One*. 2012;7:e35048.

SUPPORTING INFORMATION

Additional supporting information may be found online in the Supporting Information section at the end of this article.

How to cite this article: Velasco K, St-Louis JL, Hovland HN, et al. Functional evaluation of 16 SCHAD missense variants: Only amino acid substitutions causing congenital hyperinsulinism of infancy lead to loss-of-function phenotypes in vitro. *J Inherit Metab Dis*. 2020;1–13. https://doi.org/10.1002/jimd.12309

Supplementary Figure 1

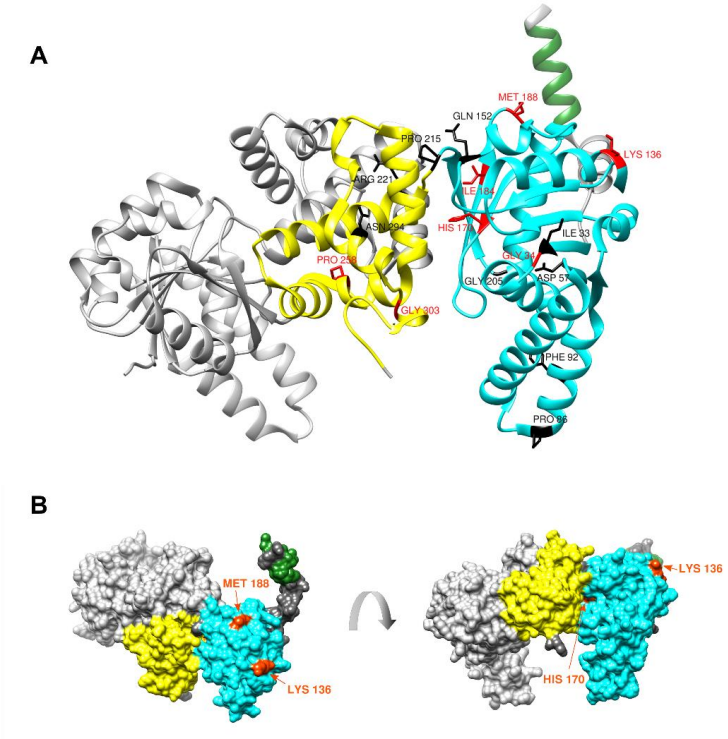

Supplementary Figure 1. Location of the studied missense variants in the 3D representation of the SCHAD protein structure. The three functional domains are colored in one of the sub-units of the SCHAD dimer: the mitochondrial import signal in green, the NAD-binding domain in blue and the dimerization domain in yellow. The second subunit is colored in grey. (A) Representation showing secondary structure elements and the location of the altered amino acids in the studied variants (variants of unknown significance in black and pathogenic variants in red). (B) Surface representation of the same structure from two different angles, showing that the amino acids Lys136 and Met188 are exposed on the surface, while His170 is buried in the catalytic site. Image of PDB ID 3RQS (Kuzin et al. 2011) created with Chimera (Pettersen et al. 2004).

References:

Kuzin A, Su M, Seetharaman J, et al (2011) Northeast Structural Genomics Consortium Target HR487. doi: 10.2210/pdb3RQS/pdb

Pettersen EF, Goddard TD, Huang CC, et al (2004) UCSF Chimera - A visualization system for exploratory research and analysis. J Comput Chem 25:1605–1612

Supplementary Figure 2

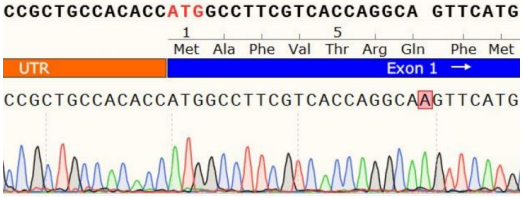

Supplementary Figure 2. Confirmation of CRISPR-Cas9-mediated disruption of SCHAD expression in HEK293 cells. DNA sequencing revealed an insertion early in the exon 1 coding sequence (the nucleotide A highlighted by a red square) in the *HADH* gene. Wildtype DNA and protein sequence are shown on top of the panel.

Supplementary Figure 3

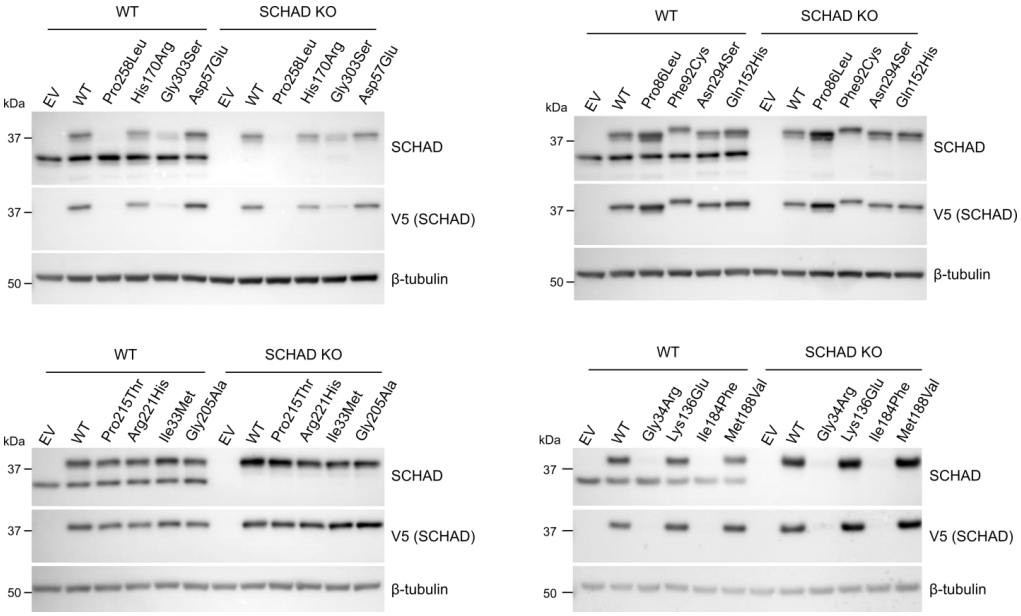

Supplementary Figure 3. Expression of all studied SCHAD variants in HEK293 wild type (WT) and SCHAD knockout (KO) cells. Western blots of whole-cell lysates from HEK293 WT and SCHAD KO cells transfected with the indicated variants are shown. One µg of protein was loaded in each lane. SCHAD was detected with anti-SCHAD (Atlas) and anti-V5 antibodies, the latter being specific for exogenous SCHAD. An anti-β-tubulin antibody was used for monitoring the loading. Note that endogenous SCHAD is present only in the WT cells (band around 34 kDa).

Supplementary Figure 4

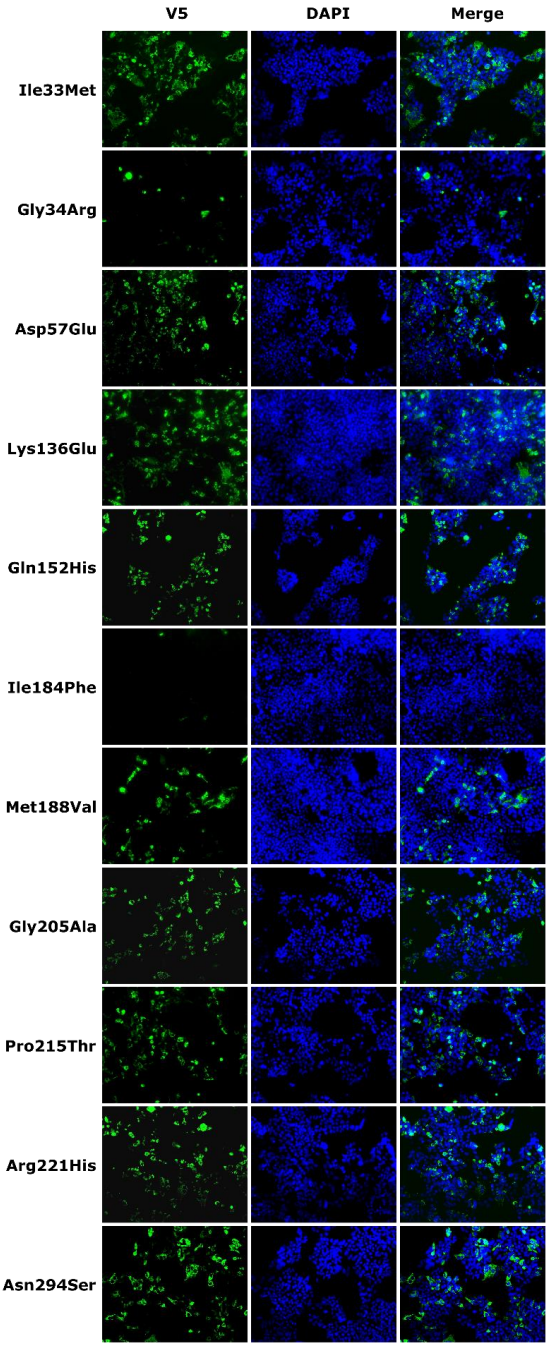

Supplementary Figure 4. Expression of SCHAD variants in HEK293 SCHAD KO cells as determined by immunofluorescence. The variants are those not shown in Figure 3. The cells were transiently transfected with the indicated SCHAD variants (V5-tagged), fixed 48 hours post-transfection, stained using anti-V5 primary antibody and fluorescent anti-mouse IgG secondary antibody (green), and counterstained with DAPI (blue). Images are representative fields from two experiments, each with two technical replicates (x200).

Supplementary Figure 5

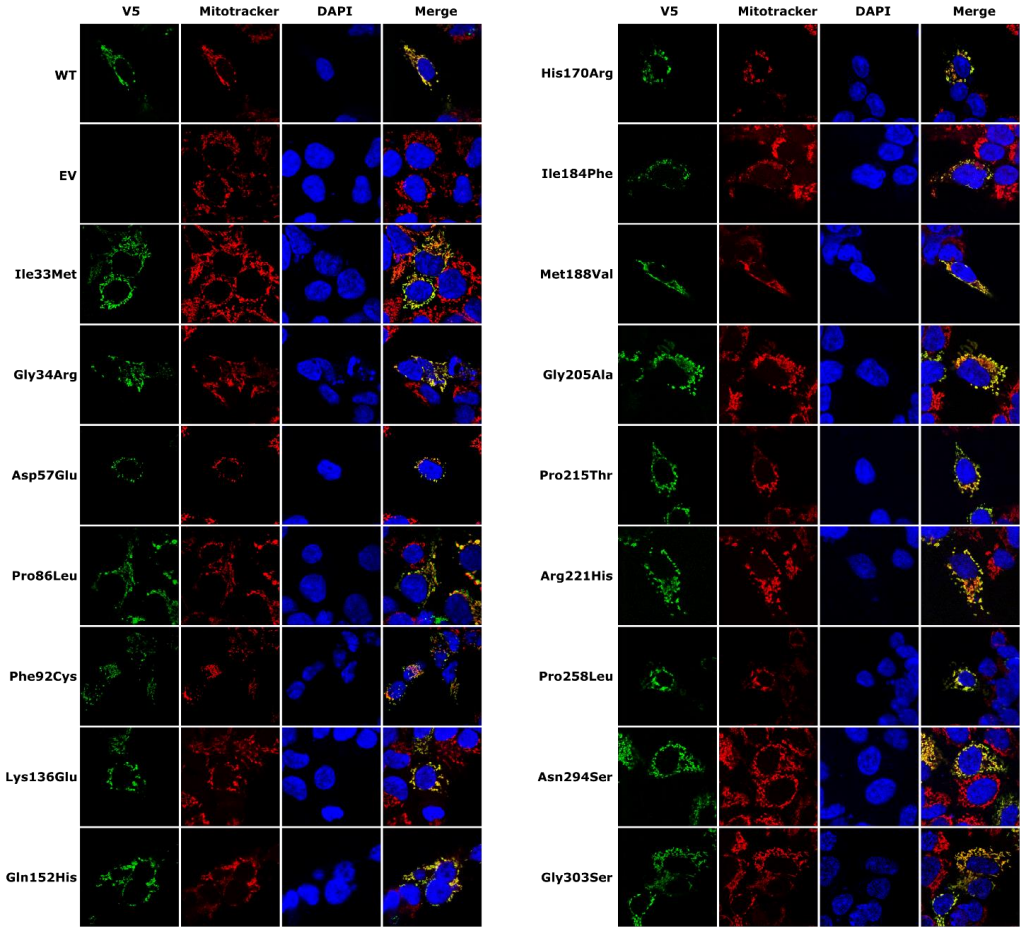

Supplementary Figure 5. Intracellular localization of SCHAD variants in HEK293 SCHAD KO cells. Cells were transiently transfected with the indicated SCHAD variants (V5-tagged). Forty-eight hours post-transfection the cells were incubated with a mitochondrial stain (MitoTracker, red), fixed, stained using anti-V5 primary antibody and fluorescent anti-mouse IgG secondary antibody (green), and counterstained with DAPI (blue). Images show representative cells from two experiments, each with two technical replicates. (x1000). EV= empty vector.

Supplementary Figure 6

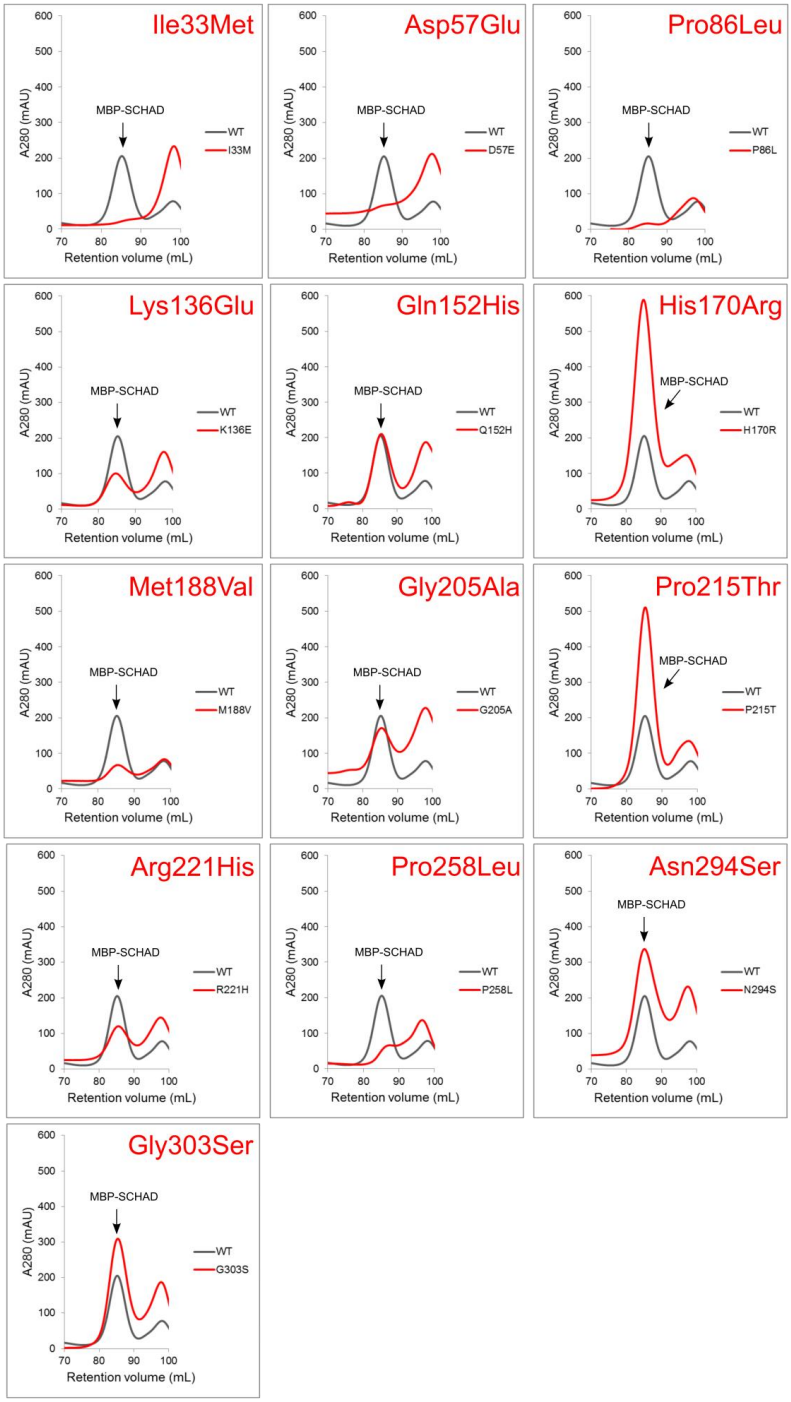

Supplementary Figure 6. Size exclusion chromatography (SEC) elution profiles of purified SCHAD variants. Each protein variant was expressed in *E. coli* BL21 (DE3) cells and purified by immobilized metal affinity chromatography. All protein from the first purification step was further processed by SEC in a Superdex 200 16/60 column. In every graph, the red line corresponds to the elution profile of the named variant compared to the profile of the WT protein (black line). Dimeric MBP-SCHAD eluted in the volume between 80-90 ml (arrow). The second peak (after 90 ml) corresponded to other proteins of lower molecular mass as analyzed by SDS-PAGE and western blot (data not shown). Although the absorbance values where MBP-SCHAD is expected to elute, are very low for the first three variants (p.Ile33Met, p.Asp57Glu and p.Pro86Leu), we were able to detect the protein by SDS-PAGE and to recover a sufficient amount for the enzymatic assays. We could not detect or recover any protein after the final purification step for the p.Gly34Arg, p.Phe92Cys and p.Ile184Phe variants (data not shown). Each purification profile is one representative image from 2-3 purification attempts.

Supplementary Figure 7

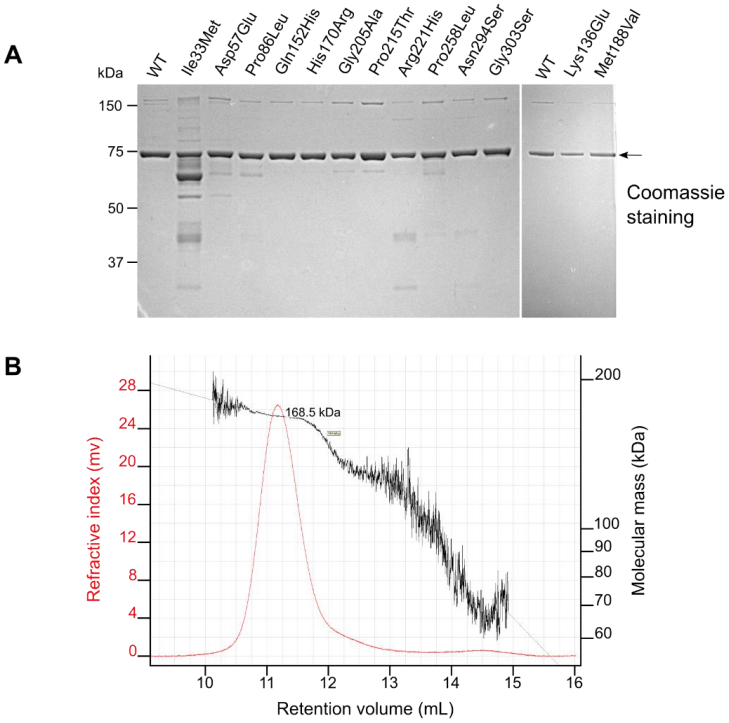

Supplementary Figure 7. Purification of recombinant MBP-SCHAD variants from *E. coli*. (A) All successfully purified SCHAD variants (0.5 µg) were analyzed by SDS-PAGE and Coomassie staining. (B) Molecular mass calculation based on SEC-MALS analysis for MBP-SCHAD WT. The red line represents the refractive index trace from an in-line Superdex 200 HR 10/30 column. The black line corresponds to the molecular mass distribution as determined by MALS with an estimated molecular mass value of ~ 168 kDa (predicted value is ~ 154 kDa).

Supplementary Figure 8

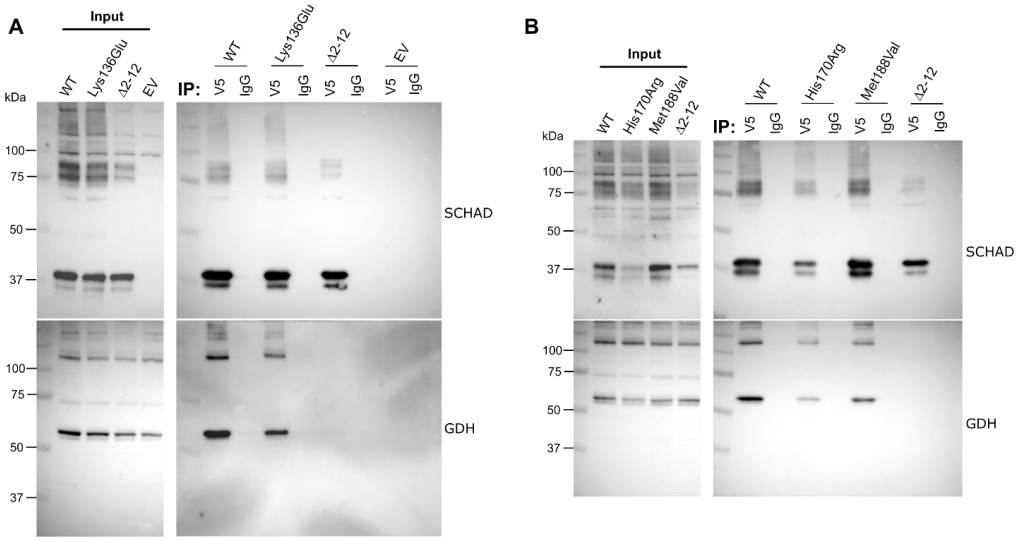

Supplementary Figure 8. Full images of western blot membranes presented in main Figure 5. (A) Wildtype SCHAD protein (WT), variant p.Lys136Glu, a SCHAD variant lacking the mitochondrial import signal (Δ2-12), and empty plasmid vector (EV). (B) WT SCHAD and variants p.His170Arg, p.Met186Val and Δ2-12. HEK 293 SCHAD KO cells were co-transfected with plasmids expressing GDH and the selected V5-tagged SCHAD variant. Forty-eight hours after transfection, cells were treated with a crosslinking reagent before lysis. Cell lysates (450 µl) with equal protein concentration (Input) were incubated with either V5 or IgG antibodies coupled to agarose beads. The proteins bound to the antibodies/beads (IP) were separated by SDS-PAGE, and SCHAD (GeneTex antibody) and GDH were visualized by western blot. Representative images of three experiments with each variant are shown.

Supplementary Table 1

Nucleotide change	Amino acid variant	Sequences of mutagenesis primers
c.99C>G	p.Ile33Met	F: 5'-gcacgtgacggtcatgggcggcgg-3' R:5'-ccgccgcccatgaccgtcacgtgc-3'
c.100G>C	p.Gly34Arg	F: 5'- cagcccgccgcggatgaccgtca-3' R: 5'-tgacggtcatccgcggcgggctg-3'
c.171C>A	p.Asp57Glu	F: 5'-acagtagtgttggtagaacagacagaggacatcct-3' R: 5'-aggatgtcctctgtctgttctaccaacactactgt-3'
c.257C>T	p.Pro86Leu	F: 5'-gaagtttgcagaaaaccttaaggccggcgatgaa-3' R: 5'-ttcatcgccggccttaaggttttctgcaaacttc-3'
c.275T>G	p.Phe92Cys	F: 5'-ccctaaggccggcgatgaatgtgtggagaaga-3' R: 5'-tcttctccacacattcatcgccggccttaggg-3'
c.406A>G	p.Lys136Glu	F: 5'-tatgttcagcagcaaactcgtccagccttttgaagag-3' R: 5'-cttctccagtcttcttgctgaacttgttctctgctac-3'
c.456G>T	p.Gln152His	F: 5'-cattagctatgcttgtaatatgcaaggaggaagtgttgc-3' R: 5'-gcaacacttcctccttgcatattacaagcatagctaatg-3'
c.509A>G	p.His170Arg	F: 5'-cgattcgctggcctccgtttcttcaacccagtg-3' R: 5'-cactgggttgaagaaacggaggccagcgaatcg-3'
c.550A>T	p. Ile184Phe	F: 5'-ctggtcattggtgttttaaagacctccacaagtttcatg-3' R: 5'-catgaaacttgtggaggtctttaaaacaccaatgaccag-3'
c.562A>G	p.Met188Val	F: 5'-cttctggctggtcactggtgttttaatgacctcc-3' R: 5'-ggaggtcattaaaacaccagtgaccagccagaag-3'
c.614G>C	p.Gly205Ala	F: 5'-actttagcaaagccctagcaaagcatcctgtttcttg-3' R: 5'-caagaaacaggatgctttgctagggctttgctaaagt-3'
c.643C>A	p.Pro215Thr	F:5'-ggttcacaataaacccagtagtgtccttgcaagaaac-3' R:5'-gtttcttgcaaggacactactgggtttattgtgaacc-3'
c.662G>A	p.Arg221His	F: 5'-tgggtttattgtgaaccacctcctggttccatacc-3' R: 5'-ggtatggaaccaggaggtggttcacaataaaccca-3'
c.773C>T	p.Pro258Leu	F: 5'-cggttaccccatgggcctatttgagcttctagatt-3' R: 5'-aatctagaagctcaaataggcccatggggtaaccg-3'
c.881A>G	p.Asn294Ser	F: 5'-gctaccagcttacttaaggatgggctgggctg-3' R: 5'-cagcccagcccatccttaagtaagctggtagc-3'
c.907G>A	p.Gly303Ser	F: 5'-gtagcagagaacaagttcagcaagaagactggagaag-3' R: 5'-cttctccagtcttcttgctgaacttgttctctgctac-3'
c.Δ4-36	p.Δ2-12	F: 5'-gtggaattccaccatgtcctcctcgtccaccg-3' R: 5'-cggtggacgaggaggacatggtggaattccac-3'

Supplementary Table 1. Primers used to introduce the studied variants in the *HADH* sequence by site-directed mutagenesis. Primers were designed according to manufacturer instructions using the QuickChange primer design program (https://www.agilent.com/store/primerDesignProgram.jsp).

Graphic design: Communication Division, UiB / Print: Skipnes Kommunikasjon AS

uib.no

ISBN: 9788230846063 (print)
9788230840382 (PDF)